ADVANCED FUNCTIONAL MATERIALS

WILEY ADVANCED

Review

Advances in Wearable Sensors: Moving toward Autonomous Intelligence

Submission ID 5726b2be-75bb-4f4d-972f-6891f6250172

Submission Version Initial Submission

PDF Generation 13 Jun 2026 14:01:02 EST by Atypon ReX

Authors

Dr. Zixuan Zhang

CRediT
Investigation, Visualization, Writing - review & editing, Writing - original draft, Project administration

Affiliations
- Department of Electrical & Computer Engineering, National University of Singapore, 4 Engineering Drive 3, 117576, Singapore
- Center for Intelligent Sensors and MEMS, National University of Singapore, 117608, Singapore
- School of Electrical and Electronics Engineering, Hubei University of Technology, Wuhan 430068, China
- School of AI, Beijing Institute of Technology, Beijing 100081, China

Mr. Shuhan He

ORCiD
https://orcid.org/0009-0003-5692-9724

CRediT
Visualization, Investigation, Writing - original draft, Writing - review & editing

Affiliations
- Department of Electrical & Computer Engineering, National University of Singapore, 4 Engineering Drive 3, 117576, Singapore
- Center for Intelligent Sensors and MEMS, National University of Singapore, 117608, Singapore
- National University of Singapore Suzhou Research Institute (NUSRI), Suzhou 215123, China

Miss Xinrong Chen

CRediT
Writing - original draft, Writing - review & editing

Affiliations
- School of Electrical and Electronics Engineering, Hubei University of Technology, Wuhan 430068, China

Mr. Xu Chen

CRediT
Writing - review & editing, Writing - original draft

Affiliations
- School of Electrical and Electronics Engineering, Hubei University of Technology, Wuhan 430068, China

Miss Luwei Wang

CRediT
Writing - original draft, Writing - review & editing

Affiliations
- Department of Electrical & Computer Engineering, National University of Singapore, 4 Engineering Drive 3, 117576, Singapore
- Center for Intelligent Sensors and MEMS, National University of Singapore, 117608, Singapore

Miss Jingfeng Xu

CRediT
Writing - review & editing, Writing - original draft

Affiliations
- Department of Electrical & Computer Engineering, National University of Singapore, 4 Engineering Drive 3, 117576, Singapore
- Center for Intelligent Sensors and MEMS, National University of Singapore, 117608, Singapore
- National University of Singapore Suzhou Research Institute (NUSRI), Suzhou 215123, China

Dr. Yunlong Xu

CRediT
Writing - original draft, Writing - review & editing

Affiliations
- Center for Intelligent Sensors and MEMS, National University of Singapore, 117608, Singapore
- National University of Singapore Suzhou Research Institute (NUSRI), Suzhou 215123, China

Prof. Hailing Fu

CRediT
Writing - review & editing, Supervision

Affiliations
- School of AI, Beijing Institute of Technology, Beijing 100081, China

Prof. Guozhi Zhang

CRediT
Supervision, Writing - review & editing

Affiliations
- School of Electrical and Electronics Engineering, Hubei University of Technology, Wuhan 430068, China

Prof. Chengkuo Lee
Corresponding Author
Submitting Author

ORCiD
https://orcid.org/0000-0002-8886-3649

CRediT
Conceptualization, Investigation, Funding acquisition, Writing - original draft, Writing - review & editing, Visualization, Validation, Methodology, Project administration, Resources, Supervision

Affiliations
- Department of Electrical & Computer Engineering, National University of Singapore, 4 Engineering Drive 3, 117576, Singapore
- Center for Intelligent Sensors and MEMS, National University of Singapore, 117608, Singapore
- School of Electrical and Electronics Engineering, Hubei University of Technology, Wuhan 430068, China
- National University of Singapore Suzhou Research Institute (NUSRI), Suzhou 215123, China

Files for peer review

All files submitted by the author for peer review are listed below. Files that could not be converted to PDF are indicated; reviewers are able to access them online.

Name	Type of File	Size	Page
AFM_Review_V3.0.docx	Main Document - MS Word	22.8 MB	Page 4

WILEY-VCH

Advances in Wearable Sensors: Moving toward Autonomous Intelligence

Zixuan Zhang, Shuhan He, Xinrong Chen, Xu Chen, Luwei Wang, Jingfeng Xu, Yunlong Xu, Hailing Fu, Guozhi Zhang* and Chengkuo Lee**

Z.Zhang, S. He, L.Wang, J.Xu, C.Lee
Department of Electrical & Computer Engineering, National University of Singapore, 4 Engineering Drive 3, 117576, Singapore

Z.Zhang, S. He, L.Wang, J.Xu, Y.Xu, C.Lee
Center for Intelligent Sensors and MEMS, National University of Singapore, 117608, Singapore

Z.Zhang, X.Chen, X.Chen, G.Zhang
School of Electrical and Electronics Engineering, Hubei University of Technology, Wuhan 430068, China

S.He, J.Xu, Y.Xu, C.Lee
National University of Singapore Suzhou Research Institute (NUSRI), Suzhou 215123, China

H.Fu
School of AI, Beijing Institute of Technology, Beijing 100081, China

E-mail: Hailing Fu (hailing.fu@bit.edu.cn); Guozhi Zhang (zhangguozhi@hbut.edu.cn); Chengkuo Lee (elelc@nus.edu.sg)

Funding: The National Foreign Experts Program (S20250239) in Hubei University of Technology, Research Platform for Biomedical and Health Technology (RP-BTH-Prof. LEE Chengkuo) in NUS (Suzhou) Research Insititute, NUS College of Design and Engineering (CDE)-Robotics Seed Grant Programme, “AI-Sensor Enhanced Medical Operation Training System (A-8003283-00-00)”, NUS College of Design and Engineering (CDE)-Robotics Seed Grant Programme, “A Multimodal Sensing/ Haptic System For lower-Limb Exoskeleton Feedback Control (A-8003281-00-00)”

Keywords: wearable electronics, hydrogel, multimodal sensing, energy harvesting, in-sensor computing,

Abstract

Wearable systems are rapidly evolving from traditional passive devices into highly integrated platforms capable of distributed sensing, self-sustaining operation, and autonomous decision-making. In recent years, with the rapid development of flexible materials, bioelectronic sensors, micro/nano fabrication, device miniaturization, and wireless communication technologies, wearable sensing platforms have been able to continuously and synchronously acquire various biophysical and biochemical signals, providing an important technological foundation for long-term health monitoring and human-computer interaction. However, existing wearable systems still face challenges in simultaneously achieving high sensitivity, multimodal sensing, long-term wearing comfort, continuous energy supply, and real-time local computation, which limits their ability to form truly closed-loop intelligent systems in complex dynamic scenarios. This review summarizes recent advances in wearable sensors from three perspectives. First, advanced wearable tactile sensors and their applications in surgical and robotic systems are discussed. Second, self-powered wearable sensors are reviewed with a focus on metamaterial-based wireless body sensor networks, functional fibers, and wearable energy harvesters. These advances aim to address key challenges related to long-term operation, wireless communication, and energy sustainability. In addition, we also explore emerging directions in autonomous wearable intelligence, including visual–tactile sensing for robotic perception, wearable tactile feedback interfaces, artificial-intelligence-assisted wearable systems, and near-sensor/in-sensor computing architectures.

1. Introduction

Wearable sensors are undergoing a conceptual transition from isolated monitoring devices to distributed intelligent systems that continuously perceive, interpret and respond to dynamic states across humans, robots and surrounding environments.[1–3] Early wearable electronics were primarily designed to measure individual physiological signals, such as heart rate, motion, body temperature, respiration, motion and plantar pressure.[4–6] Although these devices established the feasibility of continuous and non-invasive sensing beyond clinical and laboratory environments, emerging wearable systems are expected to address more complicated physiological, biomechanical, and interactive scenarios.[7,8] For example, exercise assessment requires the combined analysis of cardiovascular activity, respiration, sweat metabolites, skin temperature, and body motion.[9–12] The key challenge is therefore not simply to improve the sensitivity of individual sensors, but to coordinate spatially distributed and multimodal signals into interpretable physiological, biomechanical and interaction states. Wireless body sensor networks (WBSN) provide a system-level solution to address this challenge.[13–15] As illustrated in Figure 1, multiple sensing nodes can be distributed across the skin, textiles, footwear, prosthetic interfaces, and human–machine interfaces to form a whole-body network for synchronized data acquisition and wireless data transmission. In this framework, wearable sensors no longer operate as independent devices attached to isolated body locations, but instead function as interconnected sensing units to monitor body motion, physiological activity, tactile interaction, and environmental variations. Recent studies on near-field-enabled clothing and textile-based body area networks have shown that garments can serve not only as mechanical supports for sensors, but also as communication and power-distribution media.[16,17] Battery-free and chip-less textile sensors further suggest a path toward large-area, low-maintenance, low power-consumption sensing systems that can operate during daily activities without bulky electronics.[18,19] Thus, wireless body sensor networks represent an important step from local signal collection toward multi-dimensional coordinated perception.[20–25]

Movement posture analysis of human body is one of the most important applications of wireless body sensor networks.[26,27] Conventional wearable electronics for human motion monitoring mainly relied on accelerometers or gyroscopes to classify simple activities such as walking, running, or standing. Advanced wearable sensors combined with soft, conformal, or textile-integrated platforms have become capable of extracting richer biomechanical information. For example, Li et al. developed a flexible topological clothing platform that wirelessly interconnects multiple on-body biosensors through textile-based topological edge states.[25] By confining microwave signals along reconfigurable textile channels instead of radiating them into free space, the system enhanced on-body signal transmission by more than

three orders of magnitude and maintained robust communication under body bending and exercise. When combined with machine-learning algorithms, the clothing-based sensor network enabled reliable monitoring of heartbeat and respiration during standing, walking, jogging and running, illustrating how textile-integrated body sensor networks can move wearable motion monitoring from isolated activity recognition toward distributed physiological and biomechanical interpretation.

Exercise vital-sign monitoring extends the application of wearable sensors from movement to physiological regulation. During various physical activity, the body undergoes simultaneous changes in cardiovascular output, respiration, perspiration, skin temperature, muscle activation and mechanical loading. A single bio-sensing signal is often insufficient to distinguish training intensity, dehydration, thermal stress, fatigue, and metabolic state. Recent wearable systems have increasingly adopted multiplexed and hybrid sensing strategies.[28–30]. For example, Gao et al. developed a fully integrated wearable sweat sensor array for multiplexed in situ perspiration analysis during exercise.[23] By integrating electrochemical sensors, signal conditioning, wireless transmission and temperature calibration into a flexible wristband/headband platform, the system simultaneously measured sweat glucose, lactate, sodium, potassium and skin temperature. This work showed that exercise monitoring can move beyond regular heart rate and motion tracking toward real-time interpretation of metabolic activity, electrolyte balance and thermoregulatory state. More recent textile-based body area networks further indicate that exercise monitoring requires not only multimodal sensing,[31,32] but also robust wireless interconnection between distributed sensing nodes under motion, perspiration and environmental disturbance.

The same requirement for multimodal interpretation is also evident in intelligent transportation and driving safety. Driver state is influenced by posture, fatigue, attention, cardiovascular response, cognitive load, and environmental conditions.[33,34] Conventional camera-based monitoring can capture facial expression, gaze direction and eye closure, but its reliability is affected by illumination, occlusion, and privacy concerns. Wearable sensors integrated into seats or seat belts provide complementary information by directly tracking physiological and motion-related signals, such as heart-rate variability, electrocardiographic activity, muscle activity, galvanic skin response, respiration, and body motion. These signals can reveal fatigue or stress states and be translated by algorithms into timely alerts, adaptive assistance, and safety interventions within a human–vehicle intelligence loop. For example, Zeng et al. developed a digitally embroidered metamaterial biosensor that can be integrated into a safety harness or vehicle seat belt for contactless monitoring of heartbeat and respiration in kinetic environments.[24] By guiding wireless signals along a textile metamaterial structure, the

system detected cardiopulmonary signals through near-field interactions with the body and maintained reliable heart rate and respiration tracking in both an airline cabin simulator and a moving car.

Electronic skin further expands wearable sensors from physiological monitoring toward tactile and multisensory intelligence for human–machine interaction.[35,36] Rather than simply measuring pressure, human skin integrates normal force, shear force, strain, temperature, texture, proximity cues and dynamic contact patterns to guide perception and action. Inspired by this biological function, electronic skins have developed from pressure-sensitive films into stretchable, conformal, and three-dimensional tactile architectures. Advanced electronic skins can emulate human mechanosensation by integrating skin-like sensor array for multimodal signal acquisition, and tactile interfaces capable of perceiving pressure, temperature, texture and slip for dexterous manipulation. Beyond multimodal sensing alone, Li et al. reported a metamaterial-based self-powered electronic skin that integrates conformal mechanics, shape-memory reconfigurability and multisensory perception.[21] By combining a 4D-printed mechanical metamaterial skeleton with electret–piezoelectric and carbon-nanotube sensing components, the device can detect deformation, pressure, vibration, and pre-contact distance signals while maintaining conformal attachment to curved and dynamic biological surfaces. Wireless electronic-skin systems for joint-motion monitoring, acoustic recognition, near-field sensing and contactless game control demonstrate the evolution of electronic skin from passive tactile sensing toward mechanically adaptive, self-powered and interaction-oriented human–machine interfaces. More recently, in-sensor tactile computing has further reduced the separation between sensing and processing, enabling tactile information to be interpreted closer to the sensor surface.

Gait monitoring and smart prosthetics further represent a key step in wearable intelligence, shifting from biomechanical monitoring toward closed-loop sensing, feedback and movement assistance.[37,38] The contact surface between the foot and the ground contains rich information about plantar pressure distribution, such as gait phase, load symmetry, pressure centre trajectory, and balance stability. However, these signals only realize their full value when they are aggregated through continuous acquisition, wireless transmission, and motion interpretation. For example, Kang et al. developed an additively manufactured 3D auxetic metamaterial tactile sensor for structurally guided capacitive and resistive sensing.[22] By using a negative-Poisson-ratio lattice to concentrate local deformation under compression, the sensor improved tactile sensitivity and was further integrated into a wearable insole system for real-time gait monitoring and pronation analysis. Similar distributed wireless sensing needs exist in the field of prosthetics, because pressure and temperature at the skin-prosthetic interface directly affect

comfort, tissue health, and the long-term use of the prosthesis. For example, Kwak et al. reported a wireless, battery-free multimodal sensor system for lower-limb prostheses that continuously measures pressure and temperature at multiple skin–prosthesis interface locations.[20] The system uses soft, thin sensors placed inside the socket, while external NFC/BLE modules wirelessly power the sensors and transmit data to portable electronic devices. By enabling continuous monitoring during prosthesis use, this platform links wearable sensing to socket fitting, residual-limb protection, and personalized prosthetic management.

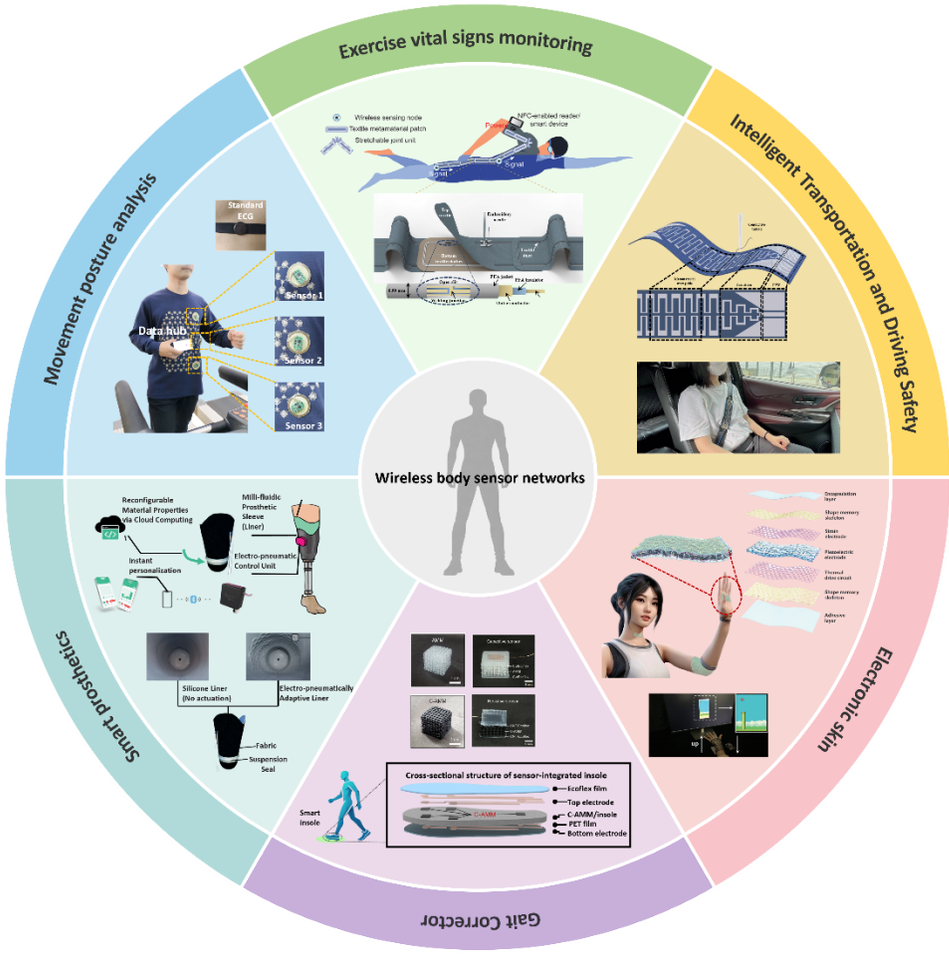


Figure 1. Applications of Wireless Body Sensor Networks. Movement posture analysis. Reprinted with permission.[25] Copyright 2026 Springer Nature. Exercise vital signs monitoring. Reprinted with permission.[23] Copyright 2024 Springer Nature. Intelligent transportation and driving safety. Reprinted with permission.[24] Copyright 2024 Springer Nature. Electronics skin. Reprinted with permission.[21] Copyright 2024 Wiley-VCH GmbH. Reprinted with permission.[22] Copyright 2025 Wiley-VCH GmbH. Smart prosthetics. Reprinted with permission.[20] Copyright 2020 AAAS.

In summary, these examples demonstrate that wearable sensors have evolved from isolated sensing components into networked systems for autonomous intelligence, shifting from local signal acquisition to collaborative perception and closed-loop assistance. Soft and conformal human-interface sensors should first enable the stable acquisition of distributed biomechanical,

physiological, tactile, and environmental signals. Second, various sensing nodes, such as those integrated with skin, clothing, footwear, seats and human–machine interfaces, can be connected through wireless body sensor networks to achieve synchronized data streams and multimodal information fusion. Therefore, in the future development of wearable sensors, sensing, wireless communication, embedded computing, energy management and feedback will need to be integrated into a continuous perception–interpretation–decision–action loop. Near computing and in-sensor computing are crucial because they allow raw tactile, motion and physiological signals to be processed close to the sensing interface, thereby reducing latency, energy consumption and privacy risks. Edge intelligence further empowers wearable systems by enabling them to recognize user intentions, predict abnormal states and generate personalized responses without relying entirely on remote cloud platforms.

This shift at the application level benefits from the parallel development of wearable sensing technologies, evolving from early, personalized electronic devices for physiological and motion monitoring to soft, skin-like, and textile-integrated systems capable of multimodal sensing. As wearable interfaces become increasingly bio-inspired, mechanically adaptive and computationally integrated, the field is moving toward tactile intelligence and in-sensor information processing. This technological progression is summarized in Figure 2. The early development of wearable electronics was closely associated with portable physiological monitoring and miniaturized sensing hardware. Early wearable electronics mainly focused on collecting physiological and biomechanical signals under mobile conditions, including cardiac, respiratory, motion, and pressure-related information.[39] Although these systems were often bulky, rigid, and dependent on external power or wired data transmission, they established the feasibility of continuous on-body sensing. During the same period, silicon micromachining and microelectromechanical systems (MEMS) provided a manufacturable route toward miniaturized pressure sensors, force sensors, accelerometers, and integrated inertial measurement units (IMUs).[40,41] By combining higher sensitivity with miniaturized and scalable device architectures, these sensors advanced tactile sensing from bulky, large, discrete components toward conformal wearable platforms for the applications of human motion monitoring, prosthetics and robotic control.

From the 1990s to the early 2000s, advances in flexible materials and micro/nanofabrication technologies began to transform wearable sensors from rigid monitoring devices into wearable, distributed platforms for a broad range of applications. Conductive polymers, thin-film electrodes, elastomeric substrates, and functional sensing layers allowed wearable sensors to move beyond rigid formats and conform to soft, curved, and deformable body interfaces.[42,43] This functional expansion further stimulated the development of large-

area tactile arrays and artificial mechanoreceptors, which aimed to mimic biological touch by converting pressure, vibration, deformation, and dynamic contact into distinguishable electrical signals. The advancement of these wearable technologies marked a transition from wearable electronics as monitoring tools toward bionic tactile interfaces that operate more intimately with the human body.

Since the 2010s, the development of wearable electronics has gradually shifted from flexible structural designs at the device level to integrated interfaces for long-term wear. In this stage, comfort, breathability, and mechanical stability have become as important as sensing performance. Functional fibers, due to their ability to be directly embedded in fabric structures, provide a viable approach to integrating wearable sensing elements, thereby improving the compatibility of devices in long-term use scenarios.[44,45] Meanwhile, epidermal electronics, through the introduction of ultra-thin, flexible, and stretchable structures, can be laminated more closely to the skin surface, reducing mechanical mismatch and motion artifacts.[46] Hydrogels and ionically conductive soft materials further expand the design space of wearable interfaces by providing tissue-like mechanical compliance, adhesion, stretchability and multimodal sensing capabilities, thereby supporting applications in health monitoring, rehabilitation assessment, motion analysis and immersive interaction.[47,48]

Between 2015 and 2020, the long-term operation of wearable tactile systems increasingly highlighted the importance of self-powered and energy-autonomous designs. Conventional wearable devices often rely on batteries, which restricts device lifetime, maintenance, and system scalability. To address these limitations, triboelectric, piezoelectric, thermoelectric, and textile-based energy harvesters have been explored to convert body motion, mechanical deformation, and thermal gradients into electrical energy.[49–51] The highly integrated systems can serve simultaneously as an energy harvester and a self-powered sensor, enabling autonomous sensing and communication. These developments provide a pathway toward sustainable wearable systems for long-term health monitoring, motion recognition, rehabilitation, and human–machine interaction. In addition, wearable sensor systems have entered a new era driven by artificial intelligence (AI), multimodal fusion, and closed-loop interaction.[52–54] At the same time, haptic feedback technologies have evolved from simple vibration modules toward multimodal, skin-conformal, and user-adaptive interfaces capable of delivering pressure, temperature, vibration, and electrotactile stimulation.[55–57] These advances have extended wearable tactile systems into interactive interfaces for AR/VR, teleoperation, rehabilitation, prosthetic control, and human–robot collaboration.[58,59] These emerging applications require tactile systems not only to detect force or deformation, but also to capture spatially resolved contact patterns, object geometry, slip, texture, and dynamic interaction

processes. By converting contact-induced deformation, marker displacement, optical reflection, or contact-dependent light transmission into camera-readable images, vision–tactile sensors can capture contact geometry, surface texture, slip, material stiffness, and multidimensional force information with high spatial resolution.[60,61] These sensors have been widely explored in robotic fingertips, soft grippers, prosthetic hands, surgical robots, and teleoperated systems.[62,63]

From 2020 onward, the future of wearable sensor systems is increasingly developed from passive interconnect fabrics toward multifunctional, self-adaptive, and edge computing platforms.[64–66] Conventional wearable systems often wireless transmit the sensor data to external processors or cloud platforms for analysis, leading to latency, energy consumption, bandwidth burden, and privacy concerns. Near-sensor/ in-sensor computing technologies aims to move feature extraction, signal processing, and inference functions closer to the sensing unit, while edge computing enables local decision-making, reducing reliance on remote computing.[67–69] For example, Li et al. developed a bio-inspired flexible spiking sensory neuron based on a high-performance VO_2 memristor for wearable human–machine interfaces.[70] The flexible VO_2 memristor, fabricated at 280 °C with a Cr_2O_3 buffer layer, exhibited forming-free threshold switching, ultrahigh endurance (>10^{12} cycles), low cycle-to-cycle and device-to-device variations, fast response (<30 ns), and excellent flexibility with bending down to a 1 mm radius. By coupling the temperature-sensitive VO_2 memristor with a flexible piezoresistive pressure sensor, the crossmodal spiking sensory neuron could synchronously encode pressure and temperature stimuli into spike signals with different frequencies and amplitudes, enabling local multimodal fusion without complex external conversion circuits.

In this review, we summarize recent advances in wearable systems and explores their evolution toward autonomous intelligence. First, it reviews advanced hydrogel-based wearable sensors and their applications in smart insoles, as well as MEMS-based tactile sensing and their applications in surgical and robotic platforms. Second, self-powered wearable sensors and systems are discussed, with emphasis on metamaterial-based wireless body sensor networks, functional fibers, wearable energy harvesters, and textile-based energy-harvesting platforms. Third, future directions toward autonomous intelligence are highlighted, including wearable haptic feedback interfaces, vision–tactile sensing for robotic perception, AI-enhanced wearable systems, and near-sensor, in-sensor and edge computing. These advancements collectively form the core theme of this paper: wearable haptic systems are evolving from flexible sensing interfaces into autonomous network platforms that integrate sensing, communication, energy management, computing, feedback, and actuation functions, with the aim of enabling human-cantered assistance and machine interaction.

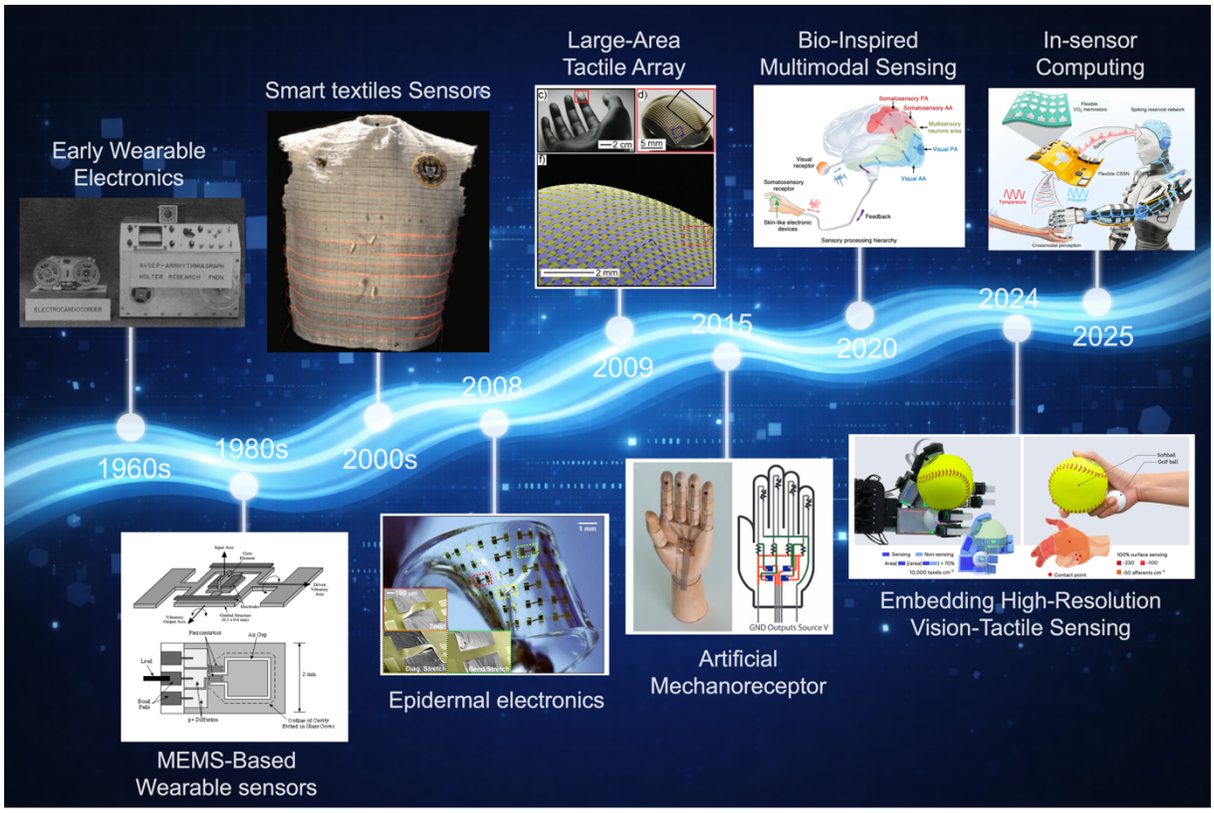


Figure 2. Evolution of wearable sensing technologies from early body-mounted electronics to bio-inspired tactile intelligence and in-sensor computing. The timeline summarizes representative milestones in wearable and tactile sensing technologies. Early wearable electronics began with body-mounted physiological monitoring systems such as the Holter electrocardiographic recorder in the 1960s. Reproduced with permission.[39] Copyright 1961, AAAS. In the following decades, MEMS-based wearable and inertial sensors, including silicon micromechanical gyroscopes and batch-fabricated silicon accelerometers, introduced miniaturized suspended structures, integrated electrodes, and piezoresistive readout for motion sensing. Reproduced with permission.[4,6] Copyright 1991 and 1979, IEEE. Smart textile sensors then enabled garment-integrated physiological monitoring through conductive textile pathways and embedded sensing elements. Reproduced with permission.[40] Copyright 1999, Springer Nature. Epidermal electronics further advanced skin-conformal bio interfaces using ultrathin, stretchable, and flexible circuit platforms for intimate physiological signal acquisition. Reproduced with permission.[42] Copyright 2008, National Academy of Sciences. Large-area tactile arrays expanded wearable sensing toward spatially distributed pressure and touch mapping on curved and deformable surfaces. Reproduced with permission.[43] Copyright 2009 Wiley-VCH Verlag GmbH & Co. KGaA, Weinheim. Artificial mechanoreceptors integrated flexible pressure sensors with organic electronic circuits to convert mechanical stimuli into digital neural-like signals. Reproduced with permission.[46] Copyright 2015, AAAS. Bio-inspired multimodal sensing systems subsequently combined visual and somatosensory information from skin-like stretchable sensors for learning-enabled gesture recognition. Reproduced with permission.[61] Copyright 2020, Springer Nature. More recently, high-resolution vision–tactile sensing has been embedded across robotic hands to support adaptive, human-like grasping and contact-rich manipulation. Reproduced with permission.[60] Copyright 2025, Springer Nature. In-sensor computing systems further integrate multimodal sensing, memory, and computation within flexible neuromorphic devices, enabling real-time perception and edge intelligence for future wearable and robotic systems. Reproduced with permission.[70] Copyright 2024, Springer Nature.

2. Advanced wearable sensors and applications

Advanced wearable sensors have been widely developed to capture tactile, biomechanical, physiological, and environmental information from the human body and its surrounding interfaces. By integrating soft materials, flexible substrates, microfabricated sensing elements, and intelligent signal processing, these systems enable continuous and conformal monitoring in applications ranging from healthcare and rehabilitation to human–machine interaction, robotics, and surgical assistance. Representative advances in hydrogel-based wearable sensing, MEMS-based tactile sensors, and the applications for wearable gait analysis and surgical robots are highlighted in this section.

2.1 Hydrogel-based wearable sensing

Driven by their intrinsic hydration, mechanical compliance, mixed ionic/electronic conductivity, and tissue-conformal compatibility, soft hydrogel-based tactile interfaces have become pivotal platforms for digital twins, biomimetic perception, human–machine interfaces (HMIs), and wearable healthcare. These applications demand high-fidelity signal transduction and robust decoding capabilities at the material-tissue interface. Current research focuses on engineering hydrogel tactile devices with tailored physical attributes and output modalities via functional doping, hybrid network architectures, and surface encapsulation. For example, coating PAAm hydrogels with an adaptive lipid bilayer (Figure 3a(i)) creates a biomimetic barrier that significantly enhances water retention.[71] The dynamic reorganization of lipid aggregates effectively seals deformation-induced microcracks, thereby improving dehydration resistance and self-healing behavior to ensure stable long-term signal fidelity. Similarly, supramolecular Fmoc-FF hydrogels in electronic skins (Figure 3a(ii)) demonstrate a functional stratification: the biodegradable upper network acts as a protective isolation layer,[72] while the lower network, doped with conductive agents like PEDOT: PSS, constitutes the primary sensing element. Coupled with adhesive designs, these systems address the rigorous skin-lamination requirements essential for wearable monitoring.

Furthermore, hydrogels utilize energy harvesting mechanisms for multimodal self-powered sensing (Figure 3a(iii)).[73] By incorporating reversible redox couples $\left(I^{-}/I_{3}^{-}\right)$, thermogalvanic hydrogels exploit thermal gradients between the human body and the environment to generate voltage or current, facilitating simultaneous strain and temperature monitoring. Concurrently, composite networks such as PVA–betaine offer a critical balance between stretchability, environmental stability (anti-freezing/drying), and biocompatibility. These interfacial engineering strategies collectively boost output magnitude and operational reliability, establishing a foundation for system-level integration.

In the context of digital twins, sensors leveraging ion migration and ion–polymer interactions (Figure 3b) achieve ultrasensitive multi-degree-of-freedom (multi-DoF) sensing by translating mechanical deformation into distinct potential signals.[74] Specifically, resolving wrist motions along X/Y axes facilitates online action mapping and virtual–physical synchronization. For biomimetic perception, piezoionic devices (Figure 3c) modulate ion transport via microscopic porosity and phase blending.[75] This mechanism enhances electrical response and permits frequency-dependent vibration perception, alongside stimuli-responsive functionalities like temperature sensing. Transcending simple sensing, a single-pixel neuromorphic unit (Figure 3d) integrating a transient voltage artificial neuron (TVAN) with a sustained potential artificial neuron (SPAN) capture both high-frequency transient cues (vibration, texture) and quasi-static signals (pressure).[76] This multimodal encoding supports "liveness" detection in fingerprint-like authentication by embedding process-dependent tactile signatures.

Regarding HMIs (Figure 3e), modulating interfacial charge dynamics and ion-transport kinetics in $Ti_3C_2T_x$ MXene-assisted gradient porous foams yield high-sensitivity tactile inputs.[77] Integration into smart gloves allows the translation of hand gestures into machine commands (e.g., robotic navigation) via wireless transmission and pattern recognition, demonstrating a closed-loop material-to-system workflow. In wearable healthcare, hydrogel sensors featuring instantaneous self-recovery and ultralow detection limits (Figure 3f),[78] when paired with LSTM sequence models, effectively classify subtle jaw deformations for temporomandibular disorder (TMD) diagnosis. Finally, bioadhesive hydrogel couplers for miniaturized ultrasound systems (Figure 3g) resolve issues of dehydration and slippage typical of conventional gels.[79] This interface ensures stable acoustic coupling for prolonged focused ultrasound (FUS) neuromodulation, as evidenced by electrophysiological suppression effects.

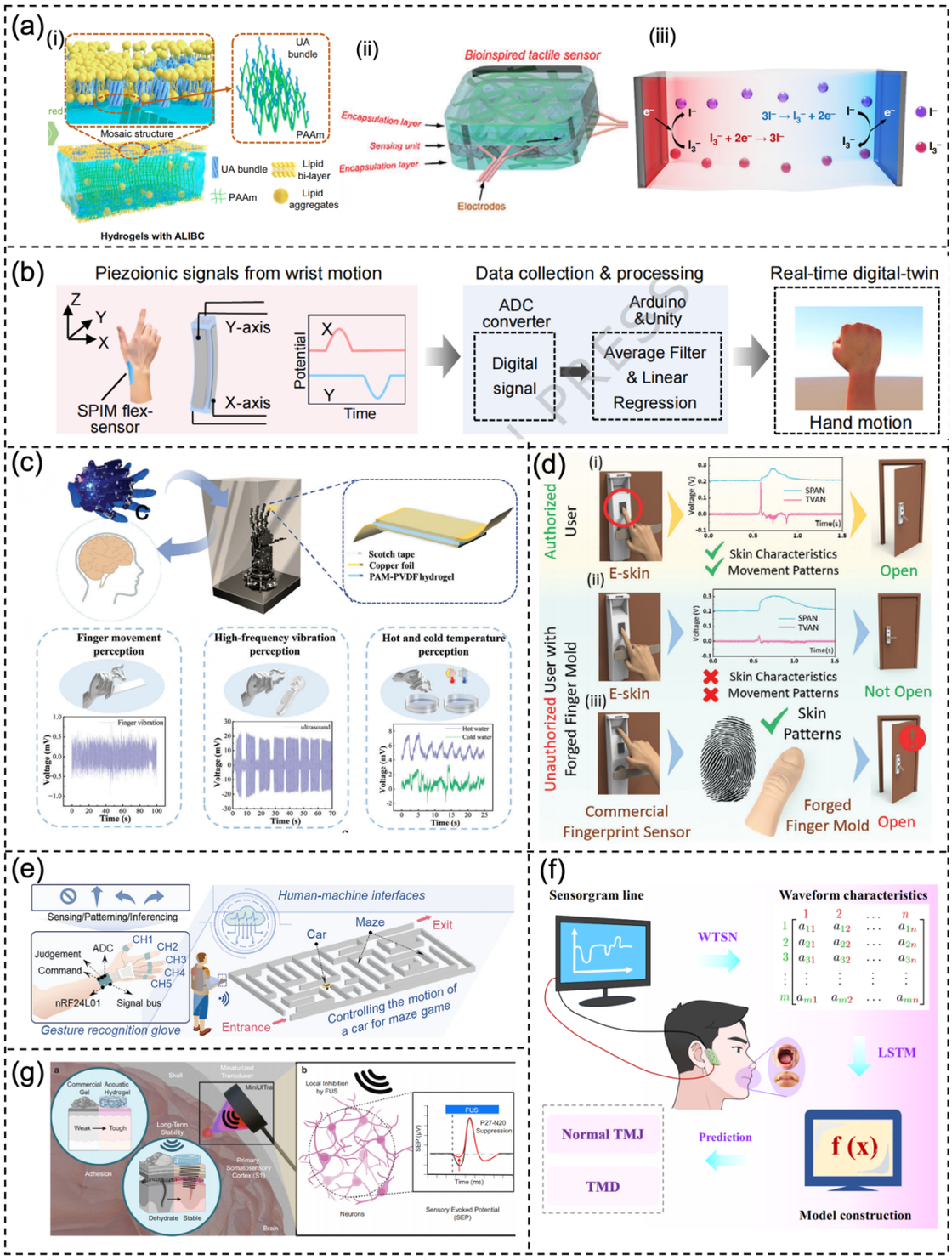


Figure 3. Hydrogel-based wearable sensing. (a) Hydrogel interface engineering: (i) ALIBC-coated PAAm for anti-dehydration and stable output. Reprinted with permission.[71] Copyright 2024 Springer Nature. (ii) Fmoc-FF/PEDOT:PSS e-skin with encapsulation-sensing layers. Reprinted with permission.[72] Copyright 2024 Wiley-VCH GmbH. (iii) I-/I3- thermogalvanic hydrogel for self-powered temperature-strain sensing. Reprinted with permission.[73] Copyright 2024 Springer Nature. (b) Piezoionic wrist-motion sensing and lightweight processing enable real-time digital-twin motion mapping. Reprinted with permission.[74] Copyright 2025 Springer Nature. (c) PAM-PVDF piezoionic hydrogel for multimodal perception: finger motion, ultrasound vibration, and hot/cold discrimination. Reprinted with permission.[75] Copyright 2024 Wiley-VCH GmbH. (d) TVAN+SPAN neuromorphic e-skin enhances touch awareness and anti-spoofing against forged fingers. Reprinted with permission.[76] Copyright 2024 Wiley-

VCH GmbH. (e) MXene-assisted gradient porous foam hydrogel glove for gesture recognition and wireless command control. Reprinted with permission.[77] Copyright 2025 Wiley-VCH GmbH. (f) Hydrogel sensor + LSTM time-series decoding for intelligent TMD diagnosis (normal TMJ vs TMD). Reprinted with permission.[78] Copyright 2025 Springer Nature. (g) Bio-adhesive hydrogel acoustic coupling enables long-term wearable FUS neuromodulation (SEP suppression). Reprinted with permission.[79] Copyright 2025 Springer Nature.

2.2 Wearable insole based on flexible substrate

Plantar monitoring has attracted increasing attention because the plantar region is one of the most informative interfaces of the human body.[80–83] The foot can provide rich biomechanical information, such as plantar pressure distribution, gait characteristics, and balance status, while also reflecting physiological conditions through temperature and biomarkers in sweat.[84–86] Consequently, wearable sensing systems based on insoles and socks have been rapidly developed in recent years.[87–89] Flexible materials such as textiles, hydrogels, and polymers have been widely adopted in these systems to meet the requirements of comfort, flexibility, and stable signal acquisition during long-term use.[90–96] These advantages have supported the growing use of wearable insoles/socks systems in applications such as human activities monitoring, gait analysis, sports training, rehabilitation assessment, and early disease warning.[97–99] As shown in Figure 4a, Y. Luo et al. propose a textile-based sock using a conductive stainless-steel thread coated with a piezoresistive nanocomposite composed of a polydimethylsiloxane (PDMS) elastomer matrix and graphite/copper nanoparticles as conductive fillers, which is applied to record and learn human–environment interactions.[99] A machine-learning-based self-supervised sensing-correction strategy was developed to enable robust sensing. In this approach, spatial–temporal contextual information was leveraged to normalize sensing responses, compensate for sensor variations, and correct malfunctioning sensors. Building on this reliable sensing capability, the system further combined plantar pressure distribution over time from tactile socks with machine-learning analysis, achieving human pose estimation. Gait information can not only characterize human daily activities but also reveal disease-related abnormalities and support clinical assessment. S. Hu et al. proposed a self-powered insole with four single-electrode-mode triboelectric nanogenerator (TENG) sensing units positioned at the first metatarsal head, fifth metatarsal head, midfoot, and heel (Figure 4b).[86] Each sensing unit consisted of a PDMS upper layer featuring an inverted-cone structure to enlarge the measurement range and a hemispherical bump on the top surface for load detection, together with an MXene/PDMS lower layer containing a central pillar and surrounding wall to enhance the electrical output. With this configuration, normal and shear plantar stress could be decoupled based on the asymmetrical outputs of the TENG units. Six gait patterns associated with different disease conditions, including regular gait, hemiplegic gait,

myopathic gait, antalgic gait, parkinsonian gait, and neuropathic gait, were detected and classified using a convolutional neural network, demonstrating the potential of the system for disease diagnosis. In addition to PDMS, hydrogel has attracted increasing interest in recent years due to its flexibility, stretchability, softness, and biocompatibility, making them promising material for wearable sensors.[98,100–102]

D. Han et al. proposed a self-powered smart insole integrating four single-electrode gel-TENG units, enabling human motion monitoring in low-temperature environments (Figure 4c).[102] A dual-network conductive gel with skin-adaptive modulus, ionic conductivity, mechanical stability and antifreezing capability, was used as the electrode and embedded within the silicone rubber layer. The smart insole achieved real-time visualization of plantar pressure distribution and successfully recognized 11 basic skiing motions with a classification accuracy of 97.1%, demonstrating its promise for intelligent activity monitoring in extreme environments. L. Song proposed an insole based on the phytic acid-induced gradient ionic hydrogel for highly sensitive, wide-range pressure monitoring (≈ 3.7 Pa to 1.2 MPa) (Figure 4d).[103] Each insole consisted of 12 sensing units, integrating the gradient ionic hydrogel and copper foil electrodes on a flexible polyimide substrate. Benefiting from the gradient structure, the insole enabled accurate monitoring of both static and dynamic plantar pressure distributions. Specifically, it could clearly distinguish different standing postures and capture pressure heat maps throughout continuous walking, demonstrating strong potential for gait analysis and human activity monitoring.

Disease monitoring and rehabilitation training have attracted increasing attention as important application areas of plantar pressure sensing. R. Xu et al. reported a hydrogel-based balance training carpet inspired with the unique sensory organ of a crocodile (Figure 4e).[101] Dome-shaped polyacrylamide-lithium chloride ionic hydrogel together with conductive knitted fabric was used to construct the iontronic meta-fabric. Based on a high-resolution 40 × 40 tactile sensing arrays, the system enabled real-time visualization of plantar pressure distributions during posture shifts and gait cycles, thereby allowing real-time assessment of motor stability, which improved efficiency of rehabilitation training.

Plantar sensing systems are increasingly being extended to sports monitoring, posture correction, and personalized exercise guidance. L. Wang et al. presented an AI-enhanced insole sensing system based on the multifunctional polyvinyl alcohol/ polyacrylamide/ lithium chloride/ glycerol ionic hydrogel for simultaneously monitoring of plantar pressure, temperature and sweat (Figure 4f).[104] Beyond gait phase detection and daily activity monitoring, the system was further applied to yoga training to demonstrate both static and dynamic detection. By integrating machine learning algorithms with embedded haptic feedback

units, the system established a virtual yoga coach avatar for yoga posture recognition, imbalance detection, and posture correction. In addition, personalized posture guidance were generated for different users by integrating random forest algorithms trained on centre-of-pressure (COP) stability data. This work offers users an immersive, face-to-face-like training experience with a virtual yoga coach, demonstrating a next-generation intelligent insole platform for interactive training.

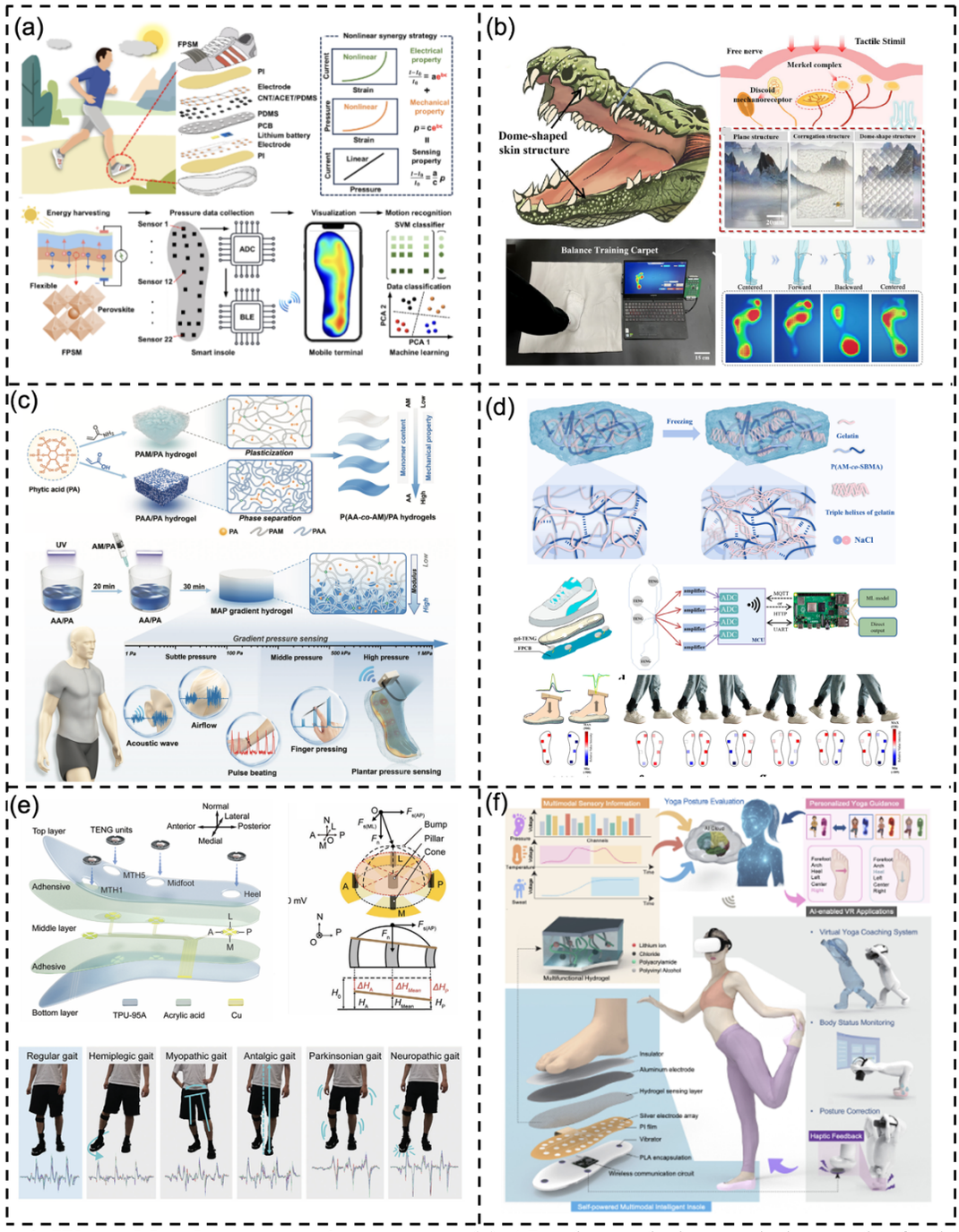


Figure 4. Wearable plantar sensing system. (a) AI-enhanced piezoresistive socks for human pose estimation. Reprinted with permission.[86] Copyright 2021 Springer Nature. (b) A self-powered triboelectric insole sensing system for disease diagnosis. Reprinted with permission.[99] Copyright 2024 Wiley-VCH GmbH. (c) A gel-TENG-based insole sensor for low-temperature environments monitoring. Reprinted with permission. [102] Copyright 2025

Wiley-VCH GmbH. (d) A gradient ionic hydrogel-based insole sensor for wide-range pressure detection. Reprinted with permission.[103] Copyright 2025 Wiley-VCH GmbH. (e) An ionic hydrogel-based carpet for rehabilitation training. Reprinted with permission.[101] Copyright 2024 Springer Nature. (f) AI-enhanced smart insole sensing system based on multifunctional hydrogel for yoga training. Reprinted with permission.[104] Copyright 2025 Wiley-VCH GmbH.

2.3 MEMS-based tactile sensing

Compared with flexible tactile sensors, MEMS technology-based tactile sensors have unique features like scalability, miniature size and high sensitivity. The great scalability and miniature size are attributed to the mature microelectronic fabrication processes, making monolithic integration possible.[105] On the other hand, some elastic or composite materials used in flexible tactile sensors are incompatible with photolithography/etching processes, limiting the form factor of flexible sensors. In order to enhance the sensitivity, microstructures are extensively investigated.[106] The transduction efficiency is increased by methods like stress concentration. Moreover, microstructures also play an important role in decoupling multiple external stimuli,[107,108] enabling multimodal sensing for MEMS-based tactile sensors.

For MEMS-based tactile sensing, decoupled multimodal sensing with a relatively large dynamic range can be challenging. As a proof of concept, Won et al. reported a three-dimensional (3D) tactile sensor, which can measure pressure, shear force, bending strain and temperature (not fully decoupled), based on monocrystalline silicon nanomembranes (Figure 5a).[109] The 3D microstructures are fabricated by bonding two-dimensional planar precursors to pre-stretched silicone substrate and compressive 3D buckling induces the final microstructures. By measuring the output difference of four piezoresistive sensing elements located on four pillars, in-plane and out-of-plane mechanical deformations can be separated. However, changes in temperature cannot be decoupled from normal force loading. This sensor design can be easily extended to a sensor array, generating a 7 * 7 pressure map with a spatial resolution of 2 mm.

The 3D buckling structures successfully capture in-plane stimuli but the fabrication process is complex and the delicate structures constrain the device to achieve higher spatial resolution. To further improve the spatial resolution and the scalability, a large-scale and multiplexed MEMS tactile sensor array (Figure 5b) is introduced by Oh et al., which can be employed to facilitate closed-loop robot control.[110] The sensing pixel is made of dual-gate piezoelectric zinc oxide (ZnO) thin-film transistors (TFTs). When force is exerted to the surface of a TFT, the channel deforms, resulting in changes in source-drain current. Furthermore, due to the dual-gate configuration, by biasing the gate voltage, the output of a single TFT can be easily switched on/off. Therefore, multiplexing is achieved intrinsically by tuning gate voltages of TFTs. In addition to normal force sensing, shear force sensing is enabled by encapsulating

TFT array with 3D PDMS pump array, which can transduce shear force to normal force. The high spatial resolution and the low latency of the system are demonstrated by a robot grip experiment, where the robot can adjust the grip force in real time based on the detected shear force to prevent slip.

Apart from piezoelectric transistor technologies, capacitive sensors are suitable for fabricating high spatial resolution, large scale tactile sensing array as well. Weichart et al. introduced a capacity-based tactile sensor array with large measurement range and large scale (up to 12*12 individually addressable sensing pixels, Figure 5c).[111] The flexible substrate, which consists of metal interconnects and polyimide (PI), is fabricated by redistribution layer (RDL) technologies. The top of the substrate, soldering bumpers and suspended membranes are constructed. The sensitivity of the sensor can be divided into two stages: when small force is applied on the bumper, the deformation of the suspended membrane yields high sensitivity; when large force is applied, the membrane touches the PI stopper and the deformation of the stopper results in large measurement range but low sensitivity.

For piezoresistive tactile sensors, temperature changes may affect the accuracy of the sensing pixels since the resistance will also change because of the thermal expansion and the temperature coefficient of resistance (TCR). To handle this issue, Xu et al. proposed a flexible, piezoresistive sensor array with temperature sensing and calibration functionality (Figure 5d).[112] In each sensing pixel, there are four bending-up cantilevers that serve as micro strain gauges. The delicate 3D structures are constructed by releasing the pre-compressed silicon oxide layer after the sacrificial layer is etched away. The four cantilevers are made of nickel chromium alloy and can capture normal and shear force. Beneath the cantilevers, there is the temperature sensing module, which is barely affected by exerted force and thus the resistance change of this module is solely affected by temperature changes. The system can effectively measure 3D forces and temperature changes and is insensitive to bending and stretching, as is illustrated in applications like wearable sensing patch.

For tactile sensing, accomplishing high sensitivity while maintaining broad linearity range remains elusive. Wang et al. offered a potential solution by devising a bio-inspired piezoresistive tactile sensor (Figure 5e).[113] The sensor follows the conventional Wheatstone bridge configuration while cavities (the so-called stress traps) are created around the piezoresistors to enhance the energy influx efficiency for better sensitivity. In addition, flexure suppression units are made to constrain large deformation of the membranes and reduce the nonlinear internal friction, in order to increase the linearity range. The tactile sensor can not only measure pressure but also classify airflows, distinguishing laminar, transitional and

turbulent flows. Combined with wavelet analysis and neural networks, the sensor is able to identify approaching objects with different shapes.

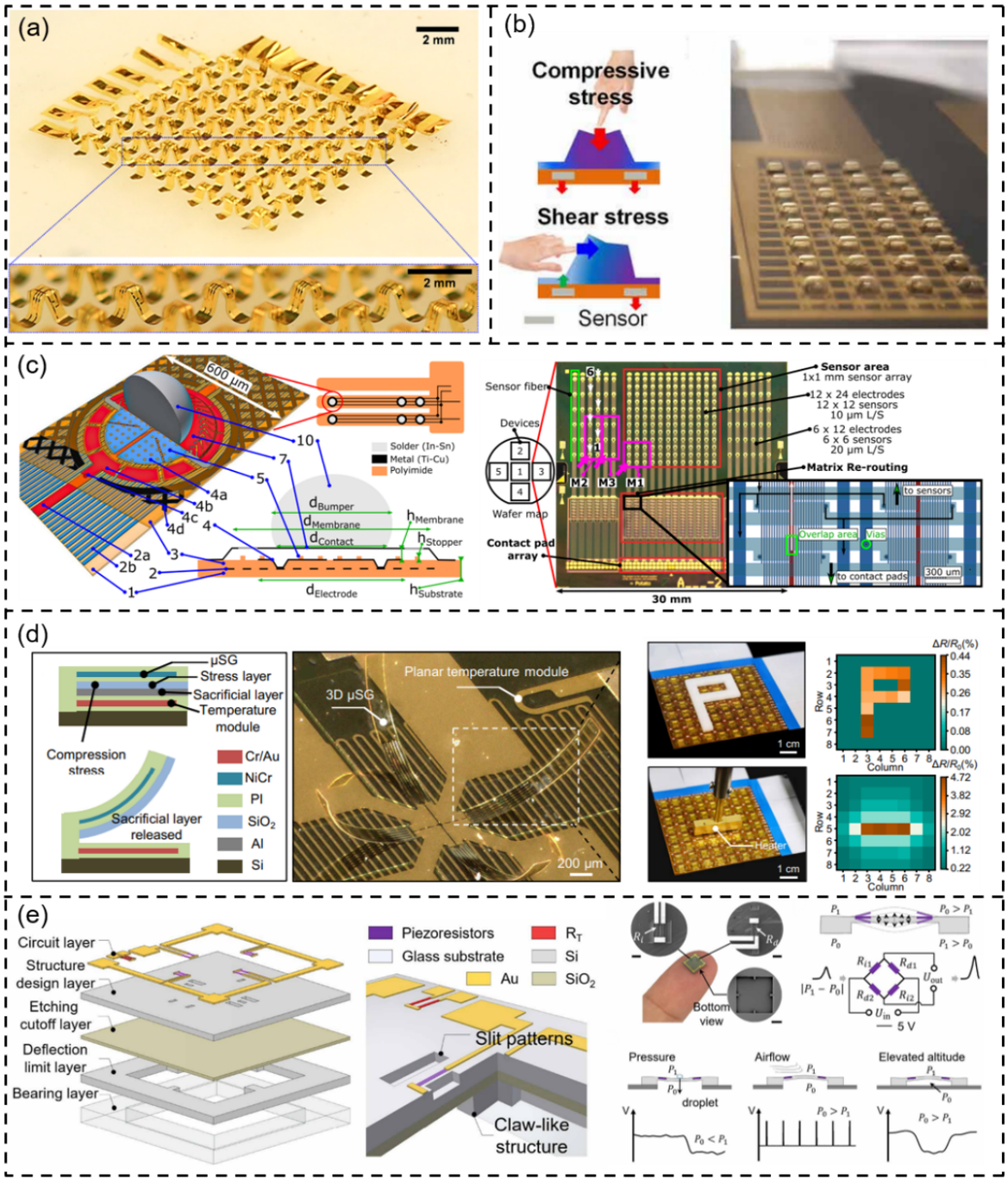


Figure 5. Microelectromechanical system technology-based tactile sensors. (a) A multimodal tactile sensor with three-dimensional structures. Reprinted with permission.[109] Copyright 2019 The American Chemical Society. (b) A large-scale, multiplexed tactile sensor based on thin-film transistors. Reprinted with permission. [110] Copyright 2020 The American Association for the Advancement of Science (AAAS). (c) A large-scale capacitive sensor array with large measurement range. Reprinted with permission.[111] Copyright 2021 IEEE. (d) A flexible piezoresistive sensor array with temperature sensing functionality. Reprinted with permission.[112] Copyright 2024 The American Association for the Advancement of Science. (e) A bio-inspired piezoresistive sensor with high sensitivity and broad linear range. Reprinted with permission.[113] Copyright 2025 AAAS.

2.4 Tactile sensing in surgical robots

Robot-assisted minimally invasive surgery (RMIS) is gaining more attention due to its advantages over traditional surgery, such as minimized trauma, fast recovery time, etc. Despite the benefits, however, RMIS usually requires teleoperation, and this prevents surgeons having accurate tactile sensations on tissues.[114] The lack of touch-based sensations has become a severe issue for RMIS since surgeons may exert excessive force on the operating tissue.[115] One promising solution is tactile sensors, which can be seamlessly integrated into surgical robots.[116] Tactile sensors can not only notify surgeons once excessive force/strain is exerted but also restore intuitive tactile sensations for surgeons in combination of haptic feedback interfaces.[117] In addition to features like miniature size and high sensitivity, recent progress in fabrication process, system integration and materials has endowed tactile sensors with modular design, arrayed and multimodal sensing and synergistic sensing-actuation ability.

For system integration, extremely low thickness makes it easy to attach tactile sensors to the surface of surgical robots. To this end, Aubeeluck et al. reported a screen-printed, ultra-thin resistive tactile sensor for endoscopic surgery (Figure 6a).[118] The sensor achieves a thickness of 110 μm and an area of 9 mm², enabling facile attachment to magnetically actuated microgrippers. Protected by polyimide encapsulation, the piezoresistive layer is screen-printed by the ink of multi-walled carbon nanotubes (MWCNTs) and thermoplastic polyurethane (TPU) composites. The piezoresistive layer and the silver interdigitated electrode are separated by the spacer layer, which is fabricated by printable silicone ink. The form factor of the spacer layer is optimized to eliminate unwanted actuation, increase sensitivity and maintain a low minimum detectable force. When force is exerted on the sensing unit, the change of contact area, together with the deformation of the piezoresistive layer, contributes to the resistance change. This tactile sensor exhibits three sensitivity modes, accomplishing an appropriate trade-off between the sensitivity and the sensing range. It provides a low-cost solution of ultra-thin tactile sensors with easy integration to surgical robots.

Compared to single-axis force sensing, 3D force sensing is preferred to better facilitate the dexterous control of surgical instruments.[119] Addressing this need, Hou et al. proposed a miniaturized 3D piezoresistive tactile sensor, which can be easily integrated to palpation probes or forceps, based on microelectromechanical system (MEMS) technology (Figure 6b).[120] The novel modular design renders the sensor with adjustable sensitivity and sensing range, making it suitable for versatile surgical tasks. Specifically, the core sensing chip with four piezoresistive cantilevers is capped with an encapsulation layer and a replaceable elastic layer. By changing the thickness and the Young's modulus of the elastic layer, sensitivity and sensing range can be tuned – high sensitivity and small sensing range are achieved by increasing the thickness and

reducing the Young's modulus and vice versa. This flexibility renders the sensor suitable for tasks requiring high sensitivity (like palpation) as well as tasks requiring large sensing range (like needle holding). The sensing output, however, is not in linear relationship with the exerted force and a neural network is trained and deployed to decouple the nonlinearity.

For tasks like tumor resection, high spatial resolution of tactile sensing is desired to accurately identify the boundary between tumor and healthy tissues. Tactile sensor array could be a good solution, but it suffers from large crosstalk among its sensing pixels. Li et al. attempted to handle this limitation by fabricating a flexible pressure sensor array with high spatial resolution and extremely low crosstalk by laser manufacturing (Figure 6c).[121] The piezoresistive tactile sensor array is prepared by a two-step laser process. Firstly, isolated piezoresistive sensing pixels made of graphene are generated by low power lasers. High power lasers are applied later to cut through the active and substrate layers, leaving interconnects between sensing pixels. By applying the theory of cantilevers, interconnects with serpentine shape are preferred, as they can not only reduce the crosstalk between pixels, but also increase the flexibility of the array, making it conformal to soft surfaces. When mounted on a Da Vinci surgical robot, this pressure sensor array successfully identifies the boundary between the dummy tumor and the normal issues.

In RMIS, direct contact sensing may not be suitable for some delicate tissues, in which case, proximity sensing can be beneficial. Meanwhile, in such situations, surgeons may still damage delicate tissues because there is no intuitive feedback from the tactile sensing component. To enhance the safety of RMIS, Li et al. introduced an assistive system consisting of a full-range proximity-tactile sensor with multimodal sensing ability and an intuitive haptic feedback interface (Figure 6d).[122] The system is composed of an ultrasonic sensor based on piezoelectric micromachined ultrasonic transducers (PMUTs) for long-range proximity sensing, a capacitive sensor for short-range proximity sensing and a triboelectric sensor for direct tactile sensing. Combined with timely vibrotactile feedback offered by a wristband, this highly integrated system ensures the surgeon to perceive approaching contact before any physical interaction occurs. Furthermore, since abnormal tissues exhibit different ultrasound echoes due to their different acoustic impedance and adsorption properties compared with normal tissues, abnormal tissues can be recognized with the help of convolutional neural networks.

Considering the limitation of form factors for surgical robots, sensors with both sensing and actuation capabilities are preferred over conventional sensors since the system does not require external actuators and can be more compact. Following this direction, Li et al. reported a bio-inspired tactile gripper-on-a-fiber (TGoF) system with synergistic sensing and actuation capabilities (Figure 6e).[123] The whole system is fabricated on the tip of a single-mode fiber

(SMF), consisting of a wave spring, a planar reflector with a scattering cone and a pH responsive gripper for actuation. The wave spring and the planar reflector together serve as a Fabry-Perot interferences sensor – when the reflector moves, the cavity length changes and based on the evolution of the interference spectra, the movement can be recognized. With respect to the gripper actuation, bovine serum albumin (BSA) is added as pH responsive muscles. When the pH value diverts from the isoelectric point, the electrostatic repulsion will induce expansion of the BSA muscles, pushing the two arms of the gripper to each other. As a demonstration, replaceable probes are installed on the gripper, and the system is used to measure the Young's modulus of zebrafish zygotes. Although for this system, only single-axis tactile information can be captured, it does illustrate the potential for synergistic sensing and actuation systems to be applied in surgical robots.

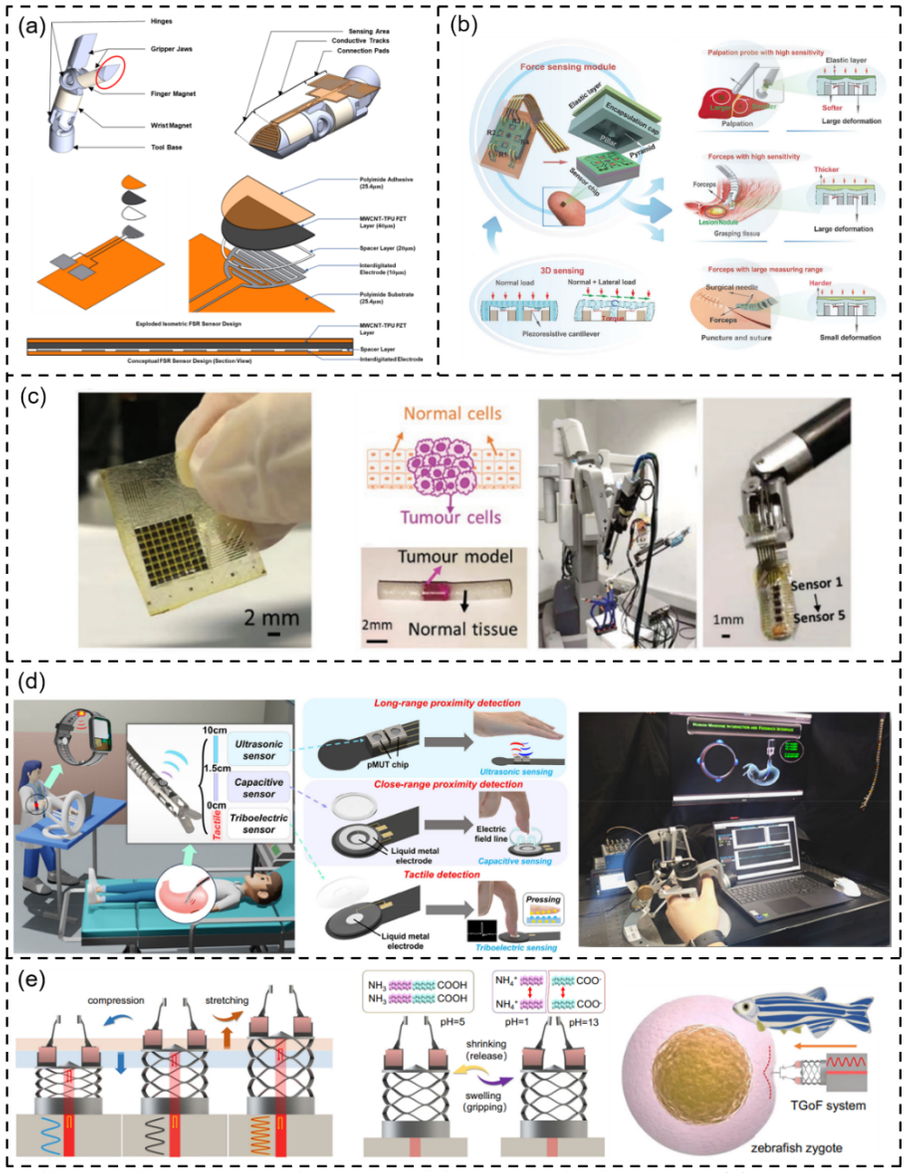


Figure 6. Tactile sensing systems integrated into surgical robots. (a) A screen-printed, ultra-thin piezoresistive tactile sensor for endoscopic surgery. Reprinted with permission.[118] Copyright 2023 The American Chemical Society. (b) A miniaturized three-dimensional tactile

sensor with modular design. Reprinted with permission.[120] Copyright 2023 Wiley-VCH GmbH. (c) A resistive tactile sensor array with high spatial resolution and low crosstalk. Reprinted with permission.[121] Copyright 2022 Wiley-VCH GmbH. (d) An assistive surgical system with full-range proximity-tactile sensing and haptic feedback ability. Reprinted with permission.[122] Copyright 2025 Wiley-VCH GmbH. (e) A bio-inspired tactile gripper-on-a-fiber system featuring synergistic sensing and actuation. Reprinted with permission.[123] Copyright 2025 Springer Nature.

3. Self-powered wearable sensors and systems

Recent progress in wearable electronics has increasingly shifted the field from externally powered sensing devices toward self-sustained systems that integrate sensing, energy harvesting, wireless communication, and intelligent data analysis. For long-term and continuous on-body operation, wearable sensors must not only maintain mechanical softness, comfort, and signal stability, but also address the limitations imposed by batteries, wired connections, and frequent recharging. Self-powered and energy-harvesting technologies therefore provide an important pathway for improving the autonomy, durability, and practical usability of wearable systems. In this section, we summarize representative advances in metamaterial-based wireless body sensor networks, functional fibers, wearable energy harvesters, and textile-based energy-harvesting platforms. Together, these studies demonstrate how energy-related design strategies can support next-generation wearable systems with improved wireless connectivity, self-powered operation, and intelligent human-centered applications.

3.1 Wireless body sensor networks based on metamaterial

WBSNs constitute a foundational layer of next-generation wearable intelligence, enabling distributed monitoring of physiological and biomechanical signals across the human body.[124–126] By interconnecting sensors that capture cardiopulmonary activity, motion dynamics, pressure distribution, and environmental interaction, WBSNs can evolve from isolated "single-point" measurements into spatially coordinated perception and feedback.[127,128] Yet, even as sensing front-ends and low-power electronics mature, the scalability and robustness of WBSNs remain fundamentally constrained by their electromagnetic architecture.[129–131] Conventional body-area networks typically rely on far-field radiative transmission, where each node behaves as an independent emitter. In this setting, the human body presents a high-permittivity, finitely conductive environment that amplifies absorption and impedance mismatch, while also promoting radiation leakage and multipath scattering. As node density rises and the body moves, radiative interference intensifies, spectral stability becomes difficult to maintain, and energy efficiency deteriorates. The practical bottleneck therefore shifts from "what can we sense" to

"how can we route signals and energy across the body in a mechanically compatible, electromagnetically controlled manner."

Metamaterials provide a route to reframe this bottleneck as a solvable architectural problem rather than an unavoidable propagation penalty. Unlike conventional materials whose electromagnetic response is determined predominantly by intrinsic composition, metamaterials derive their effective permittivity, permeability, and dispersion characteristics from deliberately engineered subwavelength architectures. By structuring periodic or resonant unit cells, the dispersion relation of electromagnetic waves can be tailored beyond natural constraints, enabling propagation constants to shift beyond the light line and supporting bound modes confined near the body surface.[132–134] In this regime, electromagnetic energy is no longer emitted isotropically into free space but propagates as surface-bound or guided modes with exponentially decaying fields away from the interface. This dispersion-engineered confinement suppresses radiation loss, minimizes tissue absorption, and establishes a spatially localized communication channel that is intrinsically resistant to environmental interference and external interception.

For example, Tian et al. proposed a method utilizing metamaterial textiles to construct spoof surface plasmon waveguides on the body surface. By structuring these textiles at a subwavelength scale, they convert wireless signals from implanted devices into surface waves that propagate along the body's contour, thereby bypassing the absorption and reflection of radio-frequency signals by biological tissues. This enables direct, low-loss wireless networking between implantable devices (Figure 7a).[135] Their work highlights the significant potential of metamaterials in enabling robust communication for WBSNs. Building on this, to further address the degradation of electromagnetic performance in wearable devices caused by mechanical deformation in practical applications, Kim et al. proposed a strain-invariant frequency-selective metasurface for wearable electronics. By integrating a strain-controlling layer around its split-ring resonator unit cells, it maintains dipole resonance at 2.4 GHz under biaxial stretching, thereby achieving selective wave transmission for target frequency bands and broadband electromagnetic interference shielding even under mechanical deformation (Figure 7b).[136] In a similar vein, Li et al. introduced flexible spoof surface plasmon polariton (SSPP) sensors capable of proximity sensing, physical contact detection, and material identification. By integrating these sensors into wearable devices, their approach enables non-invasive monitoring of physiological parameters (Figure 7c).[137] Expanding on this, Ling et al. proposed a tension-driven three-dimensional printing technique (CHARM3D) and utilized it to fabricate three-dimensional electromagnetic bandgap metamaterials, which effectively reduce the mutual coupling between adjacent antenna elements in WBSNs (Figure 7d).[138]

Additionally, Hajiaghajani et al. explored textile-integrated magneto-inductive metamaterials for near-field communication, offering a solution for multi-body area networks (BANs) that enhance both security and network expansion. Their approach allows for the seamless integration of wireless sensors onto clothing, where the metamaterial network provides a secure and flexible communication path for the devices (Figure 7e).[139] Finally, Tian et al. demonstrated that the metamaterial textiles enhance transmission efficiency by over three orders of magnitude compared to conventional radiative networks, localize wireless communication within 10 cm of the body, and allow for wireless power transfer and touch sensing. These textiles are robust to daily wear, as they contain no active electronic components, and provide a more secure, energy-efficient platform for interconnecting devices in WBSNs (Figure 7f).[140]



Figure 7. Mechanisms of Metamaterial-Based Wireless Body Sensor Networks. a) the metamaterial textile network. Adapted with permission.[135] Copyright 2023, Springer Nature. b) the multilayer configuration of the EMI-shielding metasurface. Reproduced with permission.[136] Copyright 2025, Springer Nature. c) Structure of the flexible SSPP sensor. Reproduced with permission.[137] Copyright 2026, American Chemical Society. d) Tension-driven three-dimensional printing of free-standing Field's metal structures. Reproduced with permission.[138] Copyright 2024, Springer Nature. e) Design of textile-integrated metamaterials for magneto-inductive wave propagation. Reproduced with permission.[139] Copyright 2021, Springer Nature. f) Wireless body sensor networks with metamaterial textiles. Reproduced with permission.[140] Copyright 2019, Springer Nature.

3.2 Multifunctional fibers for self-powered wearable intelligent systems

In recent years, advances in fiber electronics have created opportunities for bio-integrated systems, as fibers can be woven, sewn, stretched, and conformally integrated with textiles or biointerfaces. Compared with traditional wearabe devices, functional fibers demonstrate inherent advantages in breathability, deformability, washability, and large-area integration. Wearable systems based on fiber electronics is promising to reduce reliance on batteries by harvesting distributed energy from the human body and the surrounding environment, including body temperature, biomechanical motion, droplets, and ambient electromagnetic fields. For example, thermoelectric fibers can convert body temperature gradients into electrical energy, while triboelectric and piezoelectric fibers can convert mechanical deformation, contact, vibration, and sound waves into electrical signals. However, the practical application of energy-harvesting textiles remains limited by several challenges.

Conventional ionic conductors often suffer from strain-induced resistance variation because stretching increases the conductive path length and reduces the cross-sectional area, which will distort the signal transmission in wearable sensor systems. As shown in Figure 8a, Ye et al. designed a bicontinuous fiber through polymerization-induced phase separation, forming an interpenetrated structure composed of a solid elastomer phase and a liquid ion-conducting phase.[141] The dissolved salts spontaneously partitioned into the liquid phase, creating highly tortuous ionic channels at a self-wrinkled interface. During stretching, these tortuous channels were gradually straightened, which enhanced ionic conductivity and compensated for the geometric resistance increase. As a result, the fiber showed only a small resistance increase even at large strain, providing a stable soft cable for high-fidelity signal transmission. In addition, continuous energy delivery in a soft, scalable, and textile-compatible form remains another key challenge for fiber electronics. As shown in Figure 8b, Ding et al. developed scalable thermoelectric fibers through a gelation extrusion strategy, aiming to overcome the limited scalability and laborious PN-junction assembly of conventional thermoelectric textiles.[44] This approach directly produced continuous p-type and n-type thermoelectric fibers with improved mechanical compliance and process efficiency. It is of importance to make the fiber itself as a fundamental functional unit of textile-based electronics, rather than as a passive carrier of external devices. This research provides a scalable approach to enabling interactive functions by integrating thermoelectric conversion capabilities at the fiber level for harvesting low-grade body heat.

Beyond the material-level design of thermoelectric fibers, practical self-powered textiles require device-level integration, where individual fibers are assembled into fabric architectures capable of continuous energy harvesting under wearable conditions. As shown in Figure 8c,

Sun et al. reported a stretchable fabric that generates electrical power from woven thermoelectric fibers to address the mismatch between conventional two-dimensional thermoelectric architectures and the out-of-plane thermal gradient between the human body and the surrounding environment.[142] This system uses acrylic fibers to wrap alternating doped carbon nanotubes and weave them into the π-type thermoelectric modules. The interlocked textile architecture enabled the thermoelectric modules to stand in a three-dimensional configuration, aligning more effectively with the direction of heat flow. Unlike rigid or substrate-supported thermoelectric devices, this woven generator-maintained textile-like softness, stretchability, and conformability. The fabric achieved a peak power density of 70 mW m^{-2} under a temperature difference of 44 K and retained output stability under approximately 80% strain. Therefore, this work moves thermoelectric fibers beyond material-level energy conversion toward wearable textile-level power generation, showing that body heat can be harvested through textile architectures while preserving mechanical compliance and wearing comfort.

Extending thermoelectric energy harvesting toward broader thermal regulation and environmental adaptability, Figure 8d presents a hyperstable eutectic core-spun fiber for wearable energy harvesting and personal thermal management.[143] Sun et al. designed a core-spun functional fiber composed of a Zn-based eutectogel core and a polytetrafluoroethylene sheath. Rather than stacking separate functional layers onto fabrics, the systems directly integrated multiple functions into a single fiber architecture. The resulting fiber exhibited a synergistic piezoelectricity-enhanced triboelectric output, while also providing hydrophobicity, high mid-infrared emissivity, and visible-light reflectivity. When woven into a monolayer multifunctional textile, the fiber enabled harvesting of both mechanical energy and droplet energy, while simultaneously supporting passive personal thermal management.

In addition to harvesting the energy from body heat, self-powered textiles are also required to convert mechanical energy from body motion, contact, and vibration into usable electrical signals. As shown in Figure 8e, Dong et al. developed three-dimensional stretchable and self-encapsulated multimaterial triboelectric fibers using scalable thermal drawing of water-resistant thermoplastic elastomers and conductive composites.[144] Previous fiber-based triboelectric nanogenerators often relied on simple single-electrode configurations or fragile core–sheath structures, which limited their robustness, environmental stability, and output reliability. In this work, the proposed fiber contained stretchable conductive nanocomposite electrodes, microtextured triboelectric surfaces, an internal air gap, and an elastomeric encapsulating cladding. The contact–separation mode generate electrical outputs under compression and

stretching, even under humidity and repeated cycling. The use of a 10-m-long fiber on a stretchable surface further demonstrated its scalability and textile compatibility.

Beyond harvesting mechanical energy, triboelectric fibers can also use mechanically induced electrical signals as direct sensing outputs, enabling self-powered detection of pressure, strain, vibration, and touch without external power supply. As shown in Figure 8f, Lin et al. reported a triboelectric micro-flexure-sensitive fiber electronic system inspired by biological mechanoreceptors, particularly the Meissner corpuscle.[145] Instead of focusing on large-strain deformation, the work targeted subtle physiological bending and micro-flexure signals that are common in muscle activity, respiration, posture adjustment, and rehabilitation monitoring. The fiber was designed using a dynamic stability model of sheath–core structures and incorporated ordered nanofiber buckling at the ionic conductive interface. The incorporation of ionogel electrodes further enhanced sensitivity to electric-field changes and improved signal transmission. As a result, the fiber could detect ultra-low curvature down to 0.1 mm^{-1}. The proposed triboelectric fibers can function simultaneously as energy harvesters and self-powered physiological sensors, demonstrating that the same energy-conversion principle can support both power generation and subtle biomechanical signal perception in wearable rehabilitation and human–machine interaction systems.

Mechanical energy harvesting mainly relies on body motion, contact, and deformation, whereas wearable textiles can also benefit from ambient electromagnetic energy and wireless signal transmission, which extends fiber electronics from mechanically activated energy harvesters toward chipless wireless textile systems. As shown in Figure 8g, Yang et al. developed a single body-coupled fiber that enables ambient electromagnetic energy harvesting and wireless signal transmission without additional chips or batteries.[146] Conventional intelligent textiles generally depend on rigid silicon-based components, such as wireless modules, microprocessors, and analog-to-digital converters, which compromise softness, comfort, and energy efficiency. This system proposed a body-coupled energy interaction mechanism in which the human body participates in coupling ambient electromagnetic energy with the fiber. The fiber itself can dynamically switch between energy confinement and radiation states, enabling wireless visual–digital interaction within a miniature fiber format.

The applications of functional fibers are not limited to power generation or wireless signal transmission, but also can be serve as flexible platforms to detect minute mechanical vibrations, such as sound transmitted through the air and vibrations generated by human movement. As shown in Figure 8h, Yan et al. developed a thermally drawn composite piezoelectric fiber that can be woven into ordinary fabric to convert nanometre-scale mechanical vibrations into electrical signals.[147] Inspired by the auditory system, the fabric acts as a membrane that

converts airborne sound pressure waves into mechanical vibration modes, while the embedded piezoelectric fiber functions as the transducer that converts these vibrations into electrical output. The active layer consists of a piezoelectric P(VDF-TrFE)-based composite loaded with barium titanate particles, and an elastomeric cladding concentrates mechanical stress in the piezocomposite layer to improve sensitivity. The resulting acoustic fabric enabled sound localization, fabric-to-fabric communication, and cardiac auscultation from a shirt.

As shown in Figure 8i, Lee et al. developed a wireless stretchable and suturable fiber strain-sensing system for monitoring connective-tissue deformation.[45] Unlike planar implantable electronics, which can suffer from structural mismatch with fibrous tissues and often require difficult suturing procedures, this system was designed in a one-dimensional fiber format compatible with tendon and ligament structures. The sensor consists of two stretchable conductive fibers arranged in a double-helical structure with a hollow core, forming a capacitive strain sensor. By connecting the fiber-based capacitor to an inductive coil, the authors constructed a passive RLC resonant circuit that enables wireless readout without rigid soldering points. The sensor showed a strain sensitivity of around 12 and was demonstrated on Achilles tendon and knee ligament tissues in ex vivo and in vivo porcine models.

Building on the need for intimate bio-interfaces, Wang et al. further softens the contact between functional fibers and living systems. As shown in Figure 8j, the imperceptible augmentation of biological surfaces use in situ tethered organic bioelectronic fibers based on PEDOT:PSS. In contrast to conventional thin-film electronics or electronic textiles, which may block pores, restrict gas exchange, or mechanically perturb soft biological surfaces, this approach creates substrate-free and open fiber networks directly on living structures through orbital spinning. These organic bioelectronic fiber networks were used as on-skin electrodes for ECG and EMG recording, skin-gated organic electrochemical transistors, augmented touch interfaces, and plant-monitoring interfaces. This study therefore shifts multifunctional fiber systems from wearable power and sensing textiles toward imperceptible living interfaces, where minimal material use, breathability, conformability, and biological compatibility become as important as electrical function.

Organic fibers emphasize soft and imperceptible biointerfaces, whereas multifunctional fibers can further extend into optoelectronic applications through high-quality semiconductor fibers. As shown in Figure 8k, Wang et al. addressed the long-standing challenge in thermally drawn semiconductor fibers, where stress development and capillary instabilities during molten-core fabrication can lead to cracks, perturbations, or discontinuities in the semiconductor core. By analysing stress formation during viscous flow, core crystallization, and cooling, the authors established a mechanical design strategy to produce ultralong, fracture-

free, and perturbation-free semiconductor fibers. These exposed semiconductor wires could then be integrated with metal electrodes and polymer cladding to form flexible optoelectronic fibers and large-area optoelectronic fabrics. Compared with conventional rigid photodetectors, the fiber format allows long sensing lengths, conformability to curved surfaces, washability, and textile integration.

Finally, Khatib et al. proposed a spiral transformation strategy to convert two-dimensional microfabricated flexible electronic films into one-dimensional fiber optic devices, as shown in Figure 8l. This method can precisely control the longitudinal, angular, and radial positions of functional components within the fiber, overcoming many of the shortcomings of previous fiber optic electronic devices, such as low component density and limited functionality. The resulting Spiral-NeuroString can integrate multiple sensing and stimulation functions in a soft, deformable, and miniaturized fiber format. The authors demonstrated continuous gastrointestinal motility mapping and tissue stimulation in awake pigs, as well as long-term neural recordings in the mouse brain. They also demonstrated the potential to fabricate ultra-high channel-count fibers, accommodating up to 1280 channels in a flexible fiber with a diameter of 230 μm. Therefore, this work introduces the concept of multifunctional fiber optics to a system-level bioelectronic platform where sensing, stimulation, high-density integration, flexibility, and minimally invasive manipulation functions are integrated into a single architecture.

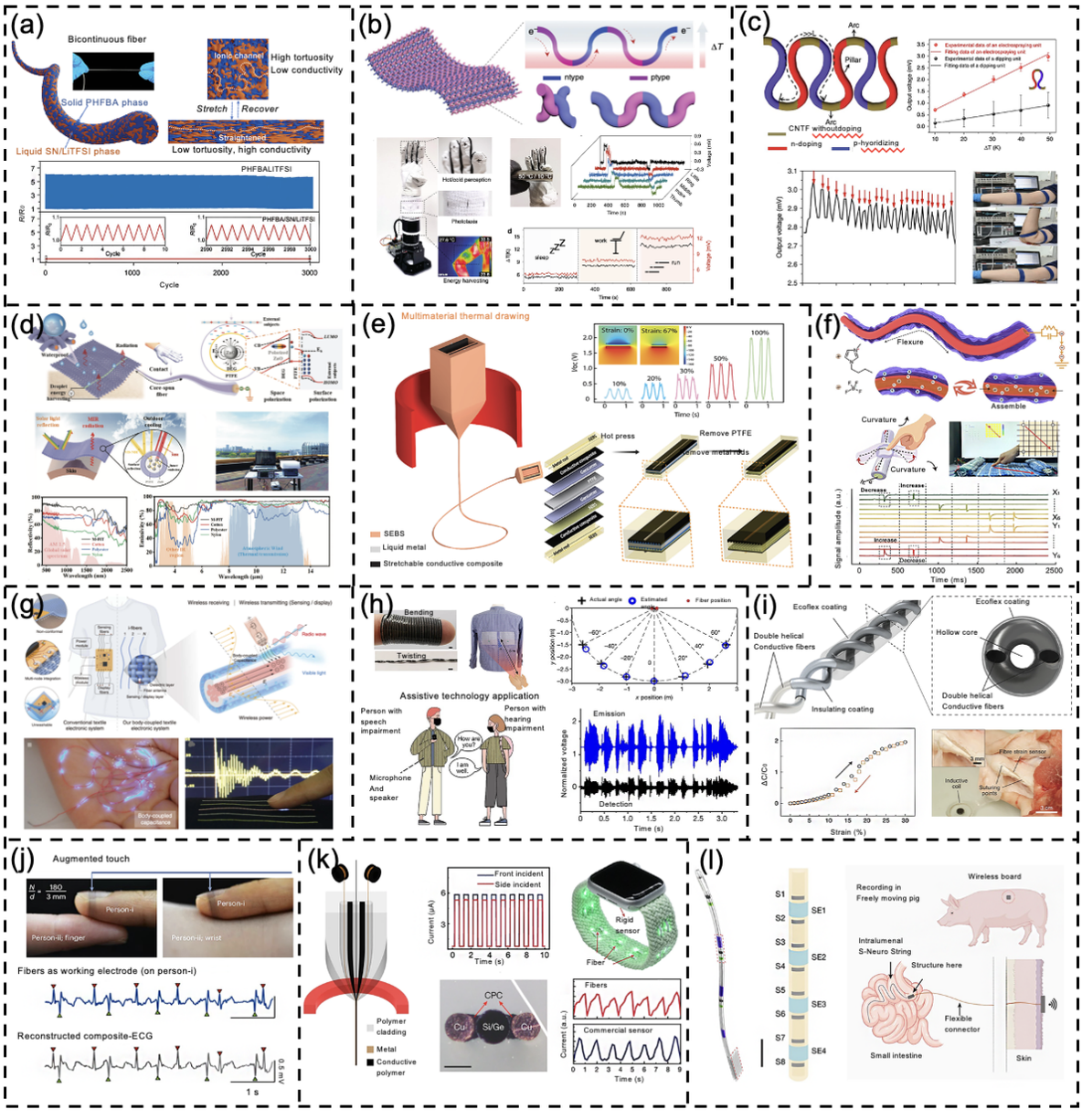


Figure 8. Multifunctional fibers for self-powered wearable intelligent systems. (a) A solid–liquid bicontinuous fiber with strain-insensitive ionic conduction for deformable fiber electronics. Reprinted with permission.[141] Copyright 2024 Wiley-VCH GmbH. (b) Scalable thermoelectric fibers for textile-based energy harvesting, touch sensing, and communication. Reprinted with permission.[44] Copyright 2020 Springer Nature. (c) A stretchable thermoelectric fabric woven from thermoelectric fibers for body-heat energy harvesting. Reprinted with permission.[142] Copyright 2020 Springer Nature. (d) A eutectic core-spun fiber for mechanical/droplet energy harvesting and personal thermal management. Reprinted with permission.[143] Copyright 2023 Wiley-VCH GmbH. (e) Stretchable and self-encapsulated triboelectric fibers for mechanical energy harvesting. Reprinted with permission.[144] Copyright 2022 AAAS. (f) Triboelectric micro-flexure-sensitive fibers for self-powered physiological motion sensing. Reprinted with permission.[145] Copyright 2024 Springer Nature. (g) A body-coupled fiber for chipless textile electronics via ambient electromagnetic energy harvesting and wireless signal transmission. Reprinted with permission.[146] Copyright 2024 AAAS. (h) A piezoelectric acoustic fiber for fabric-based sound sensing and physiological monitoring. Reprinted with permission.[147] Copyright 2022 Springer Nature. (i) A wireless suturable fiber strain sensor for connective-tissue deformation monitoring. Reprinted with permission.[45]

Copyright 2021 Springer Nature. (j) Organic bioelectronic fibers for imperceptible living-system interfaces. Reprinted with permission.[148] Copyright 2024 Springer Nature. (k) Semiconductor optoelectronic fibers enabled by mechanical design. Reprinted with permission.[149] Copyright 2024 Springer Nature. (l) High-density soft bioelectronic fibers for multimodal sensing and stimulation. Reprinted with permission.[150] Copyright 2025 Springer Nature.

3.3 Wearable textile energy harvester

The field of wearable textile energy harvesters has made significant progress in recent years at the intersection of smart textiles and energy technology[151–156]. Through innovative structural design, materials engineering, and system integration, researchers have developed a series of textile-based energy harvesting and self-powered sensing systems based on triboelectric nanogenerators and the tribovoltaic effect, providing new technological pathways for human motion energy harvesting, health monitoring, and human-computer interaction.

In terms of structural design, various textile forming technologies have been employed to construct efficient energy harvesting structures. Ahmed et al. adopted a fully weft-faced fabric structure, integrating a densely packed weft-dominated matrix with a BTO/PDMS laminated composite and copper-nickel fabric electrode to maximize triboelectric contact area, achieving excellent electrical output performance and air permeability for integration into insoles and smart trousers for gait analysis and real-time motion monitoring (Figure 9a).[157] Chen et al. fabricated a bionic double-helix braided yarn TENG using high-speed spiral braiding technology, with a latex rubber tube as the core yarn and silver-plated nylon yarn combined with ordinary nylon yarn as braiding yarns, achieving superelastic deformation up to 500% and stable performance after 36,000 stretching cycles, with applications in self-powered lamp cords, crib pre-warning systems, and yoga counting elastic cords (Figure 9b).[158] Wang et al. employed a kirigami structure to construct a unique repeatably stretchable three-dimensional structure on PDMS/$BaTiO_3$ composite films, significantly improving contact-separation efficiency and achieving an output voltage of 896V and a power density of 3380mW m^{-2}, enabling simultaneous lighting of 1636 LEDs on a skirt and monitoring of various human movements (Figure 9e).[159]

In materials engineering and interface control, researchers have enhanced device performance through functional material modification and interfacial design. Chen et al. prepared a core-sheath nanofiber yarn single-electrode TENG via scalable coaxial electrospinning, incorporating lead-free $Cs_3Bi_2Cl_9$ perovskite nanocrystals into the PVDF-TrFE matrix, simultaneously improving β-phase crystallinity, dielectric properties, and surface roughness through multiscale structural engineering, achieving high pressure sensitivity of 3.64V kPa^{-1}, a broad detection range of 50kPa, and exceptional durability exceeding 50,000

cycles, with applications in interactive Guzheng interfaces and Morse code communication systems (Figure 9c).[160] Zhang et al. constructed a three-dimensional braided core-shell tribovoltaic textile based on Ag/PEDOT: PSS Schottky contact, generating self-rectifying DC output during stretching-releasing cycles, eliminating rectifier circuits and addressing high impedance issues, achieving stable DC output of 12.2nA and low matched resistance of 20kΩ after four PEDOT: PSS coatings, enabling linear monitoring of elbow and knee joint angles and real-time detection of various exercises when stitched onto sportswear (Figure 9d).[161]

In system integration and intelligence, Xiong et al. developed a graphene textile TENG through scalable spinning, roll-to-roll dip-coating, multiaxial winding, and machine knitting processes (Figure 9f).[162] The three-dimensional cardigan stitch structure provides larger triboelectric contact area compared to plain stitch, achieving a peak power of 3.6μW under 1 Hz tapping, with graphene yarns exhibiting high tensile strength of 592MPa and excellent mechanical stability. When worn on elbow and knee joints, the textile TENG collected triboelectric signals from four motion states (slow walking, fast walking, jogging, and fast running), and a one-dimensional convolutional neural network model achieved 98.12% recognition accuracy.

In summary, these studies demonstrate the latest advances in textile-based energy harvesters in structural innovation, materials optimization, and intelligent integration. These achievements not only provide feasible solutions for self-powering of wearable devices but also show broad application prospects in health monitoring, human-computer interaction, smart sports, and rehabilitation medicine. With the deep integration of materials science, textile engineering, and artificial intelligence, textile-based energy harvesters are expected to become key components of next-generation smart textiles, driving wearable electronics toward more sustainable, intelligent, and human-centered development.

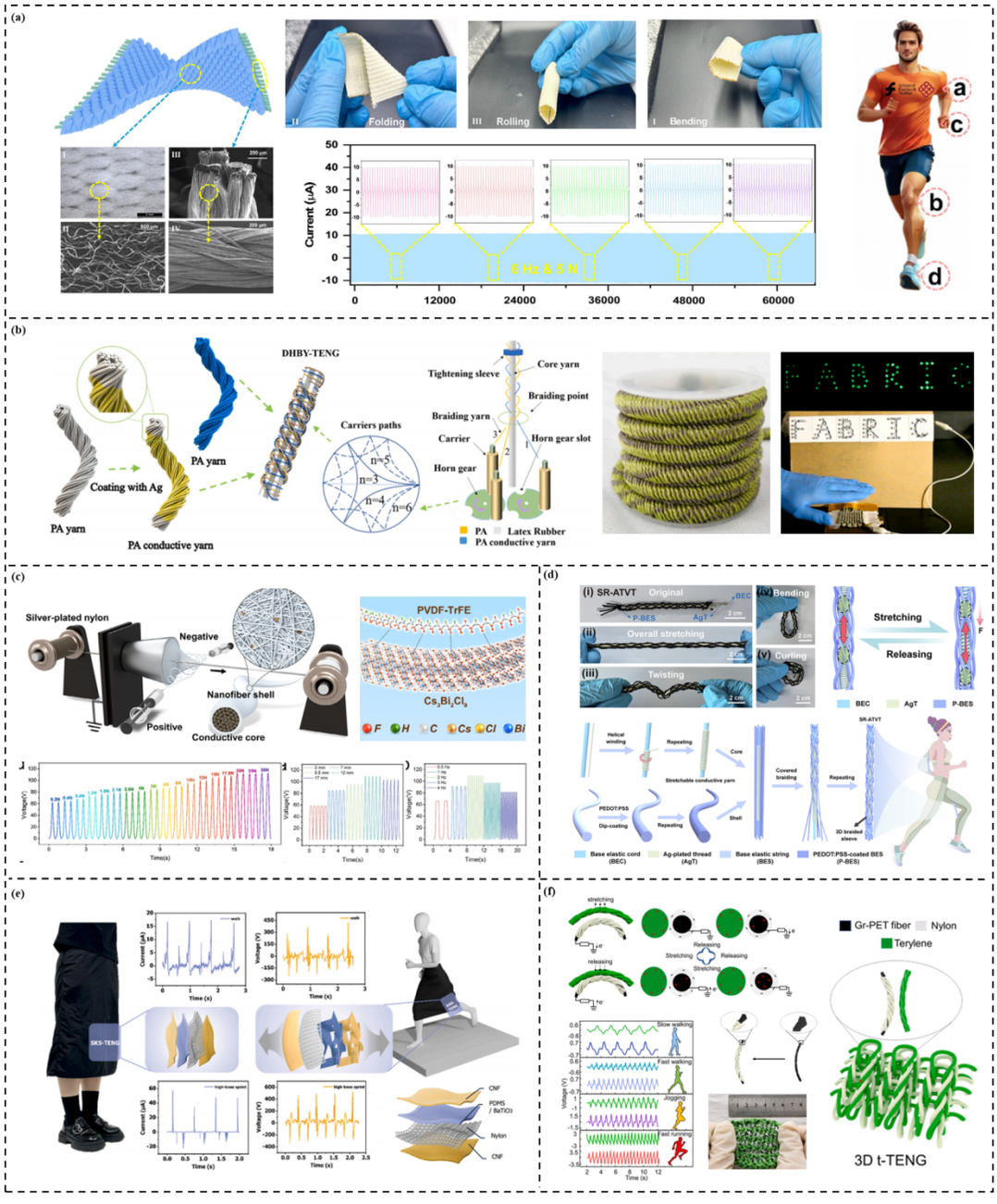


Figure 9. Wearable textile energy harvester. (a) Fully weft-faced structured fabric-based triboelectric nanogenerator with BTO/PDMS composite for gait analysis and real-time motion monitoring. Reprinted with permission.[157] Copyright 2026 Wiley-VCH GmbH. (b) Bionic double-helix braided ultra-stretchable energy-harvesting yarn for self-powered sensing and rehabilitation applications. Reprinted with permission.[158] Copyright 2025 Elsevier. (c) Core-sheath nanofiber yarn-based single-electrode triboelectric nanogenerator with Cs3Bi2Cl9 perovskite for multimodal sensing and smart musical interfaces. Reprinted with permission.[160] Copyright 2025 Wiley-VCH GmbH. (d) Stretchable all-in-one tribovoltaic textile with Ag/PEDOT:PSS Schottky contact for self-powered sport and fitness tracking. Reprinted with permission.[161] Copyright 2025 Springer Nature. (e) Stretchable kirigami-structured textile-based triboelectric nanogenerator for high-performance energy harvesting and wireless human motion monitoring. Reprinted with permission.[159] Copyright 2025 Elsevier. (f) Scalable graphene textile triboelectric nanogenerator with three-dimensional cardigan stitch for machine-learning-assisted human motion recognition. Reprinted with permission.[162] Copyright 2022 Elsevier.

3.4 Wearable energy harvester

Recent advances in wearable technology have driven a paradigm shift from rigid, battery-powered devices toward flexible, self-powered, and intelligent systems capable of continuous physiological monitoring and seamless human-machine interaction.[163–165] Among various wearable form factors, wrist-worn devices such as smart watches and wristbands have attracted significant attention due to their convenience for health tracking and gesture recognition, while waist-worn belts offer unique advantages for core body motion capture and rehabilitation training.

Wrist-worn wearable devices have emerged as a prominent form factor for health monitoring and human-computer interaction, with recent advances focusing on self-powering capabilities, multimodal sensing integration, and intelligent data analysis. In the domain of energy harvesting, Yang et al. developed high-performance p-type ductile thermoelectric materials based on AgCu(Se,S,Te) pseudoternary solid solutions, achieving figure-of-merit values of 0.45 at 300 K and 0.68 at 340K (Figure 10a).[166] Leveraging the intrinsic ductility of these materials, they fabricated π-shaped flexible thermoelectric devices with 0.1-mm-thick legs suitable for wrist wearing, utilizing polyimide-based flexible circuit boards and magnetron-sputtered tungsten/tin contact layers that achieve low contact resistivities of 2-19μΩ·cm2. At a filling factor of 72%, the device generates an output power of 203mW under a temperature difference of 1.5K, with a normalized power density of 30μW cm-2 K-2. When attached to the human wrist, the device produced an open-circuit voltage of 0.2mV under natural convection and up to 13μW with enhanced heat transfer, demonstrating stable performance after 500 bending cycles. This work establishes a foundation for self-powered wearable electronics powered by body heat.

In the field of physiological monitoring, two notable approaches have been developed for wrist-based pulse sensing. Zhao et al. developed a wearable active-pressure three-channel pulse monitoring platform inspired by traditional Chinese medicine (Figure 10b),[167] designed as a watch-like device for precise acquisition of pulse waves at the "Cun," "Guan," and "Chi" positions. The system integrates flexible pressure sensor arrays with high sensitivity (460.1kPa^{-1}) and linearity (R^2>0.999), flexible airbag arrays for active pressure control (0–50kPa), wireless transmission modules, and a companion mobile application. The ionic sensing layer, optimized through microcolumn structures and laser engraving, achieves a response time of 25ms and stability over 12,000 cycles. Through analysis of pulse wave amplitude variations under nine static pressures using a back-propagation neural network, the system predicts blood pressure with deviations meeting AAMI standards. Concurrently, Yi et al. reported the first MXene-based 3D-printed self-powered wearable physiological sensing system for continuous in Figure 10d.[168] By optimizing the flake size and rheological properties of MXene ink, they

achieved a conductivity of 5096 S/cm and shear-thinning behavior suitable for 3D printing. The MXene-based triboelectric nanogenerator delivers an output power of 816.6 mW m^{-2} when coupled with SEBS, enabling finger-tap charging, while the capacitive pressure sensor demonstrates a sensitivity of 6.03 kPa^{-1} and a response time of 80 ms, clearly resolving three characteristic peaks in the pulse waveform. The flexible circuit board supports two operating modes: in mode one, stored energy powers the capacitance-to-digital converter chip and an LED, indicating pulse rate in real time through LED flashing frequency; in mode two, detailed pulse waveforms are wirelessly transmitted to a smartphone via near-field communication for display and analysis. Together, these approaches provide complementary strategies for wrist-based continuous health monitoring.

For motion and gesture recognition, Tan et al. developed a machine learning-enabled gesture recognition wristband for full keyboard input and multi-command control in Figure 10e.[169] Their hybrid generator sensor array combines TENG and PENG elements to capture both slight contact and large-force motion information, enriching the mechanical data of gesture movements. The eight-channel sensor array collects mechanical signals from wrist surface muscle groups during 26 sign language letter gestures. Through Butterworth filtering, independent component analysis, feature extraction, and linear discriminant analysis with 600 training iterations, the model achieves a recognition accuracy of 92.6% for 26 letters, enabling sentence-level real-time sign language recognition and voice broadcasting. Complementing this work, Zhou et al. developed a conductive hydrogel doped with boric acid and KCl (PHK hydrogel) in Figure 10c.[170] The PHK hydrogel-based triboelectric nanogenerator achieves dual functions of energy harvesting and pressure sensing. A four-channel smart wristband composed of PHK TENG units conformally attaches to the wrist, capturing mechanical signals from wrist joints and muscle groups during hand movements. Using long short-term memory neural networks, the system achieves a recognition accuracy of 98.21% for handwritten Arabic numerals. These systems demonstrate the potential of wrist-worn devices for intuitive human-computer interaction and assistive communication technologies.

As a wearable form factor that conforms to the body's core area, wearable belts demonstrate unique advantages in health monitoring, motion sensing, and rehabilitation training. On one front, Zhang et al. developed a wearable belt system based on textile-based triboelectric sensors for gait analysis and waist motion capture Figure 10g.[171] The belt integrates four equidistantly sewn TENG sensors that generate distinct triboelectric signals in response to different waist motions (such as left twist and forward lean), enabling real-time robotic manipulation and virtual game interaction to enhance immersion during waist training. The sensors feature pyramid-patterned triboelectric layers encapsulated by TPU-coated fabric,

generating approximately 20V output under 100N compression force with stable performance after 5000 cyclic tests. On the other front, Hao et al. proposed a self-sensing and self-powered wearable system based on multi-source human motion energy harvesting (Figure 10f),[172] which is installed on the waist through a ball hinge. Their designed three-degree-of-freedom triboelectric nanogenerator utilizes spatial acceleration variations of the waist during different motions (such as walking, jogging, and climbing) to generate characteristic triboelectric signals, achieving 100% motion state recognition accuracy after processing with a Gated Recurrent Unit deep learning model. Meanwhile, the system integrates a knee negative energy harvester based on double frequency up-conversion technology, employing a hybrid electromagnetic-piezoelectric generation mechanism that delivers an output power of 27.01mW at a speed of 8 km/h and a power density of 0.3W/kg under 3Hz external excitation, successfully demonstrating practical applications such as powering temperature and humidity sensors and lighting up 112 LEDs. These two research directions advance wearable belts in intelligent rehabilitation and human-computer interaction from different perspectives, providing important references for the multifunctional integration and self-powering of next-generation smart belts.

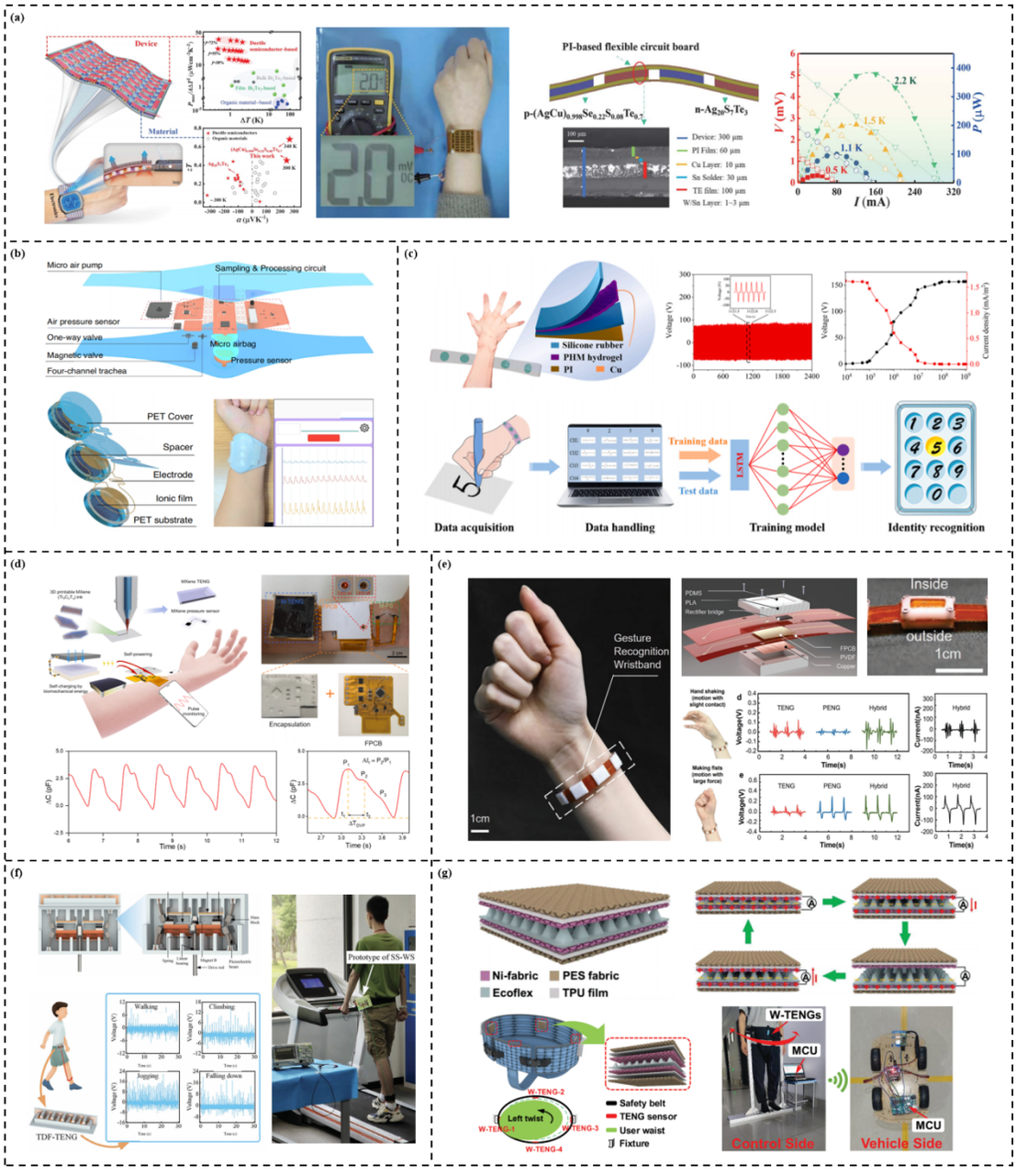


Figure 10. Wearable energy harvester. (a) High-performance p-type ductile thermoelectric materials based on AgCu(Se,S,Te) pseudoternary solid solutions for wrist-worn energy harvesting. Reprinted with permission.[166] Copyright 2022 AAAS. (b) Wearable active-pressure three-channel pulse monitoring platform inspired by traditional Chinese medicine for wrist-based physiological sensing. Reprinted with permission.[167] Copyright 2024 Springer Nature. (c) Conductive PHK hydrogel-based triboelectric nanogenerator for smart wristband with handwritten numeral recognition. Reprinted with permission.[170] Copyright 2025 Elsevier. (d) MXene-based 3D-printed self-powered wearable physiological sensing system for continuous radial artery pulse monitoring. Reprinted with permission.[168] Copyright 2022 Elsevier. (e) Machine-learning-enabled gesture recognition wristband with hybrid TENG/PENG sensor array for full keyboard input and sign-language recognition. Reprinted with permission.[173] Copyright 2022 Wiley-VCH GmbH. (f) Self-sensing and self-powered wearable system with a three-degree-of-freedom triboelectric nanogenerator for waist-motion energy harvesting and recognition. Reprinted with permission.[172] Copyright 2024 Springer Nature. (g) Textile-based triboelectric sensor belt for gait analysis and waist-motion capture in robot-aided rehabilitation. Reprinted with permission.[171] Copyright 2022 Wiley-VCH GmbH.

4. Future directions toward autonomous intelligence in wearable systems

As wearable tactile systems become increasingly soft, distributed, and energy-autonomous, their future development is moving beyond sensing alone toward closed-loop intelligent interaction. In this context, autonomous intelligence refers to the ability of wearable systems to perceive physical stimuli, process multimodal information, provide timely feedback, and support adaptive decision-making with reduced dependence on external computing or manual control. Emerging technologies such as vision–tactile sensing, advanced haptic feedback, machine-learning-assisted wearable platforms, and near-sensor/in-sensor edge computing are accelerating this transition. These directions are particularly important for applications in robotic manipulation, immersive human–machine interfaces, rehabilitation, prosthetics, and embodied intelligence, where tactile information must be rapidly interpreted and converted into meaningful feedback or action. This section discusses these emerging pathways and highlights how future wearable tactile systems may evolve from flexible sensing interfaces into autonomous, interactive, and intelligent platforms.

4.1 Wearable human machine interfaces with advanced haptic feedback

Human hands show remarkable dexterity, which is highly dependent on the high density of mechanoreceptors there.[174] Given such capacity of hands in perception and actuation, wearable glove-like human machine interfaces, which can capture hand motion accurately, hold great potential for applications like AR/VR,[175–177] sign language communication [178,179] and human-robot interaction.[180,181] In addition to tactile sensing, haptic feedback interfaces are often integrated into gloves, rendering intuitive interaction. To deliver realistic haptic sensations to the user, multimodal and user-adaptive haptic feedback gloves are investigated and implemented. Moreover, as wearable HMIs, gloves should also be compact, flexible and air permeable to increase wearing comfort, which results in ring-shape interfaces or textile-based gloves.

As an extension to glove concepts, multimodal tactile sensing and feedback rings are proposed by Sun et al. as a compact human machine interfaces (Figure 11a).[182] Triboelectric tactile sensors and pyroelectric temperature sensors are seamlessly integrated into ring-shape devices. Since the output signal of triboelectric sensors is transient, voltage integration is adopted to continuously tracking the joint angle of each finger. With this ring-shape HMI, the gesture of the user can be recognized and can be used to control a robotic hand. Furthermore, timely and multimodal haptic feedback is also essential to render immersive experience for the user in AR/VR applications. To this end, eccentric rotating mass (ERM) vibrators and nickel chromium alloy-based resistive heaters are integrated into the rings. The haptic feedback

mechanisms enable the user to feel the shape and the temperature of the grasped objects in VR space, providing comprehensive somatosensory sensations.

To increase the comfort of wearing, textile-based glove-shape HMIs are also broadly investigated. Tashakori et al. [183] reported a pair of smart textile gloves, which is able to track the hand pose in real time (Figure 11b). Piezoresistive helical sensor yarns (HSYs) are distributed over finger joints, fingertips and the palm to measure the local deformation caused by finger movement, as well as the force between the hand and the grasped object. Two nine-axis IMUs are attached to capture the wrist-joint quaternion angles. The multimodal data is analyzed by a recurrent neural network based on bidirectional long short-term memory to estimate the joint angles. The 3D movement of the hand is visualized in VR scenarios. With this real time hand motion tracking functionality, complex applications are illustrated like typing on a mock paper keyboard or drawing in-air.

Since different individuals may have different perceptions for haptic feedback delivered by human-machine interfaces, adaptively tuning the feedback parameters has become a challenge. Luo et al. introduced a low-cost textile wearable glove which can adjust the haptic feedback based on how the user reacts to haptic stimuli (Figure 11c).[184] The fabrication process is facile and scalable where piezoresistive tactile sensors and linear resonant actuators are stitched into textiles through programmable embroidery. The tactile sensing arrays achieve a high spatial resolution of 0.25 cm^2, capturing contact information during hand manipulation. Crucially, in order to achieve adaptive cross-user tactile interaction transfer, a machine learning pipeline, which is similar to the classic encoder-decoder paradigm, is employed. The encoder outputs user embedding vectors, which represent reaction speed, finger dexterity, etc. of the user while the decoder predicts the tactile output based on haptic feedback and the user embedding vectors. The user-specific haptic feedback is optimized by gradient descent in the decoder network. This schematic, where actuators can reconstruct the personalized tactile sensation via machine learning models, holds great potential for skill training or teleoperation.

Apart from training or teleoperation, wearable glove-type HMIs can also be used for rehabilitation. Kang et al. implemented a multimodal sensing and feedback system aiming to restore tactile sensations for people with traumatic spinal cord injury (Figure 11d).[185] The glove integrates copper-elastomer capacitors, spiral gold nanomembranes, and laser-induced graphene to capture pressure, temperature and finger flexion at hand respectively. On the other hand, the haptic feedback component takes the shape of an armband and can render pressure, linear displacement and vibrotactile stimuli to the user. The pressure changes measured by the glove are converted to pressure changes of the pneumatic actuators; the temperature change is

reflected by vibrotactile frequency; the finger flexion is mapped to linear displacement. The system serves as a sensor substitution interface, which can assist hand rehabilitation process.

For wearable glove-type HMIs, haptic feedback actuators usually require external power supply, which limits the minimum size and weight of the whole system. Self-powered haptic actuators, however, can solve this problem and enhance the wearing comfort of the user. Taking a step toward this direction, Xu et al. presented a self-powered electrotactile textile haptic (SPETH) glove (Figure 11e).[186] The glove harvests electrostatic energy from hand-object interaction through textile-based TENGs. The energy is stored in capacities in the power management circuit. When the capacitor voltage reaches the threshold voltage of the gas discharge tube (GDT), a pulse current is delivered to skin electrodes to stimulate mechanoreceptors as a tactile sensation. In addition to power supply units, TENGs can also serve as tactile sensors. The SPETH glove is able to recognize different gestures performed by the user, indicating its ability to provide tactile sensing and haptic feedback at the same time.

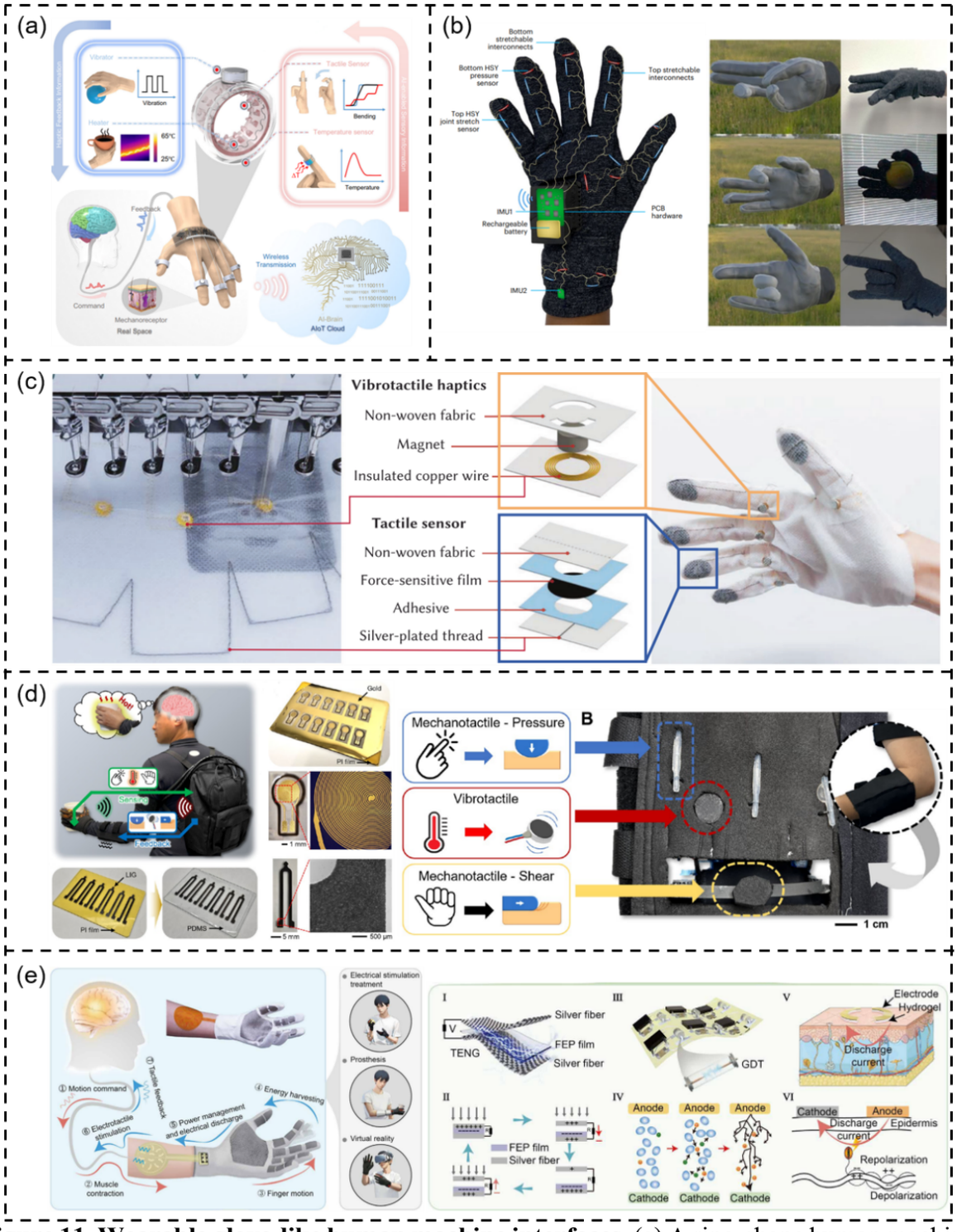


Figure 11. Wearable glove-like human machine interfaces. (a) A ring-shape human machine interface with multimodal tactile sensing and haptic feedback. Reprinted with permission.[182] Copyright 2022 Springer Nature. (b) A textile-based smart sensing glove with real time hand pose tracking functionality. Reprinted with permission.[183] Copyright 2024 Springer Nature. (c) Digitally embroidered textile gloves that can transfer tactile interaction with user-adaptive tactile feedback. Reprinted with permission.[184] Copyright 2024 Springer Nature. (d) A hand rehabilitation system based on flexible gloves and haptic actuators. Reprinted with permission.[185] Copyright 2025 The American Chemical Society. (e) A self-powered, haptic feedback glove based on triboelectric nanogenerators. Reprinted with permission.[186] Copyright 2025 The American Association for the Advancement of Science.

4.2 Vision Tactile Sensing

With the rapid development of dexterous robotic hands, soft grippers, prosthetic interfaces, and embodied intelligent systems, tactile sensors are required to capture rich contact information, including pressure distribution, fine surface texture, object geometry, material stiffness, multidimensional contact forces, and incipient slip in real time [62,187–189]. In addition, such functionality proves critical for applications ranging from VR/AR and wearable human–machine interfaces to assistive prosthetic devices designed for individuals with physical disabilities, where accurate environmental interaction and haptic awareness are operationally essential. Traditional electronic technologies, such as piezoelectric, piezoresistive, capacitive, and triboelectric sensor arrays, have been considered promising due to their high temporal resolution, thin profiles, and compatibility with flexible or wearable platforms [190–194]. However, their utility in robotic manipulation is still constrained by limited spatial resolution, dense electrode wiring, signal crosstalk, electromagnetic interference, and mechanical fragility, which impede their ability to capture detailed contact information, including fine shape features, object textures, and multidimensional contact forces. Consequently, although electronic tactile sensors have enabled many advances in flexible and wearable sensing, their application to complex robotic manipulation tasks remains limited when high-resolution, large-area, and geometry-adaptive tactile perception is required.

Vision-tactile sensors have therefore become increasingly popular in robotic hands and grippers, mainly due to their high spatial resolution, low production cost, and ease of customization [195,196]. Compared with conventional tactile sensing technologies, vision-tactile sensors are characterized by a relatively simple design, typically comprising three essential components: a soft-skinned contact module, an illumination module, and a camera module. The contact module is integral to the transduction of physical contact into a visible optical pattern that can be imaged by the camera, which not only shortens fabrication time and enhances customization potential but also allows vision-tactile sensors to be adapted to diverse robotic platforms including fingertip sensors, soft grippers, prosthetic hands, surgical robots and teleoperated manipulation systems. In fields such as surgery and healthcare, vision-tactile sensor-equipped robots can perform delicate object manipulation and, when combined with haptic feedback, enable precise tactile-assisted procedures, thereby improving both the safety and dexterity of robotic systems in healthcare and service environments. Typically, a vision-tactile sensor captures tactile images of the internal sensing region using an integrated camera–illumination module as the soft contact interface responds to external stimuli. Through mechanisms such as contact-induced deformation, marker displacement, optical reflection, surface shading, and contact-dependent light transmission, physical interactions are encoded into high-resolution visual patterns [197–199]. These tactile images can then be interpreted using

computer vision, physics-based modelling, and machine-learning algorithms to recover rich contact information, including force distribution, contact pressure, surface texture, local geometry, object stiffness, and slip state, thereby enabling robots to perceive complex shapes and dynamic interactions with high accuracy.

Consequently, vision-tactile sensors have emerged as a highly versatile and cost-effective solution for a broad range of robotic tasks, from precision manipulation and advanced object recognition to medical examination, prosthetic sensing, and adaptive humanoid grasping. Recent advances in vision–tactile sensing have evolved from early optical reconstruction of surface texture and geometry to full-hand tactile embodiment for adaptive human-like grasping. As shown in Figure 10a, the early development of vision–tactile sensing can be traced to retrographic sensing, in which mechanical contact was first converted into optical topography for high-resolution surface measurement.[200] Johnson et al. reported a retrographic sensing method for measuring surface texture and shape, which was constructed from a transparent elastomer slab coated with a reflective elastic skin. When an external object was pressed against the sensing surface, the skin deformed and conformed to the local profile of the object, thereby generating a relief replica of its surface. This deformation was imaged from the reverse side through the transparent elastomer. By arranging red, green, and blue light sources at different positions, the device captured three direction-dependent shaded images in a single RGB frame. A tailored photometric stereo algorithm was then used to reconstruct the surface gradient and generate a 2.5D height map of the contacted object. A key advantage of this approach is that the object does not need to have a well-behaved optical reflectance, because the reflective elastomer skin provides a controlled bidirectional reflectance distribution function. Therefore, the proposed sensor can image surfaces that are difficult for conventional optical methods, including transparent, specular, or spatially varying materials. This work demonstrated that a reflective elastomer skin could convert object-induced surface deformation into optical shading patterns, which were further reconstructed into 2.5D tactile topography using photometric stereo. This principle established the fundamental basis of GelSight-type sensors, where camera-captured deformation images were used to recover contact geometry, surface texture, and eventually robotic tactile information for perception and manipulation.

Building on this optical topography principle, subsequent GelSight-based systems moved beyond static surface reconstruction toward the perception of material properties and dynamic contact behaviour. In Figure 10b, Yuan et al. extended GelSight-based tactile imaging to shape-independent hardness estimation using deep learning algorithms. The GelSight sensor contains a soft elastomeric contact layer and an embedded camera that records high-resolution tactile images during pressing. When the sensor contacts objects with different hardness, both the

object and the elastomer deform, leading to changes in contact curvature, surface-normal distribution, and marker displacement. Softer objects were more readily compressed during indentation, producing smoother tactile profiles with flattened ridges, whereas harder objects retained sharper surface features and generated more localized deformation patterns. By replacing handcrafted feature extraction and strictly controlled indentation protocols with an end-to-end convolutional–recurrent learning framework, the authors enabled hardness-related temporal deformation patterns to be learned directly from raw GelSight video sequences. This learning-based strategy enabled hardness estimation under loosely controlled contact conditions, including both manual pressing and robotic gripper pressing, without requiring precise control of contact force, trajectory, or loading speed. The sensor could estimate the hardness of objects with varied shapes across a Shore 00 range of 8–87, indicating that GelSight-derived vision–tactile signals encode not only contact geometry but also force- and material-dependent deformation dynamics. Overall, this study advanced optical tactile imaging from static surface reconstruction toward learning-enabled perception of intrinsic object properties.

Following the demonstration of high-resolution optical tactile perception, the development of compact vision-tactile sensor became a key step toward practical deployment in robotic fingertips and human-scale applications. As shown in Figure 10c, Di et al. developed DIGIT Pinki, a 15-mm-diameter vision-based tactile fingertip based on fiber-optic-bundle integration.[63] Conventional camera-based tactile sensors usually require the camera, lens, illumination unit, and optical path to be packaged within the fingertip. This configuration makes miniaturization difficult, especially when the target form factor approaches human-fingertip dimensions. In DIGIT Pinki, optical fiber bundles were used as both imaging and illumination conduits. The distal elastomer sensing element was therefore separated from the camera and supporting electronics, which were placed remotely from the fingertip. This design decoupled the fingertip size from the bulk of the optical and electronic components, enabling a compact 15-mm-diameter tactile sensor smaller than an average human fingertip. Despite this design reduced form factor, the sensor still maintained high performance of tactile information with a spatial resolution of 0.22 mm and a minimum force resolution of 5 mN for both normal and shear contact forces. The system was further demonstrated in robotic and teleoperated digital palpation, including prostate-gland examination. Compared with earlier GelSight-type devices that primarily emphasized high-resolution tactile imaging, this works advanced vision-tactile sensor toward miniaturized and human-scale platforms for medical palpation, constrained robotic manipulation, compact fingertips, and prosthetic interfaces.

Another important stage in the evolution of vision-tactile sensor is the transition from empirical device fabrication to computationally guided design. As shown in Figure 10d,

Agarwal *et al.* advanced vision-based tactile sensor development from trial-and-error prototyping to simulation-driven optical co-design.[201] The performance of GelSight-type sensors depends strongly on the configuration of the optical system, including sensor geometry, internal illumination, reflective coating, and light transport. However, these parameters are difficult to optimize experimentally, because even small variations in geometry or material can substantially alter the internal light field and, consequently, the reconstructed tactile image. To address this challenge, the authors developed a physically based rendering framework for the digital design of vision-based tactile sensors. The framework parameterizes sensor geometry, coating material, illumination location, and light type, and uses optical simulation to generate synthetic tactile images prior to fabrication. Sensor performance is then quantified using an evaluation metric that measures how accurately surface normal can be recovered from RGB tactile images. The optimized design improved surface-normal reconstruction and achieved approximately a fivefold improvement over a previous human-expert design in real-world robotic embossed-text detection.

More recently, the development of vision-tactile sensor has progressed not only in sensor design methodology, but also in the underlying sensing mechanism itself. Whereas recent efforts have introduced computationally guided frameworks to optimize optical architecture and imaging performance, another emerging direction has sought to expand what vision-based tactile sensors can fundamentally perceive. As shown in Figure 10e, Lin et al. reported LightTact, a visual–tactile fingertip sensor designed for deformation-independent contact sensing.[202] Most existing vision-based tactile sensors infer contact from macroscopic deformation of a soft elastomer surface. This strategy performs well for rigid or moderately soft objects, but becomes unreliable for liquids, semi-liquids, ultra-soft materials, thin films, and other contacts that produce little or no visible indentation. LightTact addresses this limitation through an ambient-blocking optical configuration. In non-contact regions, both external ambient light and internally generated illumination are suppressed by optical isolation, such that the corresponding pixels remain nearly black. At true contact regions, the air gap is eliminated and diffuse light from the contacted surface can reach the camera, producing a bright image that preserves local appearance. This mechanism enables direct visualization of contact without relying on measurable surface deformation. As a result, LightTact achieved robust pixel-level contact segmentation across a wide range of materials, contact forces, surface appearances, and illumination conditions. The sensor was further integrated into robotic systems to demonstrate manipulation tasks that are challenging for conventional deformation-based sensors, including water spreading, facial-cream dipping, ultra-thin film interaction, and vision-language-model-assisted resistor sorting. This work broadens the operating principle of

vision-tactile sensor from deformation-to-image transduction to contact-to-image transduction, which is particularly important for delicate manipulation, soft-material handling, and human–robot interaction. More importantly, it also points toward a broader transition of vision-tactile sensor from local contact imaging at a single sensing site to distributed tactile perception in robotic manipulators.

This transition is further reflected at the system level, where the latest development of vision–tactile sensing is moving from isolated fingertip sensors toward distributed tactile embodiment across robotic hands. In Figure 10f, Zhao et al. reported F-TAC Hand, a full-hand tactile-embedded biomimetic robotic hand that integrates high-resolution vision-based tactile sensing across a large portion of the hand surface.[60] Unlike many previous vision–tactile systems that were limited to a single fingertip or parallel gripper, F-TAC Hand embedded 17 vision-based tactile sensors in six optimized configurations across the fingers and palm. This design achieved 0.1-mm spatial resolution over approximately 70% of the hand surface while preserving a full range of human-like dexterity. The tactile sensing system used photometric stereo to convert light-intensity variations into surface-gradient information. An array of encoder–decoder neural networks then mapped the captured tactile images to surface-normal information, and a Poisson solver reconstructed high-fidelity contact geometries. In addition to the hardware integration, the system incorporated a generative algorithm to synthesize human-like grasp configurations and support tactile-informed closed-loop control. The hand was validated in complex manipulation tasks, including multi-object grasping under dynamic real-world conditions. Across 600 real-world trials, the tactile-embodied system significantly outperformed non-tactile-informed alternatives, highlighting the critical role of dense tactile feedback in adaptive manipulation. This work represents an important transition from local tactile imaging to full-hand tactile embodiment, suggesting that high-resolution distributed touch could become a key enabler of embodied intelligence by supporting more adaptive, robust, and human-like robotic interaction with the physical world. Overall, the vision–tactile sensing is evolving from a high-resolution tactile imaging technique into a highly integrated perception framework for wearable interfaces, prosthetic systems, teleoperation, soft robotics, and embodied machine intelligence.

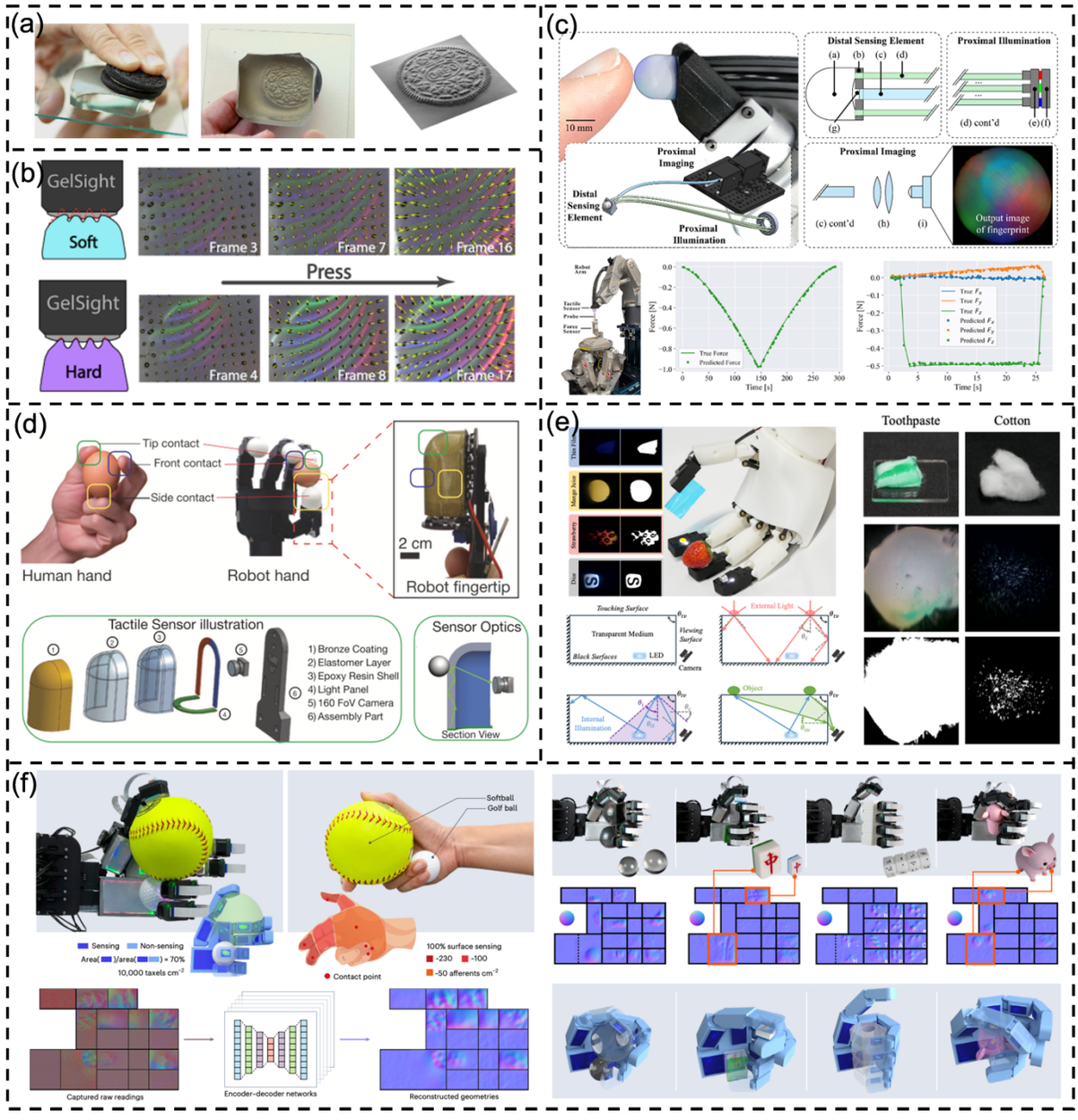


Figure 12. Recent advances in vision-tactile sensing for robotic perception. (a) GelSight-type optical tactile sensing for high-resolution reconstruction of contact geometry and surface topography. Reprinted with permission.[200] Copyright 2009 IEEE. (b) GelSight-based shape-independent hardness estimation using deep learning. Reprinted with permission.[203] Copyright 2017 IEEE. (c) DIGIT Pinki fiber-optic-bundle-based miniaturized vision-tactile fingertip. Reprinted with permission.[63] Copyright 2025 IEEE. (d) Simulation-driven optical co-design of vision-based tactile sensors. Reprinted with permission.[201] Copyright 2025 Springer Nature. (e) LightTact visual-tactile fingertip for contact-to-image transduction. Reprinted with permission. [202] Copyright 2025 The Author(s). (f) F-TAC Hand full-hand tactile-embedded biomimetic robotic hand. Reprinted with permission.[60] Copyright 2025 Springer Nature.

4.3 AI-enabled flexible electronic systems via near-sensor and in-sensor computing

Wearable sensor systems are evolving from passive signal-acquisition interfaces toward autonomous intelligent platforms that integrate flexible sensing, local computation, adaptive learning, and application-specific decision making.[204–207] Within the framework of

"Perception-Thought-Decision", the system first perceives the environment and acquires data through wearable sensors. Then, it relies on a knowledge base containing rules, models, and past experience for information processing, learning, and reasoning, forming a closed loop that evolves continuously through ongoing interaction. Within this architecture, wearable electronic systems constitute the critical interface for interacting with the physical world. By extending material optimization and device structural design toward flexibility and stretchability, wearable electronic systems can overcome the form-factor limitations of traditional rigid hardware.[208–212] This capability enables seamless integration with various complex surfaces and dynamic environments, thereby laying the foundation for intelligent perception. Together with mature micro-/nanofabrication, screen printing, additive manufacturing, and laser-cutting technologies, these methods provide a reliable basis for the scalable fabrication of high-performance flexible electronic devices.

However, an AI-enabled wearable platform is not merely a sensing unit; it requires the close coupling of compliant devices with low-power computational functions. A key research direction is therefore the optimization of where and how the "thinking" function is implemented within the system. Near-sensor and in-sensor computing architectures have been developed to shift part of the computational workload closer to, or directly into, the sensing elements.[213,214] By shortening the signal-transmission path, these architectures can reduce communication latency and energy consumption, which is essential for real-time, low-power, and autonomous wearable operation. As illustrated in Figure 13, AI-wearable electronic systems can be described through three closely related components: flexible sensing interfaces, edge-computing hardware, and data-analysis strategies. Their development is further shaped by computing architecture, algorithmic design, and application requirements.

At the device level, the sensing layer acts as the front-end interface that captures interactions between the device and the external environment. Owing to their bendability, stretchability, and mechanical compliance, flexible sensors can conformally attach to curved, irregular, or dynamically moving surfaces.[215–217] The detected physical or chemical stimuli are then transduced into electrical outputs. In conventional architectures, these analogue signals usually need to be digitized by analog-to-digital converters (ADCs) before further processing, which increases circuit complexity and power consumption.[218,219] To overcome this limitation, emerging signal-conversion and in-sensor processing strategies have been proposed to reduce, or even eliminate, the dependence on separate ADC modules. After signal acquisition, processors perform feature extraction, classification, decision-making, and actuator control, enabling closed-loop intelligent operation. Nevertheless, the rigidity of conventional chips may weaken the overall mechanical compatibility of wearable platforms. Flexible integrated circuits

and hybrid flexible–rigid electronic technologies therefore offer promising routes to combine computational capability with system-level conformability. In-sensor approaches employ transistors and memristors that are directly connected to flexible sensor networks, eliminating the need for ADCs and reducing data-transmission links. Although this approach offers high speed and efficiency, implementing complex machine learning models increases system complexity. Memristors, which mimic neuronal connections through variable resistance, are often used for neural network analog computing.[220–223] They can simultaneously perform storage and computation functions, thereby improving computational efficiency. However, memristors still face challenges related to manufacturing and stability. Analog signal processing can avoid the limitations of the von Neumann architecture. Breakthroughs beyond the von Neumann architecture enable efficient parallel computing and significantly enhance processing speed. Ultimately, at the application level, such intelligent wearable systems enable on-body health monitoring, human–machine interaction, and multisensory artificial receptors, thereby establishing a complete pathway from wearable perception to autonomous intelligence.

Advanced algorithms integrated into the processing unit facilitate the processing and analysis of data collected from wearable sensors, representing a key component for realizing AI-enabled wearable sensors.[224] As shown in Figure 13, data-analysis methods can be broadly classified into three categories: signal and statistical analytics, neural network learning, and brain-inspired computing. Early wearable sensors mainly relied on conventional signal-processing and statistical-analysis methods to extract meaningful information from raw sensing data. Classical methods, including filtering, correlation analysis, clustering, and classification, have been widely used to remove noise, identify signal patterns, and establish relationships between sensor responses and external stimuli.[217] By transforming raw electrical outputs into interpretable sensing features, these methods provide a fundamental level of intelligent perception for wearable systems. However, when facing nonlinear, multimodal, and high-dimensional signals generated by complex wearable systems, conventional methods often show limitations in feature representation, temporal modelling, and generalization capability.[225–227]

To address these challenges, neural networks have been increasingly introduced into wearable sensing platforms. Representative models include artificial neural networks (ANNs), convolutional neural networks (CNNs), recurrent neural networks (RNNs), and Transformer-based architectures.[228–230] These models enable more powerful automatic feature extraction, temporal-dependency modelling, and complex pattern recognition, thereby significantly improving the performance of wearable sensors in gesture recognition, physiological monitoring, speech decoding, and activity classification. However, as model size and network depth increase, deep neural networks (DNNs) are usually associated with higher computational

complexity, memory requirements, and energy consumption, which poses challenges for resource-constrained wearable devices, edge processors, and near-/in-sensor computing architectures.

In recent years, the field has further advanced toward brain-inspired computing, including spiking neural networks (SNNs), binary neural networks (BNNs), hyperdimensional computing (HDC), and vector symbolic architectures (VSAs).[30,231,232] Compared with conventional DNNs, these approaches offer advantages in event-driven processing, low-power inference, compact memory representation, and adaptive learning, making them particularly suitable for real-time, low-power, and resource-constrained wearable intelligent systems. Among them, VSA typically uses HDC to encode sensor data into high-dimensional hypervectors (HVs), enabling real-time on-chip computing and adaptive learning through updates of associative memory (AM). In terms of inference latency, ANN, BNN, and HDC models generally exhibit relatively low latency, CNNs typically show moderate latency, whereas DNNs often exhibit higher latency. SNNs, owing to their event-driven characteristics, show dynamic latency. In terms of power consumption, BNNs, SNNs, and HDC models generally achieve the lowest power consumption, ANNs and CNNs fall within a moderate power-consumption range, while DNNs consume the most power.[233–236] Regarding algorithmic complexity, BNNs and HDC models are relatively low in complexity, ANNs exhibit moderate complexity, whereas CNNs, SNNs, and DNNs generally involve higher complexity. Therefore, balancing recognition accuracy, inference latency, power consumption, and hardware complexity remain a major challenge for realizing autonomous intelligent wearable sensor systems based on near-sensor and in-sensor computing.

In parallel with the evolution of algorithms, the computing architecture of wearable sensors has also undergone a major transformation. In conventional cloud-computing architectures, wearable devices mainly function as front-end sensing nodes. The collected signals are transmitted to external computers, smartphones, or cloud servers for data storage, feature extraction, model inference, and decision making. This architecture benefits from powerful computational resources and is suitable for complex model training and large-scale data analysis. However, it also introduces several limitations, including high data-transmission latency, increased energy consumption, dependence on wireless connectivity, and potential privacy concerns associated with uploading personal physiological data. These limitations are particularly critical for real-time wearable applications that require rapid feedback, low-power operation, and data privacy. To overcome these limitations, wearable systems are moving toward edge-sensor computing. In this architecture, signal preprocessing, feature extraction, and model inference are locally performed by embedded processors, microcontrollers, flexible

hybrid circuits, or dedicated machine learning accelerators positioned close to the sensing units. Analog front-end circuits, ADCs, processors, wireless communication modules, and memory units are integrated into compact wearable platforms. By processing data near the human body rather than transmitting all raw signals to the cloud, edge computing reduces the communication burden, improves response speed, and enables real-time interaction. This system-level transition is particularly important for wearable sensors used in motion monitoring, electrophysiological signal decoding, closed-loop haptic feedback, and personalized healthcare, where immediate local interpretation of sensor signals is required.

A further development beyond edge computing is in-sensor computing, in which the sensing elements themselves participate in signal pre-processing, storage, or computation.[237] This architecture aims to break the conventional separation among sensing, memory, and processing, thereby reducing redundant data transmission and alleviating the bottleneck of von Neumann computing. In-sensor computing can be realized through various device concepts, including transistor-based sensing-processing units, memristive sensor arrays, neuromorphic tactile skins, capacitive analog computing arrays, and reservoir-computing sensory devices. In these systems, physical stimuli can be directly encoded into analog states, spikes, conductance changes, or high-dimensional representations, allowing sensor hardware to perform operations such as feature extraction, multiply–accumulate computation, temporal encoding, and associative learning. Such architectures are highly compatible with wearable sensors because they support low-latency, low-power, and distributed intelligence at the sensing interface. Therefore, the evolution from cloud computing to edge-sensor computing and ultimately to in-sensor computing represents a key technological route toward autonomous wearable intelligence.

The application landscape of intelligent wearable sensors reflects the transition from passive sensing to autonomous decision making. In on-body health monitoring, wearable sensors are increasingly used to continuously collect physiological and biochemical signals, including pulse, respiration, body temperature, sweat metabolites, electrophysiological activity, pressure distribution, and other health-related biomarkers.[238–240] When combined with local or in-sensor computing, these systems can perform real-time signal interpretation, abnormality detection, personalized diagnosis, and closed-loop health feedback without fully relying on external computing resources. These capabilities are essential for continuous healthcare, rehabilitation, chronic-disease management, sleep monitoring, and personalized medicine. In human–machine interaction, intelligent wearable sensors build a direct communication bridge between human motion, intention, and digital or robotic systems.[241–244] Flexible strain sensors, pressure sensors, electrophysiological sensors, smart gloves, acoustic sensors, and multimodal

wearable interfaces can capture gestures, body motions, muscle activities, speech-related signals, and tactile information. Through edge or in-sensor learning, these signals can be rapidly decoded into commands for virtual reality, augmented reality, robotic control, prosthetic operation, and immersive interaction. Compared with cloud-based recognition systems, locally intelligent wearable interfaces offer faster response, improved privacy, and better adaptability to individual users, which are crucial for practical human–machine collaboration. Beyond single-modality sensing, wearable systems are also evolving toward multisensory artificial receptors that mimic the distributed and integrated perception mechanisms of biological sensory systems.[245–247] By combining pressure, strain, temperature, chemical, humidity, electrophysiological, and optical sensing with neuromorphic or bioinspired computing, these systems can achieve multimodal fusion, cross-modal perception, and adaptive environmental awareness. Such multisensory receptors are important for electronic skins, soft robotics, artificial prostheses, smart textiles, and embodied robotic sensing systems. They allow wearable devices not only to detect isolated stimuli but also to interpret complex physical and chemical contexts in a more human-like manner.

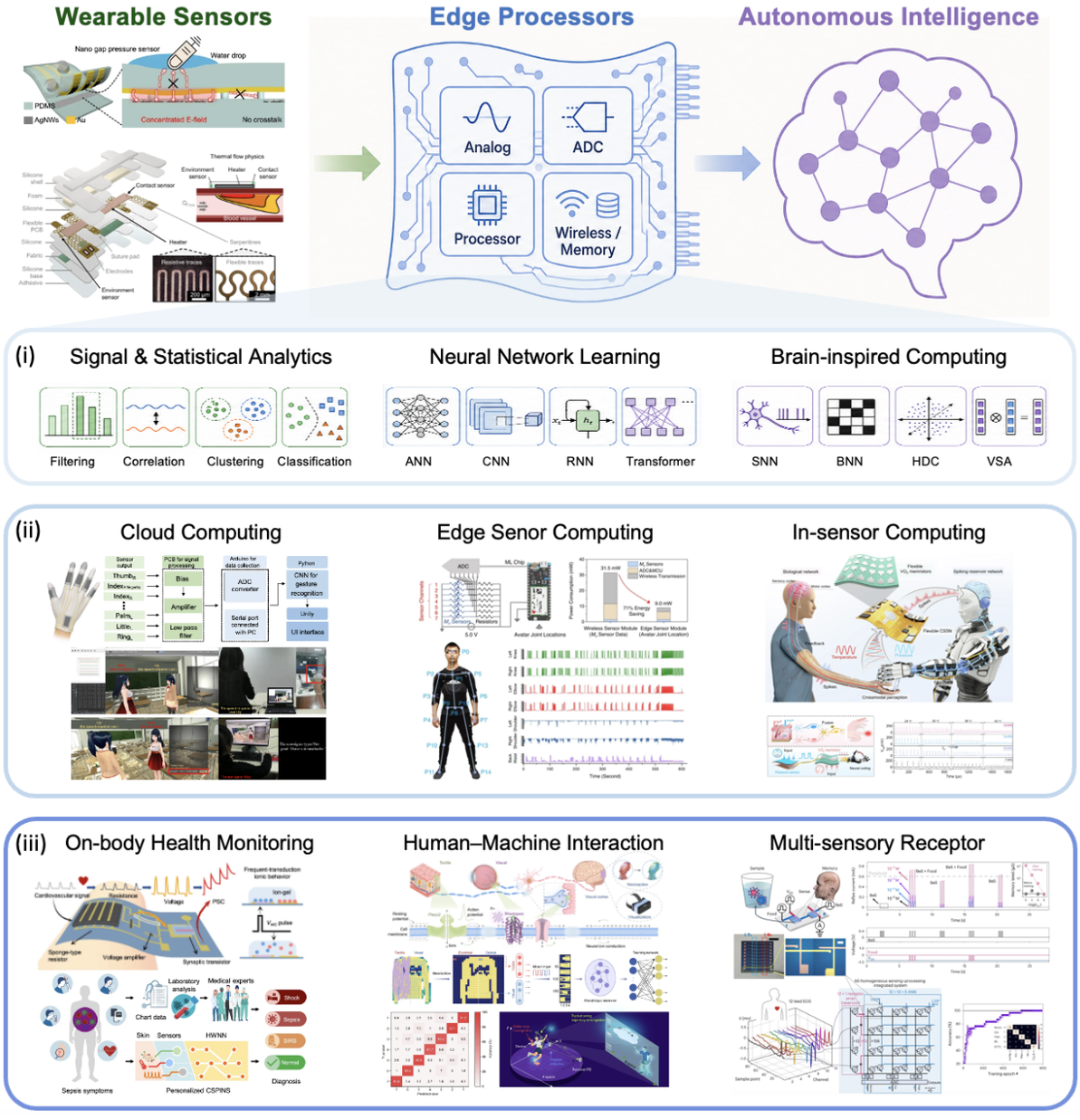


Figure 13. Comparison of in-sensor computing, near-sensor computing, and computer-aided computing as well as their implementation methods and applications. Wearable sensors. Reprinted with permission.[211] Copyright 2025 Springer Nature. Reprinted with permission.[212] Copyright 2025 Springer Nature. Example of cloud computing. Reprinted with permission.[206] Copyright 2021 Springer Nature. Example of edge sensor computing. Reprinted with permission.[70] Copyright 2022 Springer Nature. Example of in-sensor computing. Reprinted with permission.[207] Copyright 2024 Springer Nature. Application of on-body health monitoring. Reprinted with permission.[240] Copyright 2025 Springer Nature. Application of human-machine interaction. Reprinted with permission.[244] Copyright 2026 Springer Nature. Application of multi-sensory receptor. Reprinted with permission.[214] Copyright 2023 Springer Nature.

5 Conclusion

From early wearable sensing interfaces for physiological and motion monitoring to the latest developments in soft tactile systems, self-powered wearables, vision–tactile sensing, and near-/in-sensor computing, wearable tactile technologies have undergone a profound transition

from passive signal acquisition toward interactive and intelligent perception. Advances in flexible electronics, smart textiles, hydrogels, MEMS tactile sensors, and multimodal sensing architectures have enabled wearable systems to capture pressure, strain, motion, temperature, and contact information with improved sensitivity, mechanical compliance, and body-conformal integration. At the same time, the convergence between wearable tactile sensing and robotic perception has expanded the role of tactile systems beyond human monitoring, supporting applications in surgical robots, prosthetic interfaces, dexterous manipulation, immersive human–machine interaction, and embodied intelligence.

In this review, we summarized recent progress in wearable tactile systems from three interconnected perspectives. First, advanced wearable sensors and applications, including hydrogel-based interfaces, MEMS tactile sensors, and tactile sensing systems for surgical robots, were discussed as representative platforms for high-performance and application-specific tactile perception. Second, self-powered wearable sensors and systems were reviewed, covering metamaterial-based wireless body sensor networks, functional fibers, wearable energy harvesters, and textile-based energy-harvesting systems. These technologies address the long-standing limitations of wired connections, battery dependence, and frequent recharging, thereby supporting long-term, distributed, and sustainable wearable operation. Third, emerging directions toward autonomous intelligence were highlighted, including wearable haptic feedback interfaces, vision–tactile sensing for robotic perception, AI-assisted wearable systems, and near-sensor, in-sensor, and edge computing architectures. Together, these advances indicate that wearable tactile systems are evolving into closed-loop platforms that integrate sensing, energy harvesting, wireless communication, computation, feedback, and actuation.

Despite this progress, several challenges remain before fully autonomous wearable tactile systems can be widely realized. Long-term mechanical reliability, biocompatibility, breathability, and user comfort remain critical for practical on-body deployment. For high-density tactile arrays and multimodal systems, signal crosstalk, calibration drift, data redundancy, and robust decoupling of multiple stimuli still require further optimization. Self-powered wearable systems also face limitations in energy conversion efficiency, power management, and stable operation under irregular human motion. In addition, although machine learning and edge computing have greatly improved tactile perception and decision-making, current systems often still depend on external processors or cloud-based analysis, which can introduce latency, energy overhead, privacy concerns, and connectivity constraints. Achieving real-time autonomous operation therefore requires closer co-design of materials, device structures, circuits, algorithms, and system-level integration.

Looking forward, the future of wearable tactile systems will be shaped by the integration of soft materials, self-powered architectures, intelligent computation, and adaptive feedback within unified platforms. High-resolution vision–tactile sensors may provide richer contact information for robotic and prosthetic systems, while haptic interfaces can close the loop between tactile perception and human sensation. Energy-harvesting textiles and wireless body sensor networks may enable more sustainable and maintenance-free wearable platforms. Meanwhile, near-sensor and in-sensor computing will move intelligence closer to the physical interface, reducing data transmission and enabling faster, more private, and more energy-efficient decision-making. Through these converging directions, wearable tactile systems are expected to progress from flexible sensing devices into autonomous intelligent interfaces that seamlessly connect humans, robots, and environments.

Acknowledgements

This work is supported by The National Foreign Experts Program (S20250239) in Hubei University of Technology, the Research Platform for Biomedical and Health Technology (RP-BTH-Prof. LEE Chengkuo) in NUS (Suzhou) Research Insititute, NUS College of Design and Engineering (CDE)-Robotics Seed Grant Programme, “AI-Sensor Enhanced Medical Operation Training System (A-8003283-00-00)”, NUS College of Design and Engineering (CDE)-Robotics Seed Grant Programme, “A Multimodal Sensing/ Haptic System For lower-Limb Exoskeleton Feedback Control (A-8003281-00-00)”

Data Availability Statement

((include as appropriate, including link to repository))

Received: ((will be filled in by the editorial staff))
Revised: ((will be filled in by the editorial staff))
Published online: ((will be filled in by the editorial staff))

References

[1] Q. Shi, B. Dong, T. He, Z. Sun, J. Zhu, Z. Zhang, C. Lee, *InfoMat* **2020**, *2*, 1131.

[2] F. Arab Hassani, Q. Shi, F. Wen, T. He, A. Haroun, Y. Yang, Y. Feng, C. Lee, *Smart Mater. Med.* **2020**, *1*, 92.

[3] H. Souri, H. Banerjee, A. Jusufi, N. Radacsi, A. A. Stokes, I. Park, M. Sitti, M. Amjadi, *Adv. Intell. Syst.* **2020**, *2*, 2000039.

[4] P. H. Veltink, H. J. Bussmann, W. de Vries, W. J. Martens, R. C. Van Lummel, *IEEE Trans. Rehabil. Eng.* **1996**, *4*, 375.

[5] Shih-Chin Gong, Chengkuo Lee, *IEEE Sens. J.* **2001**, *1*, 340.

[6] C. V. C. Bouten, K. T. M. Koekkoek, M. Verduin, R. Kodde, J. D. Janssen, *IEEE Trans. Biomed. Eng.* **1997**, *44*, 136.

[7] S. Lee, W. Y. X. Peh, J. Wang, F. Yang, J. S. Ho, N. V. Thakor, S. C. Yen, C. Lee, *Adv. Sci.* **2017**, *4*, DOI 10.1002/advs.201700149.

[8] T. Liu, M. Zhang, Z. Li, H. Dou, W. Zhang, J. Yang, P. Wu, D. Li, X. Mu, *Nat. Commun.* **2025**, *16*, 2363.

[9] F. Wen, T. He, H. Liu, H. Y. Chen, T. Zhang, C. Lee, *Nano Energy* **2020**, *78*, 105155.

[10] J. Wang, H. Wang, N. V. Thakor, C. Lee, *ACS Nano* **2019**, *13*, 3589.

[11] Y. Yang, X. Guo, M. Zhu, Z. Sun, Z. Zhang, T. He, C. Lee, *Adv. Energy Mater.* **2023**, *13*, 1.

[12] C. Xu, Y. Song, J. R. Sempionatto, S. A. Solomon, Y. Yu, H. Y. Y. Nyein, R. Y. Tay, J. Li, W. Heng, J. Min, A. Lao, T. K. Hsiai, J. A. Sumner, W. Gao, *Nat. Electron.* **2024**, *7*, 168.

[13] N. Kumar Koditala, P. Shekar Pandey, in *2018 Int. Conf. Res. Intell. Comput. Eng.*, IEEE, **2018**, pp. 1–5.

[14] Z. Zhou, K. Chen, X. Li, S. Zhang, Y. Wu, Y. Zhou, K. Meng, C. Sun, Q. He, W. Fan, E. Fan, Z. Lin, X. Tan, W. Deng, J. Yang, J. Chen, *Nat. Electron.* **2020**, *3*, 571.

[15] J. H. Han, K. M. Bae, S. K. Hong, H. Park, J. Kwak, H. S. Wang, D. J. Joe, J. H. Park, Y. H. Jung, S. Hur, C. D. Yoo, K. J. Lee, *Nano Energy* **2018**, *53*, 658.

[16] P. Pitchappa, M. Manjappa, C. P. Ho, Y. Qian, R. Singh, N. Singh, C. Lee, *Appl. Phys. Lett.* **2016**, *108*, 111102.

[17] C. Xu, Z. Ren, H. Zhou, J. Zhou, D. Li, C. Lee, *Adv. Funct. Mater.* **2024**, *34*, 2314482.

[18] F. Wen, H. Wang, T. He, Q. Shi, Z. Sun, M. Zhu, Z. Zhang, Z. Cao, Y. Dai, T. Zhang, C. Lee, *Nano Energy* **2020**, *67*, 104266.

[19] H. Li, H. Gong, T. H. Wong, J. Zhou, Y. Wang, L. Lin, Y. Dou, H. Jia, X. Huang, Z. Gao, R. Shi, Y. Huang, Z. Chen, W. PARK, J. Y. Li, H. Chu, S. Jia, H. Wu, M. Wu, Y.

Liu, D. Li, J. Li, G. Xu, T. Chang, B. Zhang, Y. Gao, J. Su, H. Bai, J. Hu, C. K. Yiu, C. Xu, W. Hu, J. Huang, L. Chang, X. Yu, *Nat. Commun.* **2023**, *14*, 7539.

[20] K. J. Won, H. Mengdi, X. Zhaoqian, C. H. Uk, L. J. Yoon, A. Raudel, Y. Jessica, C. Xuexian, L. Cunman, P. Manish, J. Inhwa, K. Jongwon, N. Myeong, K. Kyeongha, G. Xu, O. Christopher, G. Dominic, R. Dennis, K. D. Hyun, M. Surabhi, L. Claire, Y. Da Som, P. Yoonseok, C. Ryan, B. Anthony, X. Shuai, H. Yonggang, F. Stefania, R. J. A., J. W. Kwak, M. Han, Z. Xie, H. U. Chung, J. Y. Lee, R. Avila, J. Yohay, X. Chen, C. Liang, M. Patel, I. Jung, J. Kim, M. Namkoong, K. Kwon, X. Guo, C. Ogle, D. Grande, D. Ryu, D. H. Kim, S. Madhvapathy, C. Liu, D. S. Yang, Y. Park, R. Caldwell, A. Banks, S. Xu, Y. Huang, S. Fatone, J. A. Rogers, *Sci. Transl. Med.* **2020**, *12*, eabc4327.

[21] N. Li, L. Liu, Y. Liu, J. Leng, *Adv. Funct. Mater.* **2024**, *34*, 1.

[22] M. Kang, H. G. Choi, K. Park, S. Pyo, *Adv. Funct. Mater.* **2025**, *35*, 1.

[23] X. Zhu, K. Wu, X. Xie, S. W. Anderson, X. Zhang, *Nat. Commun.* **2024**, *15*, 1.

[24] Q. Zeng, X. Tian, D. T. Nguyen, C. Li, P. Chia, B. C. K. Tee, C. Wu, J. S. Ho, *Nat. Electron.* **2024**, *7*, 1025.

[25] Z. Li, Z. Liu, Z. Wang, Y. Deng, S. Yang, J. Chen, Q. Zeng, Y. Zhong, H. Yang, Z. Xiong, X. Tian, G. Li, Y. Chen, H. Jing, J. S. Ho, C. W. Qiu, *Nat. Electron.* **2026**, *9*, DOI 10.1038/s41928-025-01516-w.

[26] L. Xu, S. Zhong, T. Yue, Z. Zhang, X. Lu, Y. Lin, L. Li, Y. Tian, T. Jin, Q. Zhang, C. Lee, *EcoMat* **2024**, *6*, 1.

[27] C.-H. Chen, P.-W. Lee, Y.-H. Tsao, Z.-H. Lin, *Nano Energy* **2017**, *42*, 241.

[28] A. Moin, A. Zhou, A. Rahimi, A. Menon, S. Benatti, G. Alexandrov, S. Tamakloe, J. Ting, N. Yamamoto, Y. Khan, F. Burghardt, L. Benini, A. C. Arias, J. M. Rabaey, *Nat. Electron.* **2020**, *4*, 54.

[29] G. Moon, J. R. Choi, C. Lee, Y. Oh, K. H. Kim, D. Kim, *Biosens. Bioelectron.* **2020**, *164*, DOI 10.1016/j.bios.2020.112335.

[30] A. Moin, A. Zhou, A. Rahimi, A. Menon, S. Benatti, G. Alexandrov, S. Tamakloe, J. Ting, N. Yamamoto, Y. Khan, F. Burghardt, L. Benini, A. C. Arias, J. M. Rabaey, *Nat. Electron.* **2021**, *4*, 54.

[31] T. He, Q. Shi, H. Wang, F. Wen, T. Chen, J. Ouyang, C. Lee, *Nano Energy* **2019**, *57*, 338.

[32] J. Zhu, M. Cho, Y. Li, T. He, J. Ahn, J. Park, T. L. Ren, C. Lee, I. Park, *Nano Energy* **2021**, *86*, 106035.

[33] Q. Abbas, A. Alsheddy, *IEEE Access* **2021**, *9*, 47530.

[34] X. Lu, H. Tan, H. Zhang, W. Wang, S. Xie, T. Yue, F. Chen, *Nat. Commun.* **2025**, *16*,

1080.

[35] Y. Xu, Z. Sun, Z. Bai, H. Shen, R. Wen, F. Wang, G. Xu, C. Lee, *Nat. Commun.* **2024**, *15*, 6022.

[36] J. C. Yang, J. Mun, S. Y. Kwon, S. Park, Z. Bao, S. Park, *Adv. Mater.* **2019**, *31*, 1904765.

[37] Z. Zhang, T. He, M. Zhu, Z. Sun, Q. Shi, J. Zhu, B. Dong, M. R. Yuce, C. Lee, *npj Flex. Electron.* **2020**, *4*, 29.

[38] P. Arens, D. A. Quirk, W. Pan, Y. Yacoby, F. Doshi-Velez, C. J. Walsh, *Sci. Adv.* **2025**, *11*, eadu2099.

[39] N. J. Holter, *Science (80-.).* **1961**, *134*, 1214.

[40] C. Gopalsamy, S. Park, R. Rajamanickam, S. Jayaraman, *Virtual Real.* **1999**, *4*, 152.

[41] W. A. Gill, I. Howard, I. Mazhar, K. McKee, *Sensors* **2022**, *22*, DOI 10.3390/s22197405.

[42] D. H. Kim, J. Song, M. C. Won, H. S. Kim, R. H. Kim, Z. Liu, Y. Y. Huang, K. C. Hwang, Y. W. Zhang, J. A. Rogers, *Proc. Natl. Acad. Sci. U. S. A.* **2008**, *105*, 18675.

[43] H. C. Ko, G. Shin, S. Wang, M. P. Stoykovich, J. W. Lee, D. Kim, J. S. Ha, Y. Huang, K. Hwang, J. A. Rogers, *Small* **2009**, *5*, 2703.

[44] T. Ding, K. H. Chan, Y. Zhou, X.-Q. Wang, Y. Cheng, T. Li, G. W. Ho, *Nat. Commun.* **2020**, *11*, 6006.

[45] J. Lee, S. J. Ihle, G. S. Pellegrino, H. Kim, J. Yea, C. Y. Jeon, H. C. Son, C. Jin, D. Eberli, F. Schmid, B. L. Zambrano, A. F. Renz, C. Forró, H. Choi, K. I. Jang, R. Küng, J. Vörös, *Nat. Electron.* **2021**, *4*, 291.

[46] B. C.-K. Tee, A. Chortos, A. Berndt, A. K. Nguyen, A. Tom, A. McGuire, Z. C. Lin, K. Tien, W.-G. Bae, H. Wang, P. Mei, H.-H. Chou, B. Cui, K. Deisseroth, T. N. Ng, Z. Bao, *Science (80-.).* **2015**, *350*, 313.

[47] H. Yuk, J. Wu, X. Zhao, *Nat. Rev. Mater.* **2022**, *7*, 935.

[48] A. K. Mishra, T. J. Wallin, W. Pan, P. Xu, K. Wang, E. P. Giannelis, B. Mazzolai, R. F. Shepherd, *Sci. Robot.* **2020**, *5*, eaaz3918.

[49] L. Huang, S. Lin, Z. Xu, H. Zhou, J. Duan, B. Hu, J. Zhou, *Adv. Mater.* **2020**, *32*, 1902034.

[50] Z. Bai, T. He, Z. Zhang, Y. Xu, Z. Zhang, Q. Shi, Y. Yang, B. Zhou, M. Zhu, J. Guo, C. Lee, *Nano Energy* **2022**, *94*, 106956.

[51] Q. Shi, T. He, C. Lee, *Nano Energy* **2019**, *57*, 851.

[52] C. Wang, T. He, H. Zhou, Z. Zhang, C. Lee, *Bioelectron. Med.* **2023**, *9*, 17.

[53] X. Guo, T. He, Z. Zhang, A. Luo, F. Wang, E. J. Ng, Y. Zhu, H. Liu, C. Lee, *ACS*

Nano **2021**, *15*, 19054.

[54] Y. Pang, X. Zhu, T. He, S. Liu, Z. Zhang, Q. Lv, P. Yi, C. Lee, *Adv. Mater.* **2024**, *2404763*, 1.

[55] M. Zhu, Z. Sun, Z. Zhang, Q. Shi, T. He, H. Liu, T. Chen, C. Lee, *Sci. Adv.* **2020**, *6*, DOI 10.1126/sciadv.aaz8693.

[56] Z. Sun, Z. Zhang, C. Lee, *Nat. Electron.* **2023**, *6*, 941.

[57] B. Dong, Z. Zhang, Q. Shi, J. Wei, Y. Ma, Z. Xiao, C. Lee, *Sci. Adv.* **2022**, *8*, eabl9874.

[58] S. Duan, Q. Shi, J. Hong, D. Zhu, Y. Lin, Y. Li, W. Lei, C. Lee, J. Wu, *ACS Nano* **2023**, *17*, 1355.

[59] H. Guo, X. Pu, J. Chen, Y. Meng, M. H. Yeh, G. Liu, Q. Tang, B. Chen, D. Liu, S. Qi, C. Wu, C. Hu, J. Wang, Z. L. Wang, *Sci. Robot.* **2018**, *3*, 1.

[60] Z. Zhao, W. Li, Y. Li, T. Liu, B. Li, M. Wang, K. Du, H. Liu, Y. Zhu, Q. Wang, K. Althoefer, S. C. Zhu, *Nat. Mach. Intell.* **2025**, *7*, 889.

[61] M. Wang, Z. Yan, T. Wang, P. Cai, S. Gao, Y. Zeng, C. Wan, H. Wang, L. Pan, J. Yu, S. Pan, K. He, J. Lu, X. Chen, *Nat. Electron.* **2020**, *3*, 563.

[62] S. Gao, Y. Dai, A. Nathan, *Adv. Intell. Syst.* **2022**, *4*, 2100074.

[63] J. Di, Z. Dugonjic, W. Fu, T. Wu, R. Mercado, K. Sawyer, V. R. Most, G. Kammerer, S. Speidel, R. E. Fan, G. Sonn, M. R. Cutkosky, M. Lambeta, R. Calandra, *IEEE Trans. Robot.* **2025**, *41*, 62.

[64] B. Li, P. Chen, H. Liu, W. Guo, X. Cao, J. Du, C. Zhao, J. Zhang, *Nat. Comput. Sci.* **2021**, *1*, 221.

[65] Z. Zhang, X. Liu, H. Zhou, S. Xu, C. Lee, *Small Struct.* **2024**, *5*, DOI 10.1002/sstr.202300325.

[66] W. Y. B. Lim, Z. Xiong, D. Niyato, X. Cao, C. Miao, S. Sun, Q. Yang, **2022**, 1.

[67] F. Zhou, Y. Chai, *Nat. Electron.* **2020**, *3*, 664.

[68] X. Liu, C. Sun, Z. Guo, X. Xia, Q. Jiang, X. Ye, J. Shang, Y. Zhang, X. Zhu, R. Li, *Adv. Sci.* **2023**, *10*, 29.

[69] Z. Ren, Z. Zhang, Y. Zhuge, Z. Xiao, S. Xu, J. Zhou, C. Lee, *Nano-Micro Lett.* **2025**, *17*, 261.

[70] Z. Li, Z. Li, W. Tang, J. Yao, Z. Dou, J. Gong, Y. Li, B. Zhang, Y. Dong, J. Xia, L. Sun, P. Jiang, X. Cao, R. Yang, X. Miao, R. Yang, *Nat. Commun.* **2024**, *15*, DOI 10.1038/s41467-024-51609-x.

[71] M. Bai, Y. Chen, L. Zhu, Y. Li, T. Ma, Y. Li, M. Qin, W. Wang, Y. Cao, B. Xue, *Nat. Commun.* **2024**, *15*, DOI 10.1038/s41467-024-54879-7.

[72] Y. Wang, Q. Geng, H. Lyu, W. Sun, X. Fan, K. Ma, K. Wu, J. Wang, Y. Wang, D.

Mei, C. Guo, P. Xiu, D. Pan, K. Tao, *Adv. Mater.* **2024**, *36*, 1.

[73] Z. Wang, N. Li, X. Yang, Z. Zhang, H. Zhang, X. Cui, *Microsystems Nanoeng.* **2024**, *10*, DOI 10.1038/s41378-024-00693-6.

[74] Y. Fang, H. Ouyang, Y. Cheng, Y. Zhou, L. Shi, J. Sun, G. W. Ho, R. Wang, *Nat. Commun.* **2025**, 1.

[75] X. Lu, Y. Chen, Y. Zhang, J. Cheng, K. Teng, Y. Chen, J. Shi, D. Wang, L. Wang, S. You, Z. Feng, Q. An, *Adv. Mater.* **2024**, *36*, 1.

[76] X. Guo, Z. Sun, Y. Zhu, C. Lee, *Adv. Mater.* **2024**, *2406778*, 1.

[77] Z. Hui, Y. Wang, Z. Zhang, R. Zhang, J. Zhou, W. Hou, L. Yin, H. Dai, Z. Xia, T. Zhang, W. Huang, G. Sun, *Adv. Mater.* **2025**, *37*, 1.

[78] Y. Yan, L. Yu, X. Zhang, Q. Han, Z. Yang, X. Lu, J. Wang, H. Xu, Q. Chen, H. Zhao, *Nat. Commun.* **2025**, *16*, DOI 10.1038/s41467-025-55996-7.

[79] K. W. K. Tang, J. Jeong, J. C. Hsieh, M. Yao, H. Ding, W. Wang, X. Liu, I. Pyatnitskiy, W. He, W. D. Moscoso-Barrera, A. R. Lozano, B. Artman, H. Huh, P. S. Wilson, H. Wang, *Nat. Commun.* **2025**, *16*, DOI 10.1038/s41467-025-60181-x.

[80] I. Almuteb, R. Hua, Y. Wang, *Smart Heal.* **2022**, *25*, 100301.

[81] S. Subramaniam, S. Majumder, A. I. Faisal, M. J. Deen, *Sensors* **2022**, *22*, 438.

[82] X. Wu, Y. Khan, J. Ting, J. Zhu, S. Ono, X. Zhang, S. Du, J. W. Evans, C. Lu, A. C. Arias, *Adv. Electron. Mater.* **2020**, *6*, DOI 10.1002/aelm.201901310.

[83] B. Baro, S. Khimhun, U. Das, S. Bayan, *Nano Energy* **2023**, *108*, 108212.

[84] Y. Tian, L. Zhang, C. Zhang, B. Bao, Q. Li, L. Wang, Z. Song, D. Li, *Exploration* **2024**, *4*, DOI 10.1002/EXP.20230109.

[85] X. Wu, Y. Khan, J. Ting, J. Zhu, S. Ono, X. Zhang, S. Du, J. W. Evans, C. Lu, A. C. Arias, *Adv. Electron. Mater.* **2020**, *6*, DOI 10.1002/aelm.201901310.

[86] S. Hu, H. Li, W. Lu, T. Han, Y. Xu, X. Shi, Z. Peng, X. Cao, *Adv. Funct. Mater.* **2024**, *34*, 1.

[87] W. Li, K. Zou, J. Guo, C. Zhang, J. Feng, J. You, G. Cheng, Q. Zhou, M. Kong, G. Li, C. F. Guo, J. Yang, *ACS Nano* **2024**, *18*, 14672.

[88] H. Zhou, Y. Gui, G. Gu, H. Ren, W. Zhang, Z. Du, G. Cheng, *Small* **2025**, *21*, 1.

[89] A. Mensah, S. Liao, J. Amesimeku, J. Li, Y. Chen, Y. Hao, J. Yang, Q. Wang, F. Huang, Y. Liu, Q. Wei, P. Lv, *Adv. Fiber Mater.* **2024**, *6*, 1746.

[90] J. Shi, S. Liu, L. Zhang, B. Yang, L. Shu, Y. Yang, M. Ren, Y. Wang, J. Chen, W. Chen, Y. Chai, X. Tao, *Adv. Mater.* **2020**, *32*, 1901958.

[91] Q. Zheng, X. Dai, Y. Wu, Q. Liang, Y. Wu, J. Yang, B. Dong, G. Gao, Q. Qin, L. Huang, *BMEMat* **2023**, *1*, 1.

[92] Y. Yang, T. He, P. Ravindran, F. Wen, P. Krishnamurthy, L. Wang, Z. Zhang, P. P. Kumar, E. Chae, C. Lee, *Sci. Adv.* **2024**, *10*, 1.

[93] Q. Shi, Z. Zhang, T. He, Z. Sun, B. Wang, Y. Feng, X. Shan, B. Salam, C. Lee, *Nat. Commun.* **2020**, *11*, 4609.

[94] T. He, H. Wang, J. Wang, X. Tian, F. Wen, Q. Shi, J. S. Ho, C. Lee, *Adv. Sci.* **2019**, *6*, DOI 10.1002/advs.201901437.

[95] Y. Hao, Z. Zhang, Y. Chen, S. Wang, Y. Tong, P. Lv, Q. Wei, C. Lee, *Nano-Micro Lett.* **2026**, *18*, 198.

[96] X. Guo, Z. Sun, Y. Zhu, C. Lee, *Adv. Mater.* **2024**, *36*, 2406778.

[97] Q. Wang, H. Guan, C. Wang, P. Lei, H. Sheng, H. Bi, J. Hu, C. Guo, Y. Mao, J. Yuan, M. Shao, Z. Jin, J. Li, W. Lan, *Sci. Adv.* **2025**, *11*, DOI 10.1126/sciadv.adu1598.

[98] M. Chen, X. An, F. Zhao, P. Chen, J. Wang, M. Zhang, A. Lu, *Nano-Micro Lett.* **2025**, *17*, 205.

[99] Y. Luo, Y. Li, P. Sharma, W. Shou, K. Wu, M. Foshey, B. Li, T. Palacios, A. Torralba, W. Matusik, *Nat. Electron.* **2021**, *4*, 193.

[100] B. Ying, X. Liu, *iScience* **2021**, *24*, 103174.

[101] R. Xu, T. Xu, M. She, X. Ji, G. Li, S. Zhang, X. Zhang, H. Liu, B. Sun, G. Shen, M. Tian, *Nano-Micro Lett.* **2025**, *17*, 90.

[102] D. Han, Y. Cai, X. Wang, W. Zhang, X. Li, Z. Hou, J. Liu, D. Song, W. Xu, *Adv. Funct. Mater.* **2025**, *35*, 2501362.

[103] L. Song, Z. Wang, S. Chen, Y. Shen, J. Yin, R. Wang, *Adv. Mater.* **2025**, *37*, 2417978.

[104] L. Wang, X. Guo, Z. Zhang, C. Lee, *Adv. Funct. Mater.* **2026**, *36*, 1.

[105] B. Hu, D. Xu, Y. Shao, Z. Nie, P. Liu, J. Li, L. Zhou, P. Wang, N. Huang, J. Liu, Y. Lu, Z. Wu, B. Wang, Y. Mei, M. Han, R. Li, E. Song, *Sci. Adv.* **2024**, *10*, eadp8804.

[106] N. Thanh-Vinh, N. Binh-Khiem, H. Takahashi, K. Matsumoto, I. Shimoyama, *Sensors Actuators, A Phys.* **2014**, *215*, 167.

[107] M. Han, L. Chen, K. Aras, C. Liang, X. Chen, H. Zhao, K. Li, N. R. Faye, B. Sun, J.-H. Kim, W. Bai, Q. Yang, Y. Ma, W. Lu, E. Song, J. M. Baek, Y. Lee, C. Liu, J. B. Model, G. Yang, R. Ghaffari, Y. Huang, I. R. Efimov, J. A. Rogers, *Nat. Biomed. Eng.* **2020**, *4*, 997.

[108] Z. Liu, X. Hu, R. Bo, Y. Yang, X. Cheng, W. Pang, Q. Liu, Y. Wang, S. Wang, S. Xu, Z. Shen, Y. Zhang, *Science (80-.).* **2024**, *384*, 987.

[109] S. M. Won, H. Wang, B. H. Kim, K. Lee, H. Jang, K. Kwon, M. Han, K. E. Crawford, H. Li, Y. Lee, X. Yuan, S. B. Kim, Y. S. Oh, W. J. Jang, J. Y. Lee, S. Han, J. Kim, X. Wang, Z. Xie, Y. Zhang, Y. Huang, J. A. Rogers, *ACS Nano* **2019**, *13*, 10972.

[110] H. Oh, G. C. Yi, M. Yip, S. A. Dayeh, *Sci. Adv.* **2020**, *6*, 1.
[111] J. Weichart, C. Roman, C. Hierold, *J. Microelectromechanical Syst.* **2021**, *30*, 915.
[112] C. Xu, Y. Wang, J. Zhang, J. Wan, Z. Xiang, Z. Nie, J. Xu, X. Lin, P. Zhao, Y. Wang, S. Zhang, J. Zhang, C. Liu, N. Xue, W. Zhao, M. Han, *Sci. Adv.* **2024**, *10*, eadp6094.
[113] P. Wang, C. Zhang, B. Li, X. Meng, Y. Ding, J. Zhang, S. Niu, Z. Han, L. Lin, L. Ren, *Sci. Adv.* **2025**, *11*, eady5008.
[114] D. A. Aubeeluck, C. Forbrigger, S. Mohseni Taromsari, T. Chen, E. Diller, H. E. Naguib, *ACS Appl. Electron. Mater.* **2024**, *6*, 6365.
[115] W. Othman, Z.-H. A. Lai, C. Abril, J. S. Barajas-Gamboa, R. Corcelles, M. Kroh, M. A. Qasaimeh, *Front. Robot. AI* **2022**, *8*, DOI 10.3389/frobt.2021.705662.
[116] T.-H. Chang, Y. Tian, C. Li, X. Gu, K. Li, H. Yang, P. Sanghani, C. M. Lim, H. Ren, P.-Y. Chen, *ACS Appl. Mater. \& Interfaces* **2019**, *11*, 10226.
[117] A. Gerald, S. Russo, *Nat. Rev. Mater.* **2024**, *9*, 86.
[118] D. A. Aubeeluck, C. Forbrigger, S. M. Taromsari, T. Chen, E. Diller, H. E. Naguib, *ACS Appl. Mater. \& Interfaces* **2023**, *15*, 34008.
[119] C. Hou, H. Gao, X. Yang, G. Xue, X. Zuo, Y. Li, D. Li, B. Lu, H. Ren, H. Liu, L. Sun, *Microsystems \& Nanoeng.* **2024**, *10*, 141.
[120] C. Hou, K. Wang, F. Wang, H. Li, L. Lou, S. Zhang, Y. Gu, H. Liu, T. Chen, L. Sun, *Adv. Funct. Mater.* **2023**, *33*, 2302812.
[121] Y. Li, J. Long, Y. Chen, Y. Huang, N. Zhao, *Adv. Mater.* **2022**, *34*, 2200517.
[122] D. Li, T. Ji, Y. Sun, Z. Zhang, A. Li, M. Qu, D. Lv, J. Xie, H. Liu, *Adv. Sci.* **2025**, *12*, e02353.
[123] C.-X. Li, Y.-Q. Liu, D.-D. Han, S.-L. Qu, Y.-L. Zhang, *Nat. Commun.* **2025**, *16*, 11513.
[124] A. Hajiaghajani, P. Rwei, A. H. Afandizadeh Zargari, A. R. Escobar, F. Kurdahi, M. Khine, P. Tseng, *Nat. Commun.* **2023**, *14*, 7522.
[125] R. Lin, H.-J. Kim, S. Achavananthadith, S. A. Kurt, S. C. C. Tan, H. Yao, B. C. K. Tee, J. K. W. Lee, J. S. Ho, *Nat. Commun.* **2020**, *11*, 444.
[126] J. Lee, M. Lee, J. Kim, H. Kim, J. Yu, N. Kim, J. Lee, *npj Flex. Electron.* **2025**, *9*, 109.
[127] S. Niu, N. Matsuhisa, L. Beker, J. Li, S. Wang, J. Wang, Y. Jiang, X. Yan, Y. Yun, W. Burnett, A. S. Y. Poon, J. B. H. Tok, X. Chen, Z. Bao, *Nat. Electron.* **2019**, *2*, 361.
[128] M. O. Munoz, R. Foster, Y. Hao, *IEEE Trans. Antennas Propag.* **2012**, *60*, 3397.
[129] P. Bedi, S. Das, S. B. Goyal, P. K. Shukla, S. Mirjalili, M. Kumar, *Expert Syst. Appl.* **2022**, *210*, 118477.
[130] J. Lorenzo, A. Lázaro, R. Villarino, D. Girbau, *IEEE Trans. Antennas Propag.* **2016**,

64, 4447.

[131] M. Salayma, A. Al-Dubai, I. Romdhani, Y. Nasser, *ACM Comput. Surv.* **2018**, *50*, 1.

[132] D. K. Oh, H. Kang, D. Kang, J. Kim, J. Rho, *Nat. Rev. Mater.* **2026**, *11*, 375.

[133] Q. Liu, Z. Qian, C. Zhang, V. Babeshko, *Int. J. Mech. Sci.* **2025**, *307*, 110919.

[134] K. Zhang, J. Ji, Y. Huang, H. Wang, D. Xiao, X. Kang, X. Guo, *Thin-Walled Struct.* **2025**, *208*, 112797.

[135] X. Tian, Q. Zeng, S. A. Kurt, R. R. Li, D. T. Nguyen, Z. Xiong, Z. Li, X. Yang, X. Xiao, C. Wu, B. C. K. Tee, D. Nikolayev, C. J. Charles, J. S. Ho, *Nat. Commun.* **2023**, *14*, 1.

[136] D. Kim, S. J. Hwang, J. Ryu, J.-C. Choi, W. Kim, H. Y. Jeong, P. Lee, S. Chung, *npj Flex. Electron.* **2025**, *9*, 122.

[137] Y. Li, S. Zhang, X. Li, C. Lee, M. Zhu, T. Chen, *ACS Appl. Mater. Interfaces* **2026**, *18*, 3262.

[138] S. Ling, X. Tian, Q. Zeng, Z. Qin, S. A. Kurt, Y. J. Tan, J. Y. H. Fuh, Z. Liu, M. D. Dickey, J. S. Ho, B. C. K. Tee, *Nat. Electron.* **2024**, *7*, 671.

[139] H. Qin, A. Hajiaghajani, A. R. Escobar, A. H. A. Zargari, A. Jimenez, F. Kurdahi, P. Tseng, *ACS Appl. Nano Mater.* **2023**, *6*, 19158.

[140] X. Tian, P. M. Lee, Y. J. Tan, T. L. Y. Wu, H. Yao, M. Zhang, Z. Li, K. A. Ng, B. C. K. Tee, J. S. Ho, *Nat. Electron.* **2019**, *2*, 243.

[141] H. Ye, B. Wu, S. Sun, P. Wu, *Adv. Mater.* **2024**, *36*, 1.

[142] T. Sun, B. Zhou, Q. Zheng, L. Wang, W. Jiang, G. J. Snyder, *Nat. Commun.* **2020**, *11*, 572.

[143] Z. Sun, Y. Hu, W. Wei, Y. Li, Q. Zhang, K. Li, H. Wang, C. Hou, *Adv. Mater.* **2024**, *36*, 1.

[144] C. Dong, A. Leber, D. Yan, H. Banerjee, S. Laperrousaz, T. Das Gupta, S. Shadman, P. M. Reis, F. Sorin, *Sci. Adv.* **2022**, *8*, 1.

[145] S. Lin, W. Yang, X. Zhu, Y. Lan, K. Li, Q. Zhang, Y. Li, C. Hou, H. Wang, *Nat. Commun.* **2024**, *15*, 2374.

[146] W. Yang, S. Lin, W. Gong, R. Lin, C. Jiang, X. Yang, Y. Hu, J. Wang, X. Xiao, K. Li, Y. Li, Q. Zhang, J. S. Ho, Y. Liu, C. Hou, H. Wang, *Science (80-.).* **2024**, *384*, 74.

[147] W. Yan, G. Noel, G. Loke, E. Meiklejohn, T. Khudiyev, J. Marion, G. Rui, J. Lin, J. Cherston, A. Sahasrabudhe, J. Wilbert, I. Wicaksono, R. W. Hoyt, A. Missakian, L. Zhu, C. Ma, J. Joannopoulos, Y. Fink, *Nature* **2022**, *603*, 616.

[148] W. Wang, Y. Pan, Y. Shui, T. Hasan, I. M. Lei, S. G. S. Ka, T. Savin, S. Velasco-Bosom, Y. Cao, S. B. P. McLaren, Y. Cao, F. Xiong, G. G. Malliaras, Y. Y. S. Huang,

Nat. Electron. **2024**, *7*, 586.

[149] Z. Wang, Z. Wang, D. Li, C. Yang, Q. Zhang, M. Chen, H. Gao, L. Wei, *Nature* **2024**, *626*, 72.

[150] M. Khatib, E. T. Zhao, S. Wei, J. Park, A. Abramson, E. S. Bishop, A. L. Thomas, C. H. Chen, P. Emengo, C. Xu, R. Hamnett, S. E. Root, L. Yuan, M. J. Wurdack, T. Zaluska, Y. Lee, K. Parkatzidis, W. Yu, D. Chakhtoura, K. K. Kim, D. Zhong, Y. Nishio, C. Zhao, C. Wu, Y. Jiang, A. Zhang, J. Li, W. Wang, F. Salimi-Jazi, T. A. Rafeeqi, N. M. Hemed, J. B. H. Tok, X. Qian, X. Chen, J. A. Kaltschmidt, J. C. Y. Dunn, Z. Bao, *Nature* **2025**, *645*, 656.

[151] Z. Zheng, X. Ma, M. Lu, H. Yin, L. Jiang, Y. Guo, *ACS Appl. Mater. Interfaces* **2024**, *16*, 10746.

[152] J. Kim, J. H. Noh, S. Chun, S. J. Kim, H. J. Sim, C. Choi, *Nano Lett.* **2023**, *23*, 7623.

[153] J. Peng, F. Ge, W. Han, T. Wu, J. Tang, Y. Li, C. Wang, *J. Mater. Sci. Technol.* **2025**, *212*, 272.

[154] Q. Liang, D. Zhang, T. He, Z. Zhang, H. Wang, S. Chen, C. Lee, *ACS Nano* **2024**, *18*, 600.

[155] M. Zhu, Q. Shi, T. He, Z. Yi, Y. Ma, B. Yang, T. Chen, C. Lee, *ACS Nano* **2019**, *13*, 1940.

[156] T. He, Z. Sun, Q. Shi, M. Zhu, D. V. Anaya, M. Xu, T. Chen, M. R. Yuce, A. V. Y. Thean, C. Lee, *Nano Energy* **2019**, *58*, 641.

[157] T. Ahmed, Y. Gao, M. Y. So, J. Zhang, X. Liu, G. F. I. Toki, J. Lu, T. Chen, B. Xu, *Small* **2026**, DOI 10.1002/smll.202514093.

[158] L. Chen, F. Ning, L. Jin, J. Wu, G. Jiang, P. Ma, H. Yu, F. Wang, Z. Wang, C. Chen, *Nano Energy* **2025**, *138*, DOI 10.1016/j.nanoen.2025.110832.

[159] Y. Wang, Y. Gao, D. Tan, F. Nip, H. Fu, B. Xu, *Nano Energy* **2025**, *142*, 111196.

[160] Y. Chen, J. Huang, Z. Liu, Y. Zou, J. Chen, Z. Liu, Y. Zhu, *Adv. Funct. Mater.* **2025**, *23166*, 1.

[161] X. Zhang, Y. Wu, H. Yu, C. Menon, *Adv. Fiber Mater.* **2025**, *7*, 926.

[162] Y. Xiong, L. Luo, J. Yang, J. Han, Y. Liu, H. Jiao, S. Wu, L. Cheng, Z. Feng, J. Sun, Z. L. Wang, Q. Sun, *Nano Energy* **2023**, *107*, DOI 10.1016/j.nanoen.2022.108137.

[163] A. Shiwei, X. Gao, C. Lu, D. Yao, M. Lu, M. Zhang, Y. Sun, H. Fang, D. Li, *IEEE Sens. J.* **2022**, *22*, 12547.

[164] H. Varghese, B. S. Athira, A. Chandran, *IEEE Sens. J.* **2023**, *23*, 13925.

[165] D. Wang, M. Wang, Z. Zhang, T. Liu, C. Meng, S. Guo, *IEEE Internet Things J.* **2024**, *11*, 40787.

[166] Q. Yang, S. Yang, P. Qiu, L. Peng, T. R. Wei, Z. Zhang, X. Shi, L. Chen, *Science (80-.).* **2022**, *377*, 854.

[167] Y. Zhao, Q. Sun, S. Mei, L. Gao, X. Zhang, Z. Yang, X. Nan, H. Zhang, C. Xue, J. Li, *Microsystems Nanoeng.* **2024**, *10*, DOI 10.1038/s41378-024-00703-7.

[168] Q. Yi, X. Pei, P. Das, H. Qin, S. W. Lee, R. Esfandyarpour, *Nano Energy* **2022**, *101*, 107511.

[169] P. Tan, X. Han, Y. Zou, X. Qu, J. Xue, T. Li, Y. Wang, R. Luo, X. Cui, Y. Xi, L. Wu, B. Xue, D. Luo, Y. Fan, X. Chen, Z. Li, Z. L. Wang, *Adv. Mater.* **2022**, *34*, 1.

[170] L. Zhou, D. Zhang, K. Li, H. Zhang, C. Yang, *Nano Energy* **2025**, *140*, 111072.

[171] Q. Zhang, T. Jin, J. Cai, L. Xu, T. He, T. Wang, Y. Tian, L. Li, Y. Peng, C. Lee, *Adv. Sci.* **2022**, *9*, 1.

[172] D. Hao, Y. Gong, J. Wu, Q. Shen, Z. Zhang, J. Zhi, R. Zou, W. Kong, L. Kong, *Small* **2024**, *20*, 1.

[173] P. Tan, X. Han, Y. Zou, X. Qu, J. Xue, T. Li, Y. Wang, R. Luo, X. Cui, Y. Xi, L. Wu, B. Xue, D. Luo, Y. Fan, X. Chen, Z. Li, Z. L. Wang, *Adv. Mater.* **2022**, *34*, 1.

[174] R. S. Johansson, A. B. Vallbo, *J. Physiol.* **1979**, *286*, 283.

[175] M. Zhu, Z. Sun, Z. Zhang, Q. Shi, T. He, H. Liu, T. Chen, C. Lee, *Sci. Adv.* **2020**, *6*, 1.

[176] M. Zhu, Z. Sun, C. Lee, *ACS Nano* **2022**, *16*, 14097.

[177] S. Wang, Y. Yao, W. Deng, X. Chu, T. Yang, G. Tian, Y. Ao, Y. Sun, B. Lan, X. Ren, X. Li, T. Xu, L. Huang, Y. Liu, J. Lu, W. Yang, *ACS Nano* **2024**, *18*, 11183.

[178] Z. Zhou, K. Chen, X. Li, S. Zhang, Y. Wu, Y. Zhou, K. Meng, C. Sun, Q. He, W. Fan, E. Fan, Z. Lin, X. Tan, W. Deng, J. Yang, J. Chen, *Nat. Electron.* **2020**, *3*, 571.

[179] X. H. Li, M. Z. Li, J. Y. Li, Y. Y. Gao, C. R. Liu, G. F. Hao, *Plant Biotechnol. J.* **2024**, *22*, 1516.

[180] H. Li, H. Niu, H. Kan, E.-S. Kim, N.-Y. Kim, Y. Li, *Adv. Sci.* **2025**, *12*, e09740.

[181] D. Xing, Z. Wang, M. Zhang, S. Liu, W. Yang, R. Yin, H. Liu, C. Liu, C. Shen, *Adv. Funct. Mater.* **n.d.**, *n/a*, e29907.

[182] Z. Sun, M. Zhu, X. Shan, C. Lee, *Nat. Commun.* **2022**, *13*, 5224.

[183] A. Tashakori, Z. Jiang, A. Servati, S. Soltanian, H. Narayana, K. Le, C. Nakayama, C. Yang, Z. J. Wang, J. J. Eng, P. Servati, *Nat. Mach. Intell.* **2024**, *6*, 106.

[184] Y. Luo, C. Liu, Y. J. Lee, J. DelPreto, K. Wu, M. Foshey, D. Rus, T. Palacios, Y. Li, A. Torralba, W. Matusik, *Nat. Commun.* **2024**, *15*, DOI 10.1038/s41467-024-45059-8.

[185] T. W. Kang, Y. J. Lee, B. Rigo, I. Soltis, J. Lee, H. Kim, G. Wang, N. Zavanelli, E. Ayesh, W. Sohail, H. Majditehran, S. H. Kozin, F. L. I. I. I. Hammond, W.-H. Yeo, *ACS Nano* **2025**, *19*, 5613.

[186] G. Xu, H. Wang, G. Zhao, J. Fu, K. Yao, S. Jia, R. Shi, X. Huang, P. Wu, J. Li, B. Zhang, C. K. Yiu, Z. Zhou, C. Chen, X. Li, Z. Peng, Y. Zi, Z. Zheng, X. Yu, *Sci. Adv.* **2025**, *11*, DOI 10.1126/SCIADV.ADT0318.

[187] Y. Yang, X. Guo, M. Zhu, Z. Sun, Z. Zhang, T. He, C. Lee, *Adv. Energy Mater.* **2022**, *2203040*, 1.

[188] Z. Sun, M. Zhu, Z. Zhang, Z. Chen, Q. Shi, X. Shan, R. C. H. Yeow, C. Lee, *Adv. Sci.* **2021**, *8*, 2100230.

[189] M. Zhu, Z. Sun, T. Chen, C. Lee, *Nat. Commun.* **2021**, *12*, 2692.

[190] Z. Huang, Y. Shen, J. Li, M. Fey, C. Brecher, *Sensors* **2021**, *21*, 6340.

[191] Y. Gao, H. Ota, E. W. Schaler, K. Chen, A. Zhao, W. Gao, H. M. Fahad, Y. Leng, A. Zheng, F. Xiong, C. Zhang, L.-C. Tai, P. Zhao, R. S. Fearing, A. Javey, *Adv. Mater.* **2017**, *29*, 1701985.

[192] D. Kwon, T. I. Lee, J. Shim, S. Ryu, M. S. Kim, S. Kim, T. S. Kim, I. Park, *ACS Appl. Mater. Interfaces* **2016**, *8*, 16922.

[193] B. Zhang, J. Li, J. Zhou, L. Chow, G. Zhao, Y. Huang, Z. Ma, Q. Zhang, Y. Yang, C. K. Yiu, J. Li, F. Chun, X. Huang, Y. Gao, P. Wu, S. Jia, H. Li, D. Li, Y. Liu, K. Yao, R. Shi, Z. Chen, B. L. Khoo, W. Yang, F. Wang, Z. Zheng, Z. Wang, X. Yu, *Nature* **2024**, *628*, 84.

[194] Y. Wan, Z. Qiu, Y. Hong, Y. Wang, J. Zhang, Q. Liu, Z. Wu, C. F. Guo, *Adv. Electron. Mater.* **2018**, *4*, 1700586.

[195] Y.-H. Xin, K.-M. Hu, R.-J. Xiang, Y.-L. Gao, J.-F. Zhou, G. Meng, W.-M. Zhang, *Appl. Phys. Rev.* **2025**, *12*, DOI 10.1063/5.0249440.

[196] K. He, *IEEE Trans. Instrum. Meas.* **2025**, *74*, 1.

[197] W. Yuan, S. Dong, E. Adelson, *Sensors* **2017**, *17*, 2762.

[198] H. Li, Y. Lin, C. Lu, M. Yang, E. Psomopoulou, N. F. Lepora, *IEEE Sens. J.* **2025**, *25*, 35672.

[199] S. Wang, M. Lambeta, P. Chou, R. Calandra, **2022**, 1.

[200] M. K. Johnson, E. H. Adelson, *2009 IEEE Conf. Comput. Vis. Pattern Recognit.* **2010**, 1070.

[201] A. Agarwal, A. Wilson, T. Man, E. Adelson, I. Gkioulekas, W. Yuan, *Commun. Eng.* **2025**, *4*, DOI 10.1038/s44172-025-00350-4.

[202] C. Lin, B. Huo, M. Yu, E. Ruppel, B. Chen, J. Francis, D. Zhao, *ArXiv* **2025**.

[203] W. Yuan, C. Zhu, A. Owens, M. A. Srinivasan, E. H. Adelson, *Proc. - IEEE Int. Conf. Robot. Autom.* **2017**, 951.

[204] Z. Xiang, S. Sheshadri, S. H. Lee, J. Wang, N. Xue, N. V. Thakor, S. C. Yen, C. Lee,

Adv. Sci. **2016**, *3*, DOI 10.1002/advs.201500386.

[205] Y. Hwang, B. Park, S. Hwang, S. Choi, H. S. Kim, A. R. Kim, J. W. Choi, J. Yoon, J. Kwon, Y. Kim, *Small Methods* **2023**, *7*, 1.

[206] F. Wen, Z. Zhang, T. He, C. Lee, *Nat. Commun.* **2021**, *12*, 5378.

[207] H. Yang, J. Li, X. Xiao, J. Wang, Y. Li, K. Li, Z. Li, H. Yang, Q. Wang, J. Yang, J. S. Ho, P.-L. Yeh, K. Mouthaan, X. Wang, S. Shah, P.-Y. Chen, *Nat. Commun.* **2022**, *13*, 5311.

[208] E. Ozer, J. Kufel, S. Prakash, A. Raisiardali, O. Kindgren, R. Wong, N. Ng, D. Jausseran, F. Alkhalil, D. Kong, G. Hills, R. Price, V. J. Reddi, *Nature* **2024**, *634*, 341.

[209] D. Zhong, C. Wu, Y. Jiang, Y. Yuan, M. G. Kim, Y. Nishio, C. C. Shih, W. Wang, J. C. Lai, X. Ji, T. Z. Gao, Y. X. Wang, C. Xu, Y. Zheng, Z. Yu, H. Gong, N. Matsuhisa, C. Zhao, Y. Lei, D. Liu, S. Zhang, Y. Ochiai, S. Liu, S. Wei, J. B. H. Tok, Z. Bao, *Nature* **2024**, *627*, 313.

[210] J. Biggs, J. Myers, J. Kufel, E. Ozer, S. Craske, A. Sou, C. Ramsdale, K. Williamson, R. Price, S. White, *Nature* **2021**, *595*, 532.

[211] J. S. Yang, M. K. Chung, J. Y. Yoo, M. U. Kim, B. J. Kim, M. S. Jo, S. H. Kim, J. B. Yoon, *Nat. Commun.* **2025**, *16*, DOI 10.1038/s41467-025-57232-8.

[212] Y. Deng, H. M. Arafa, T. Yang, H. Albadawi, R. J. Fowl, Z. Zhang, V. Kandula, A. Ramesh, C. Correia, Y. Huang, R. Oklu, J. A. Rogers, A. S. Carlini, *Nat. Commun.* **2025**, *16*, 1.

[213] D. Liu, X. Tian, J. Bai, S. Wang, S. Dai, Y. Wang, Z. Wang, S. Zhang, *Nat. Electron.* **2024**, *7*, 1176.

[214] S. Wang, X. Chen, C. Zhao, Y. Kong, B. Lin, Y. Wu, Z. Bi, Z. Xuan, T. Li, Y. Li, W. Zhang, E. Ma, Z. Wang, W. Ma, *Nat. Electron.* **2023**, *6*, 281.

[215] H. C. Ates, P. Q. Nguyen, L. Gonzalez-Macia, E. Morales-Narváez, F. Güder, J. J. Collins, C. Dincer, *Nat. Rev. Mater.* **2022**, *7*, 887.

[216] X. Xiao, J. Yin, J. Xu, T. Tat, J. Chen, *ACS Nano* **2024**, *18*, 22734.

[217] S. Chen, S. Fan, Z. Qiao, Z. Wu, B. Lin, Z. Li, M. A. Riegler, M. Y. H. Wong, A. Opheim, O. Korostynska, K. M. Nielsen, T. Glott, A. C. T. Martinsen, V. H. Telle-Hansen, C. T. Lim, *Adv. Mater.* **2025**, *37*, 1.

[218] Y. Chen, M. Nazhamaiti, H. Xu, Y. Meng, T. Zhou, G. Li, J. Fan, Q. Wei, J. Wu, F. Qiao, L. Fang, Q. Dai, *Nature* **2023**, *623*, 48.

[219] J. Choi, J. Shin, D. Kang, D. S. Park, *IEEE J. Solid-State Circuits* **2016**, *51*, 130.

[220] Y. Zhu, C. Wu, Z. Xu, Y. Liu, H. Hu, T. Guo, T. W. Kim, Y. Chai, F. Li, *Nano Lett.* **2021**, *21*, 6087.

[221] D. Lee, M. Park, Y. Baek, B. Bae, J. Heo, K. Lee, *Nat. Commun.* **2022**, *13*, 5223.
[222] X. Feng, X. Liu, K. W. Ang, *Nanophotonics* **2020**, *9*, 1579.
[223] P. Kumar, K. Zhu, X. Gao, S.-D. Wang, M. Lanza, C. S. Thakur, *npj 2D Mater. Appl.* **2022**, *6*, 8.
[224] C. Xu, S. A. Solomon, W. Gao, *Nat. Mach. Intell.* **2023**, *5*, 1344.
[225] W. Yang, R. T. Tan, S. Wang, J. Liu, *Proc. IEEE Comput. Soc. Conf. Comput. Vis. Pattern Recognit.* **2020**, 1717.
[226] P. Pitchappa, A. Kumar, H. Liang, S. Prakash, N. Wang, A. A. Bettiol, T. Venkatesan, C. Lee, R. Singh, *Adv. Opt. Mater.* **2020**, *8*, 2000101.
[227] K. Wakamori, R. Mizuno, G. Nakanishi, H. Mineno, *Comput. Electron. Agric.* **2020**, *168*, 105118.
[228] Z. Zhang, Q. Shi, T. He, X. Guo, B. Dong, J. Lee, C. Lee, *Nano Energy* **2021**, *90*, 106517.
[229] J. Zhou, Z. Zhang, B. Dong, Z. Ren, W. Liu, C. Lee, *ACS Nano* **2023**, *17*, 711.
[230] Y. Yang, Q. Shi, Z. Zhang, X. Shan, B. Salam, C. Lee, *InfoMat* **2022**, 1.
[231] J. Han, M. Kang, J. Jeong, I. Cho, J. Yu, K. Yoon, I. Park, Y. Choi, *Adv. Sci.* **2022**, *9*, 1.
[232] F. Wang, F. Hu, M. Dai, S. Zhu, F. Sun, R. Duan, C. Wang, J. Han, W. Deng, W. Chen, M. Ye, S. Han, B. Qiang, Y. Jin, Y. Chua, N. Chi, S. Yu, D. Nam, S. H. Chae, Z. Liu, Q. J. Wang, *Nat. Commun.* **2023**, *14*, 1938.
[233] Z. Xu, F. Zhang, E. Xie, C. Hou, L. Yin, H. Liu, M. Yin, L. Yin, X. Liu, Y. Huang, *Research* **2024**, *7*, DOI 10.34133/research.0497.
[234] T. Aina, *J. Electr. Electron. Eng.* **2025**, *13*, 143.
[235] D. Kleyko, D. Rachkovskij, E. Osipov, A. Rahimi, *ACM Comput. Surv.* **2023**, *55*, DOI 10.1145/3558000.
[236] X. Tian, Z. Liu, C. Guo, J. Yang, J. Chen, S. Lyu, H. Bi, F. Qiao, X. Wu, Y. Lu, *IEEE Sensors Lett.* **2021**, *5*, 27.
[237] X. Wu, S. Wang, W. Huang, Y. Dong, Z. Wang, W. Huang, *Nat. Commun.* **2023**, *14*, DOI 10.1038/s41467-023-36205-9.
[238] H. Hu, H. Huang, M. Li, X. Gao, L. Yin, R. Qi, R. S. Wu, X. Chen, Y. Ma, K. Shi, others, *Nature* **2023**, *613*, 667.
[239] M. Wang, Y. Yang, J. Min, Y. Song, J. Tu, D. Mukasa, C. Ye, C. Xu, N. Heflin, J. S. McCune, T. K. Hsiai, Z. Li, W. Gao, *Nat. Biomed. Eng.* **2022**, *6*, 1225.
[240] Y. Choi, P. Jin, S. Lee, Y. Song, R. Y. Tay, G. Kim, J. Yoo, H. Han, J. Yeom, J. H. Cho, D. H. Kim, W. Gao, *Nat. Commun.* **2025**, *16*, DOI 10.1038/s41467-025-60854-7.

[241] L. Liu, Q. Shi, Z. Sun, C. Lee, *Nano Energy* **2021**, *86*, 106154.

[242] S. Sundaram, P. Kellnhofer, Y. Li, J. Y. Zhu, A. Torralba, W. Matusik, *Nature* **2019**, *569*, 698.

[243] H. Liu, W. Dong, Y. Li, F. Li, J. Geng, M. Zhu, T. Chen, H. Zhang, L. Sun, C. Lee, *Microsystems Nanoeng.* **2020**, *6*, 16.

[244] Z. Wang, J. Lin, Y. Zhu, R. Sun, Q. Lin, X. Hu, J. Sun, Y. Jiang, K. You, H. Fu, X. Guo, Y. Wang, D. Li, L. Lin, F. Li, Y. Liu, Y. Zhao, W. Huang, *Nat. Commun.* **2026**, *17*, DOI 10.1038/s41467-025-67316-0.

[245] J. H. Yoon, Z. Wang, K. M. Kim, H. Wu, V. Ravichandran, Q. Xia, C. S. Hwang, J. J. Yang, *Nat. Commun.* **2018**, *9*, 417.

[246] Y. Kim, A. Chortos, W. Xu, Y. Liu, J. Y. Oh, D. Son, J. Kang, A. M. Foudeh, C. Zhu, Y. Lee, S. Niu, J. Liu, R. Pfattner, Z. Bao, T. W. Lee, *Science (80-.).* **2018**, *360*, 998.

[247] L. Massari, G. Fransvea, J. D'Abbraccio, M. Filosa, G. Terruso, A. Aliperta, G. D'Alesio, M. Zaltieri, E. Schena, E. Palermo, E. Sinibaldi, C. M. Oddo, *Nat. Mach. Intell.* **2022**, *4*, 425.

Title ((no stars))

ToC figure ((Please choose one size: 55 mm broad × 50 mm high **or** 110 mm broad × 20 mm high. Please do not use any other dimensions))